DOE/METC--91/4105

DE91 002001

Evaluation of Dust Cake Filtration at High Temperature With Effluence From an Atmospheric Fluidized-Bed Combustor

Technical Note

By
R. A. Dennis

U.S. Department of Energy
Office of Fossil Energy
Morgantown Energy Technology Center
P.O. Box 880
Morgantown, West Virginia 26507-0880

August 1990

ABSTRACT

The results of a test series designed to evaluate dust cake filtration properties at high temperature (1,300 °F) with particulate from an atmospheric fluidized-bed combustor (AFBC) are presented. The tests explored filtration phenomena on a single, full-size, ceramic, candle filter and on a small-scale disc filter. The AFBC was fired with Pittsburgh No. 8 coal with limestone sand as the sorbent. Combustor exhaust gas typically exited with a particulate concentration of 7,500 ppmw. Three separate particulate size distributions and loadings were generated for the study using two different cyclone configurations and the unaltered combustor exhaust gas. The main variable explored in the candle filter tests was particle size distribution; the disc filter tests examined dust cake thickness, particulate size distribution, and filter face velocity. Three candle filter tests and 11 disc filter tests were conducted. The main result from the study indicated that on average a 33% reduction in mean particulate size produced a 498% increase in the dust-cake specific flow resistance (K_2).

TABLE OF CONTENTS

TABLE OF CONTENTS
(Continued)

LIST OF FIGURES

LIST OF FIGURES
(Continued)

LIST OF FIGURES
(Continued)

LIST OF FIGURES
(Continued)

LIST OF FIGURES
(Continued)

LIST OF FIGURES
(Continued)

LIST OF TABLES

EXECUTIVE SUMMARY

In the spring of 1989, two separate test series were simultaneously conducted at the U.S. Department of Energy's (DOE's) Morgantown Energy Technology Center (METC) to examine applied and fundamental behavior of dust cake filtration under high temperature and high pressure (HTHP) conditions. The purpose was to provide information on dust-cake filtration properties to gas stream cleanup researchers associated with the Tidd 70 megawatt (MW) pressurized fluidized-bed combustor (PFBC). The two test facilities included (1) a high-pressure natural-gas combustor with injected particulate, which was fed to two full-size candle filters; and (2) an atmospheric fluidized-bed combustor (AFBC) with coal and limestone sorbent to generate a particulate-laden combustion exhaust gas, which was sent to a single full-size candle filter and a small-scale disc filter. Several major conclusions from these studies are noted below.

- On average reducing the mean particulate size by 33% and the associated loading carried in the filtrate will increase the dust cake specific flow resistance (K_2) by 498%.

- High-temperature and high-pressure filtration can be successfully performed with ceramic candle filters at moderate filtration face velocities and reasonable system pressure drops.

- Off-line filter cleaning can produce a filter system with a higher apparent permeability than that produced with on-line filter cleaning at the same face velocity.

1.0 INTRODUCTION

An experimental test campaign was conducted at the U.S. DOE's METC. The purpose was to explore the filtration properties of dust derived from the fluidized-bed combustion of coal. Results from the investigation address near-term design issues related to HTHP particulate filtration tests to be conducted at the Tidd 70 MW PFBC in Brilliant, Ohio.

Since the DOE is supporting a demonstration test period at the Tidd PFBC, fundamental and process design questions concerning PFBC particulate filtration and the behavior of dust cakes must be answered. Answering these questions means that the particulate cleanup equipment envisioned for the Tidd facility can be selected, designed, and installed within an appropriate time frame. In addition, the ancillary equipment (cyclones) and operational/design guidelines (face velocity, pressure drop, cleaning cycles, particle concentration, size distribution, and filter porosity) must be specified so that the most amenable dust cake can be formed. This test campaign attempts to provide information that may be used to answer some of these questions.

Two different test facilities were designed and constructed. Each facility emphasized different aspects of dust cake filtration in a PFBC application. This approach was taken since METC is not equipped with a PFBC that could simulate the exact filtration conditions expected at the Tidd PFBC. The two separate test facilities consisted of (1) a high-pressure natural-gas combustor with injected and entrained particulate, which was fed to two full-size candle filters (Zeh, Chiang, and Ayers May 1990); and (2) an atmospheric fluidized-bed combustor using coal and limestone sorbent to generate a particulate-laden exhaust gas, which was sent to a single full-size candle filter and a small-scale disc filter. The effects of pressure, cleaning techniques, and face velocity on dust-cake filtration properties were explored with the pressurized natural-gas combustion. The effects of particulate size distribution, face velocity, and cake thickness on dust cake filtration were studied with the AFBC test facility. This report describes the AFBC particulate test facility and the results from the test series.

The overall objective of these tests was to provide Tidd PFBC gas-stream-cleanup researchers with operational and design guidelines that could be implemented prior to and during the demonstration test period scheduled for January 1992. Specific issues addressed in this investigation include (1) the effect of particulate size distribution on specific flow resistance (K_2) in a dust cake filtration application, and (2) the effect of filter face velocity and cake thickness on K_2.

2.0 EXPERIMENTAL APPROACH

Fundamental and applied filtering phenomena as they might occur under Tidd PFBC conditions were studied. The tests were conducted in order to evaluate the effects of various operating parameters on HTHP barrier-filter dust-cake filtration. A 6-inch inside diameter AFBC was designed and built to provide a particulate-laden gas stream. A portion of the effluent from this combustor was fed to two filtering vessels: one housed a full-size ceramic candle filter, the other held a 4.25-inch ceramic disc filter. Mean particle size was varied with cyclones in the full-size candle filter tests, and the effects on dust cake filtration were evaluated. The disc filter was used to study fundamental aspects of dust cake filtration where particle size, dust cake thickness, and face velocity were varied. A conventional experimental approach was used for the full-size candle-filter test series; the work of Leith and Allan (1986) was used to analyze the effect of particle size on K_2. The approach used in the disc filter tests was similar to that in the studies by Holland and Rothwell (Holland and Rothwell 1977a, 1977b; Rothwell 1985).

The AFBC tests were not conducted at high pressure because it was believed that certain dust-cake filtration phenomena at high pressure could be studied at low pressure In addition, since particulate size distribution and morphology play a large role in dust cake filtration, it was decided to use an AFBC as the particulate source, rather than using simulated or re-entrained particles.

3.0 EXPERIMENTAL TEST FACILITY

To study dust cake filtration phenomena, an AFBC with an inside diameter (ID) of 6 inches was used to generate a particulate-laden gas stream. In an attempt to simulate the particulate that may be derived from the Tidd PFBC, a similar fuel and sorbent were used as the reactants in this combustor. Pittsburgh No. 8 coal, ground to a 12 by 10 mesh size, was fed to the combustor at a rate of 10 lb/h, and Greer limestone, ground to 12 by 0 mesh, was used as the sulfur sorbent and fed at a rate of 1.5 lb/h. These fuel and sorbent feed rates provided a calcium to sulfur molar ratio of 1.6:1. The 6-in. AFBC provided a particulate-laden process stream to both a full-size candle filter at a nominal flow rate of 1,200 scf/h, and to a ceramic disc filter with an active filter area of 14.2 in^2 at a nominal flow rate of 65 scf/h. Approximately one half of the effluent from the combustor was sampled to provide the particulate-laden gas stream; the remaining exhaust was vented to the atmosphere. Gases transported from the combustor to the filter vessels were guard-heated and carried in 1-in. tubing. Figure 1 is a schematic layout of the filtering vessels and combustor test facility, and Figure 2 shows a simplified process and instrumentation diagram.

3.1 Description of the 6-Inch Atmospheric Fluidized-Bed Combustor

A 14-in. Schedule 40, carbon steel vessel was used to house a 6-in. ID AFBC. A schematic of this vessel is shown in Figure 3. The combustor was designed with an internal bed temperature of 1,600 °F and a nominal operating pressure of 35 psig. Operating at 1 to 2 atm provided enough system pressure to drive the particulate-laden gas stream through the two downstream filter vessels, associated piping, and flow control loops.

Two linings of a castable refractory were poured in the combustor bed section to provide a vessel skin temperature under 500 °F and a wear-resistant inner combustor surface. One layer of refractory was used in the freeboard. Plibrico HyRezist was used as the inner wear-resistant layer with a thermal conductivity of 7.5 Btu in/h ft^2 °F at 1,500 °F, and Plibrico LWI-20 was used as the insulating outer layer with a thermal conductivity of 1.7 Btu in/h ft^2 °F at 1,500 °F. The internal combustor dimensions were a 6-in. diameter by 4-ft long section, a 1-ft transition section, and a 9-in. diameter by 4-ft long freeboard.

Fluidizing air was injected into a refractory-lined combustor plenum and allowed to flow through a conical distributor plate. The distributor plate cone had a 90° included angle and 180 holes drilled open to a 0.062-in. diameter. The distributor plate holes were staggered and drilled on six concentric circles, providing an open area of approximately 2%. A 0.5-in. central fluidizing jet was located at the apex of the cone. Flow rates of the main fluidizing air and the fluidizing jet were independently controlled and rated at 1,000 to 5,000 scf/h and 500 to 1,500 scf/h, respectively. Providing separate and variable flow configurations allowed flexibility in operation and various modes of fluidization to be obtained (i.e., bubbling, slugging, or spouted).

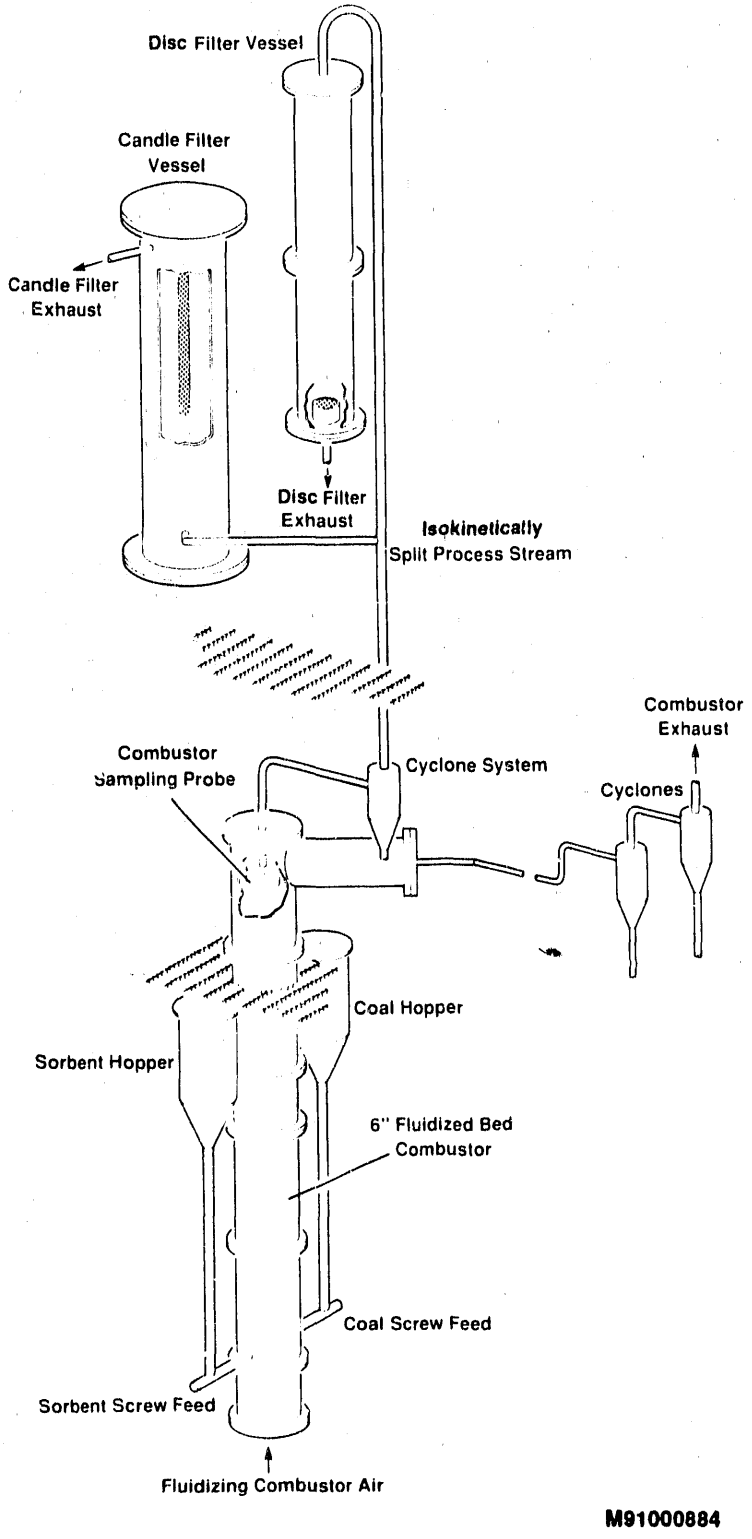

Figure 1. Conceptual Schematic of the AFBC Particulate-Cleanup Test Facility

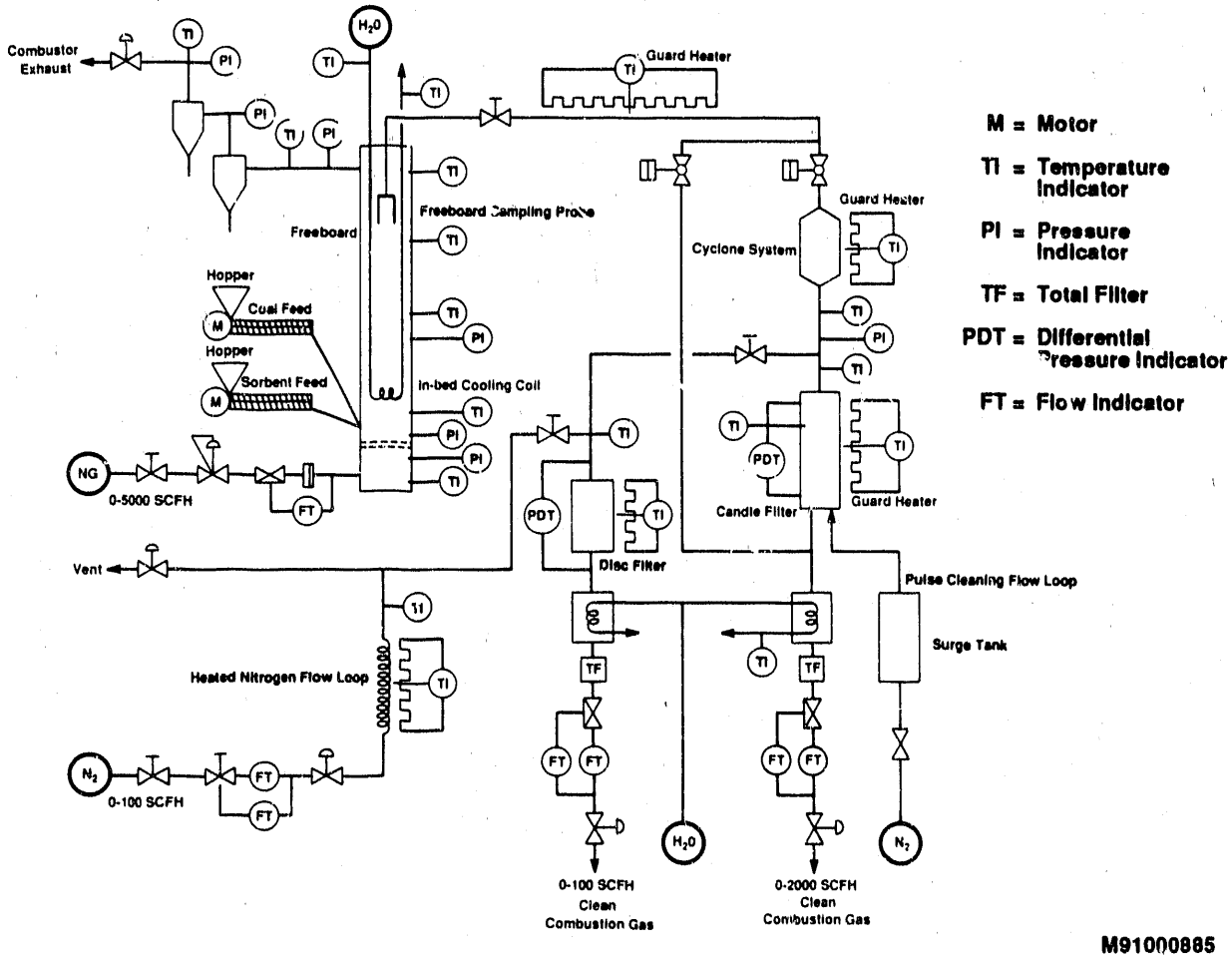

Figure 2. Simplified Process Flow and Instrumentation Diagram of the AFBC Particulate-Cleanup Test Facility

Fuel and sorbent were fed through the wall of the combustor 2 inches above the distributor plate. The penetrations for the two feed systems were 180° apart. Both material feed systems were pressure balanced to the combustor. To accomplish this, impulse lines were run from a central surge tank to the respective material lockhoppers and from the surge tank to the combustor freeboard. The screw feed systems were water cooled. Nitrogen was injected down the central screw-driven material conveying passage, and also through eight concentric 0.062-in. diameter holes at the end of the feeder. Overflow drains were provided at four elevations (9.5, 12.5, 15.5, and 21.5 in.), permitting flexibility in selecting a desired bed height.

Particulate-laden gas from the combustor was discharged in two separate flow legs. The main combustor exhaust consisted of a primary and a secondary cyclone, a total filter, a back-pressure control valve, and an exhaust plenum.

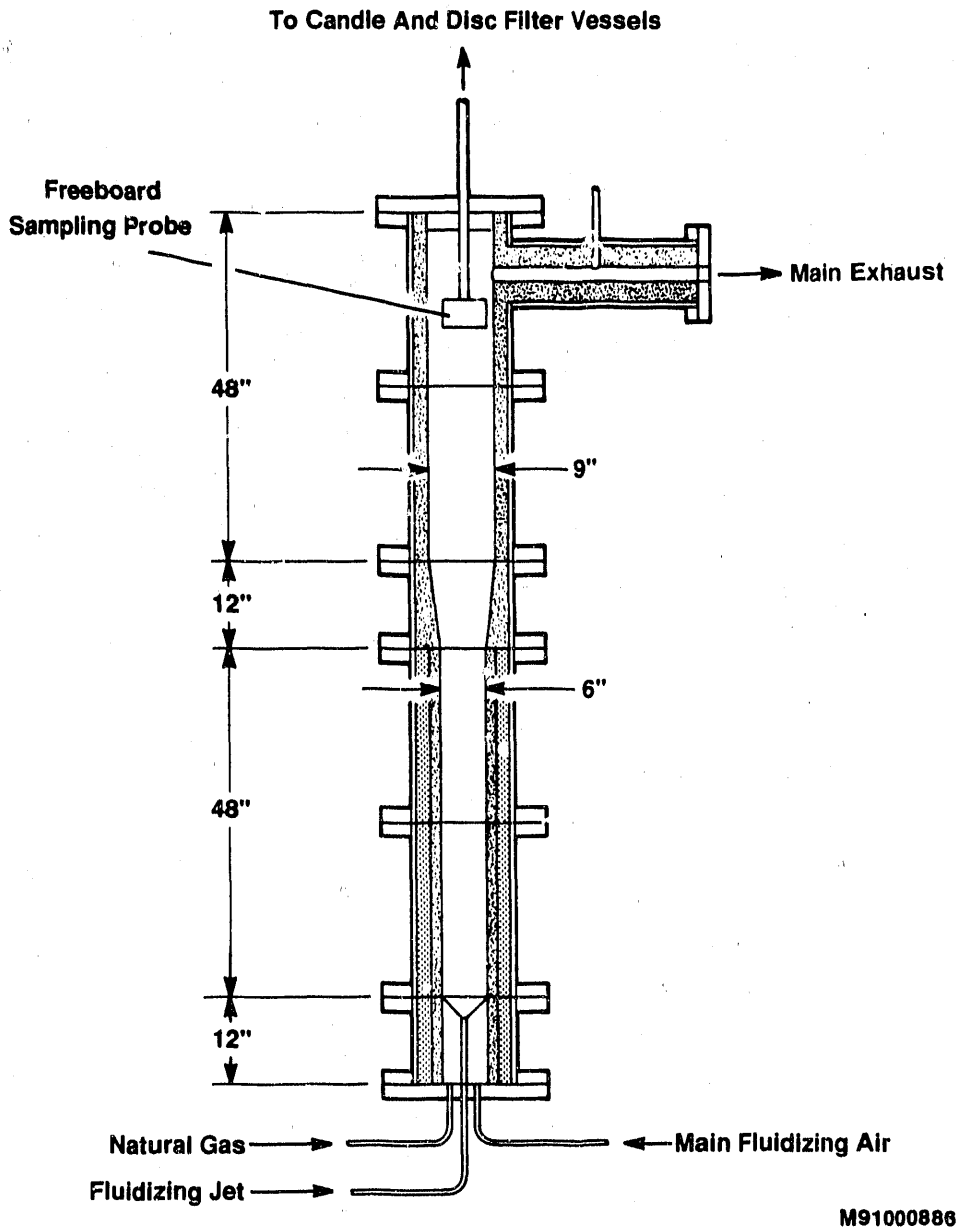

Figure 3. Schematic of 6-Inch AFBC Vessel

The back-pressure control valve was used to maintain a desired combustor operating pressure. The second exhaust leg was used to provide the particulate-laden gas stream to the filter vessels. This flow was sampled in the combustor freeboard through a 6-in. long section of 5-in. Schedule 40, carbon steel pipe. The closed end of this sampling canister was attached to a 1-in. stainless steel tube, which conveyed the gas out of the combustor. The inlet to the sampling can was positioned in the freeboard 7 feet above the combustor distributor plate. Combustor pressure forced flow through this sample line.

The flow was controlled by back-pressure flow-control systems on the downstream side of the candle and disc filter vessels.

Combustor temperatures were measured at elevations of 3.0, 6.0, 9.0, 12.0, 36.0, 63.0, and 96.0 in. above the distributor plate. Pressure drop measurements were made across the distributor plate and across several bed heights. To help moderate combustion temperatures, an in-bed cooling coil was provided. The coil was fabricated from 0.375 x 0.035 in. wall thickness, 304 stainless steel (ss) tubing with 10 wraps on a 3.5-in. ID. This provided 1.0 ft^2 of heat transfer area. The position of the coil within the bed was varied. Depending on the position of the in-bed cooling coil, water flow rates were typically between 40 and 60 gal/h.

3.2 Description of the Candle Filter Vessel

The components of the candle filter vessel consisted of the vessel enclosure, guard-heating system, filter tubesheet assembly, laser-based dust-cake thickness-detection system, and the filter blow-back cleaning system. The vessel enclosure, shown in Figure 4, consists of a 20-in. Schedule 40, carbon steel pipe; a blind and slip-on flange provided the closure on each end. The vessel length from flange face to flange face was 70 in. The vessel was lined with Plibrico Airlite castable insulation (1.0 Btu in/h ft^2 at 1,500 °F) to form a 9-in. ID. The insulating liner began in the center of the top support ring 10.25 in. below the top of the raised face flange and extended for 48 in. A 4-in. thick shelf of insulation was located 22 in. below the top surface of the insulation; the shelf was cast in place, reducing the ID to 6 in. This shelf served to support the top zone of the vessel's guard heaters. The cast refractory extended 22 in. below the 4-in. shelf to the center of the bottom support ring.

Four sight-glass penetrations were made through the shelf. Penetrations for the sight glasses were made every 90°, with one line of sight directly through the center of the vessel and the second slightly off the center axis (approximately 1.18 in.). The off-axis penetration was made to view the tangential surface of the candle filter. The off-axis set of windows provided access for the dust cake thickness detection system, which is described below.

Guard heating in the candle filter vessel was required to maintain the internal cavity of the vessel at the desired operating temperature of 1,500 °F. This heating system consisted of two separate zones that were individually controlled with variable transformers. Each zone contained two half-section heating units (Thermcraft, Inc., Model RL 194) that formed a complete cylinder when positioned in the vessel. When in the cylindrical configuration, the ID was 7 in., the outside diameter (OD) was 8.5 in., and the length was 18 in. Each zone had a recommended maximum temperature of 1,850 °F with a power output of 5,640 W. The upper and lower heating zones were separated by the 4-in. thick shelf, which supported the upper heating cylinder and permitted optical access to the filter element. A shroud was positioned between the heaters and the filter; the shroud was fabricated from a 5-in.

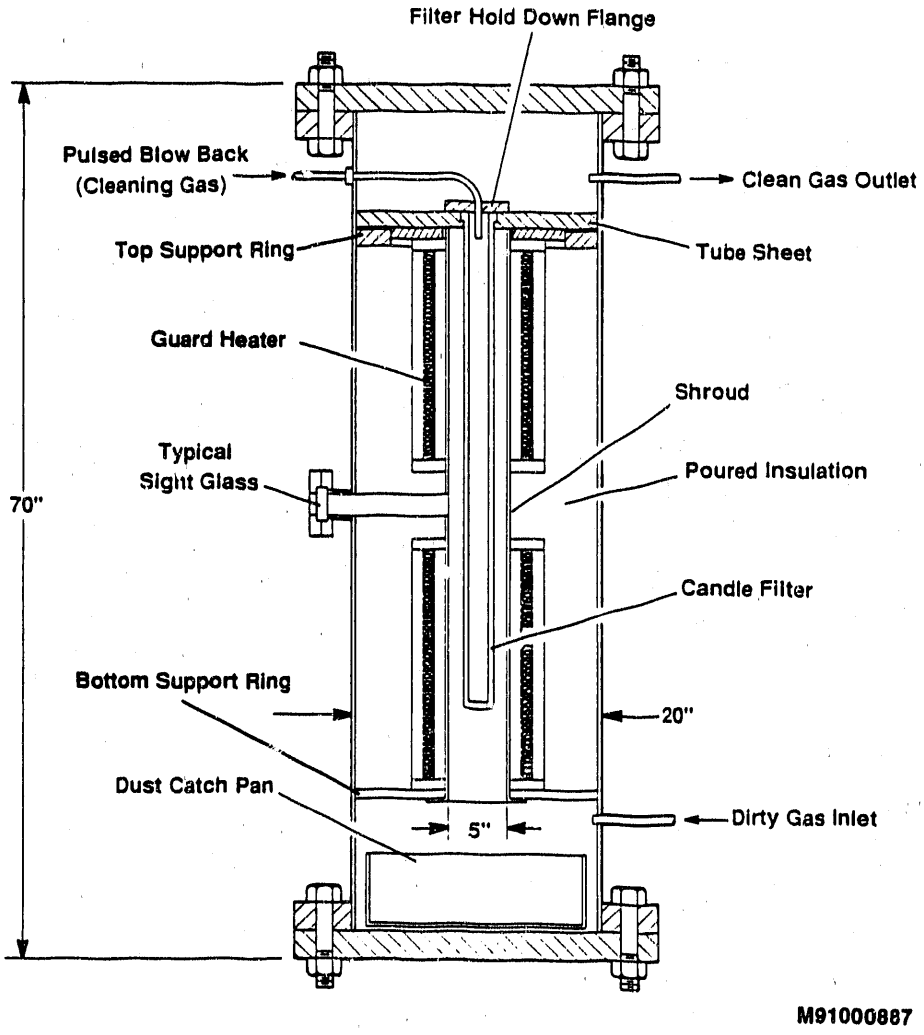

Figure 4. Schematic of Candle Filter Vessel

Schedule 10, ss pipe. The shroud was flanged and supported by the bottom support ring. The purpose of the shroud was to prevent dust from contaminating the heating elements and to permit more uniform heating of the candle filter.

For all of the tests, the same Refractron Corp. RI-20 candle filter was used. The dimensions and configuration of the filter are shown in Figure 5. Silicon carbide was used to fabricate the filter; the silicon carbide was isostatically pressed to the basic shape and then was machined to the final dimensions. The flange and bottom cap of the filter were glued in place. The mean and large pore sizes for this filter composition were measured by an American Society for Testing and Materials (ASTM) bubble test to be 43 and

77 μm, respectively.[1] The slope for pressure drop versus face velocity was determined to be 0.7 in H_2O min/ft for air at ambient conditions.[1,2] A maximum working temperature of 1,800 °F and a room-temperature modulus of rupture of about 1,950 psi were suggested for filters of this configuration and material.

The filter tubesheet assembly shown in Figure 6 consists of a tubesheet disc, filter gasketing material, and a hold-down flange. The tubesheet disc, which was supported on the top support ring, was fabricated from 304 ss with a finished thickness of 1.5 in. Graph-lock gasketing material was used to maintain the pressure seal between the tubesheet and the top support ring. The dimensions and tolerance for the candle-filter tubesheet interface were taken from Institute of Gas Technology (IGT) specifications (1987). The hold-down flange shown in the IGT specifications was not used in this assembly because of the high-pressure drop associated with the design. A new hold-down flange (shown in Figure 6) was employed that lowered the restriction on the exiting filtered gas stream.

Even though the new hold-down flange was designed with a lower pressure drop, the gasketing technique and tolerances remained the same. Three gaskets were used: (1) an Interam I-10 (3M Company) was used at the filter flange tubesheet interface, (2) an Interam I-10 was used at the hold-down flange filter-flange interface, and (3) a metal O-ring gasket was used at the tube-sheet hold-down flange interface. The first gasket was the only required pressure seal; the second Interam gasket was required to account for the difference in thermal expansion between the metal flange, the tubesheet, and the ceramic filter. The metal O-ring gasket was an IGT design and was only required if multiple candle filters were used with the exiting gas stream being separately controlled through dedicated manifolds.

The laser-based detection system for dust-cake thickness (Figure 7) was developed to measure the build-up of dust on the candle filter. In principle, the operation of this device relies on converting an obstructed laser beam into a proportional current. As the dust is filtered and a dust cake builds up, the laser beam is attenuated or blocked, which proportionally reduces the current produced by a light-receiving photo diode.

To help improve the linearity of the device, a mask was used to form a square beam from the center of a normally circular collimated laser beam. Such a beam has a more constant intensity because of the Gaussian intensity distribution of the original beam. The light was also split into two parallel beams of equal intensity, with one beam serving as a reference. The reference beam accounted for any attenuation or blockage caused by the access windows or internal and external airborne dust. During the signal processing, the ratio

---

[1] P. Eggerstedt, Industrial Filter and Pump Manufacturing Company. January 20, 1989. Personal Communication with K. Pater, METC.

[2] P. Eggerstedt, Industrial Filter and Pump Manufacturing Company. October 2, 1989. Personal Communication with C. Zeh, METC.

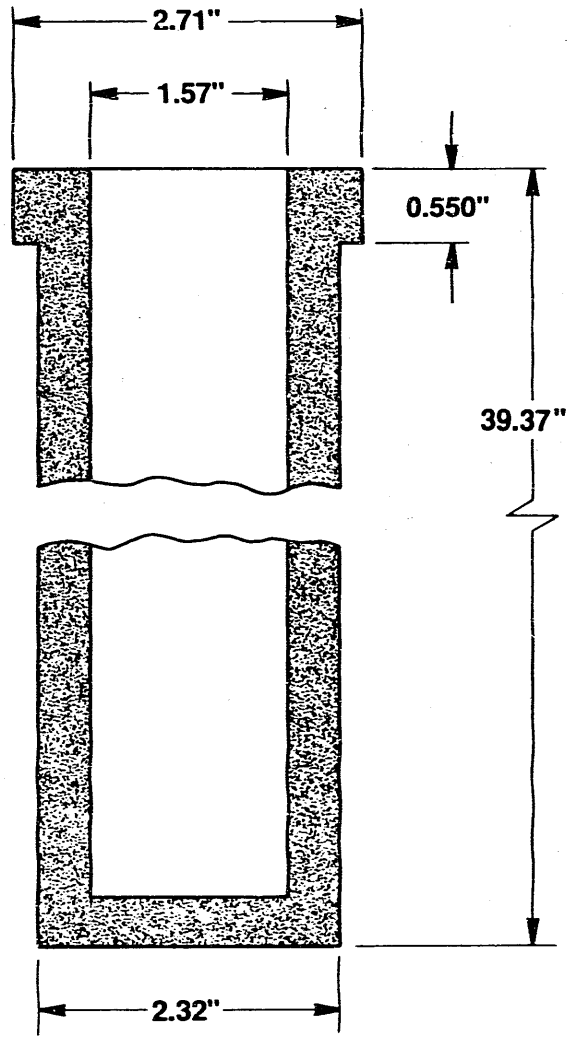

Figure 5. Dimensions of the Refractron RI-20 Candle Filter

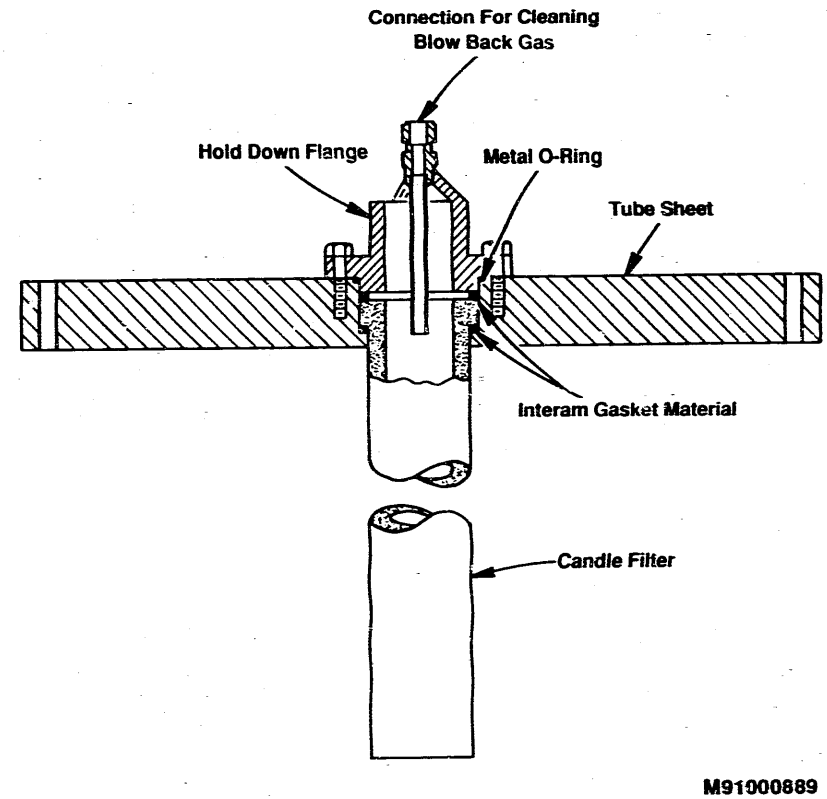

Figure 6. Candle-Filter Tubesheet and Hold-Down Flange

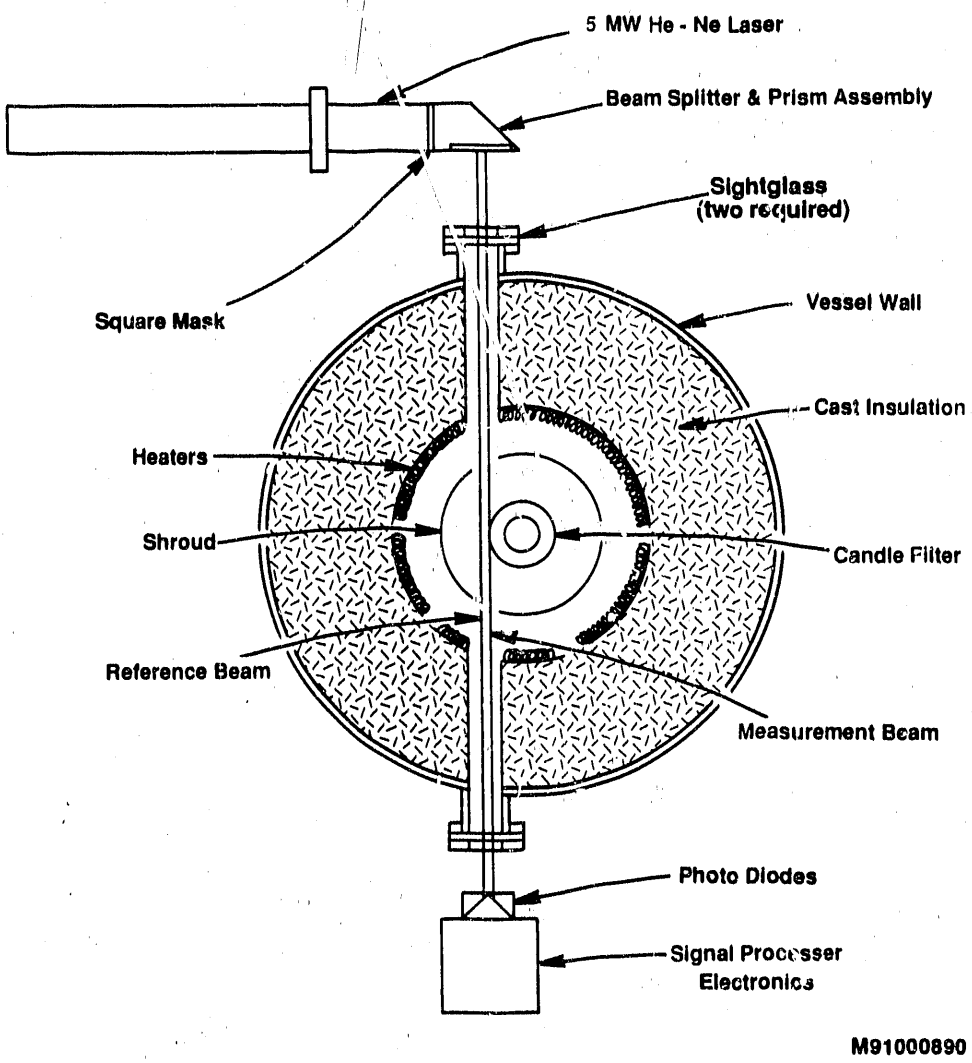

Figure 7. Candle-Filter Dust-Cake-Thickness Detector

of the generated current from both beams was measured and was calibrated to be proportional to the amount the measurement beam was blocked.

The candle-filter blow-back system consisted of a reservoir tank, switching valve, solenoid valve, pulse timers, and associated tubing. The purpose of the blow-back system was to clean the candle filter with a short pulse of nitrogen. Enough nitrogen is needed to reverse the flow of the filtrate and to remove the collected dust cake. The pulse of nitrogen should be large and fast enough so that cleaning is uniform along the length of the candle. Overpressuring the filter during a cleaning cycle could result in the shattering of the dust cake as it is removed, resulting in dust re-entrainment prior to settling.

The blow-back system reservoir-tank provided a volume of 2.3 ft^3, with the pressure regulated to 225 psig from a 600 psig nitrogen source. The

solenoid was connected to the reservoir tank by 59 in. of half-inch ss tubing with a wall thickness of 0.035 in. A switching valve was located approximately 6 in. from the solenoid valve. The purpose of the switching valve was to direct the pulsed nitrogen to either the candle or disc filter. From the switching valve, 35 in. of 0.5 in. ss tubing ran to just inside the candle filter vessel. The final connection from inside the vessel to the 0.375 in. tube on the top of the hold-down flange was made with a 10 in. long, 0.5 in. flexible metal hose.

Two timers connected in series controlled the duration, frequency, and composition of the blow-back pulse train leaving the solenoid valve and entering the candle filter vessel. One timer controlled the frequency and length of each pulse train delivered, while the second controlled the composition. For instance, a pulse train could be delivered every hour for 5 seconds (frequency and length) with a 1-second pulse on, followed by a 1-second pulse off, repeating for 5 seconds (composition).

3.3 Description of the Disc Filter Vessel

This vessel consisted of the vessel enclosure, guard-heating system, and a disc-filter support assembly. The disc filter vessel shown in Figure 8 was assembled from two spool pieces of flanged 12-in. Schedule 40, carbon steel pipe. The overall height of the assembled spool pieces was 75 in. Support rings were welded in place towards the bottom of each spool piece to support the guard heaters. Several penetrations were made through the vessel wall to accommodate guard-heater temperature measurements. At the bottom of the vessel, the filter stage flange was mounted to a machined-open 12-in. blind flange, which supported the disc filter holder.

Three cylindrical sections of guard heaters were provided in the vessel to maintain the desired operating temperature. Two cylindrical sections were positioned in the upper-flow development cavity, and one cylindrical section was located where the disc filter was positioned. Each of the two upper cylindrical sections was fabricated from two heating elements (Thermcraft, Inc., RL 184) with a 6-in. ID, a 7.5-in. OD, and a length of 24 in. The maximum recommended temperature for these heating elements was 1,850 °F, with a total power output of 13.6 kW for these two cylindrical sections.

The third set of guard-heating elements was positioned in the bottom portion of the vessel to provide guard heat to the disc filter holder. These two half-cylinders were fabricated from heating elements (Thermcraft, Inc., RL 181) with a 6 in. ID, a 7.5-in. OD, and a length of 6 in. The total power output of this cylindrical section was 2.3 kW. The maximum recommended operating temperature for these elements was also 1,850 °F.

Blanket-type insulation (Durablanket HD, by Carborundum Co.) was used in the two spool pieces. Two layers of this insulation were wrapped around each set of heating elements before being slipped into the vessel cavity. Fiber board insulation was used on the disc-filter holder assembly (Duraboard HD, by Carborundum Co.), formed into doughnut shapes, stacked, and cemented in place.

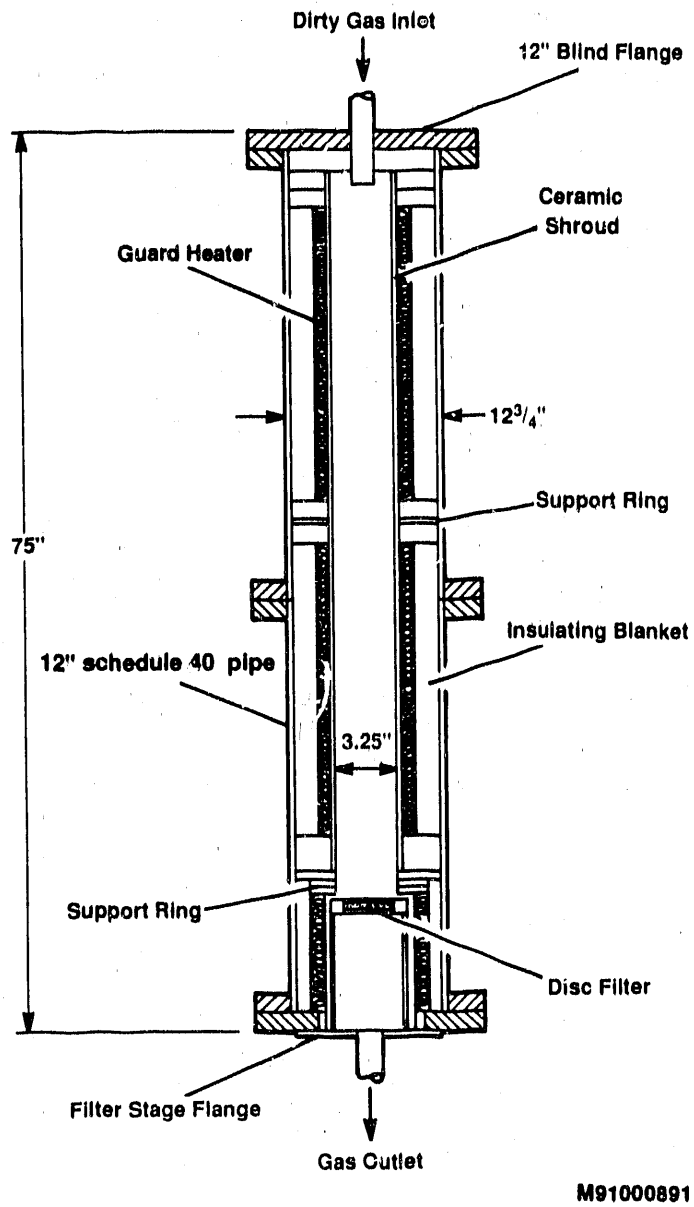

Figure 8. Schematic of Disc Filter Vessel

Each heating zone was independently controlled with continuously variable power transformers.

A shroud fabricated from a 60 in. length of 4-in. Schedule 10, ss pipe was placed in the flow cavity of the disc filter vessel. The shroud prevented dust from settling on the heating elements and provided for more uniform heating along the length of the flow cavity. The shroud was flanged on one end and was mounted to the bottom of the lower support ring.

A disc filter holder (Figure 9) was used to mount the disc filter in the vessel and to form the pressure seal between the clean and dirty sides of the

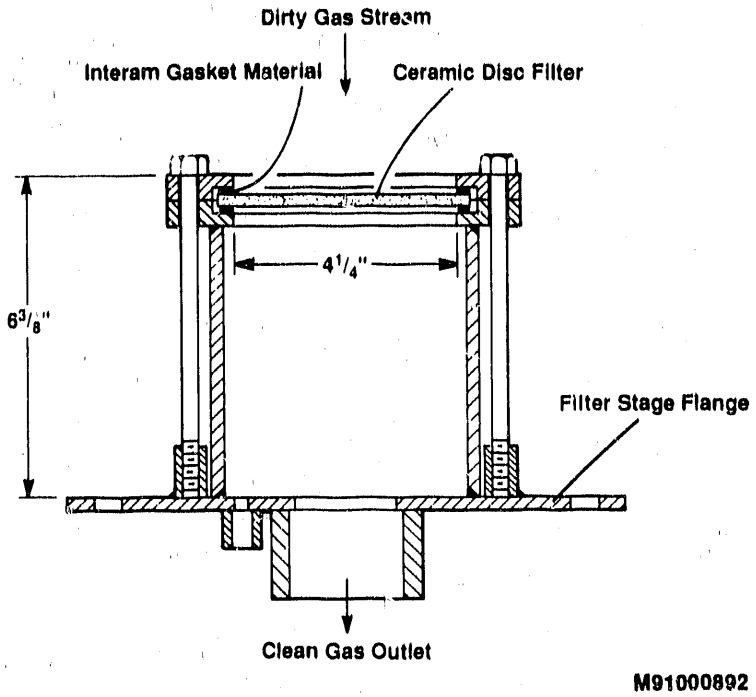

Figure 9. Schematic of Disc Filter Holder

filter. Interam I-10 was used as the gasketing material on both sides of the disc filter. The holder was fabricated from 304 ss to withstand the hot and cold cyclic service conditions. The stud bolts for the assembly were threaded to bolt holes, which were centered on a ring attached to the filter stage flange. This design allowed the threaded connections to operate at a lower temperature, thus preventing galling and seizure.

3.4 Description of the Cyclone System

The cyclone system consisted of three cyclonic separation devices with designed d_{50} cut sizes of 2.3 μm (cyclone 1), 1.5 μm (cyclone 2), and 0.8 μm (cyclone 3). Respective inlet design velocities were 30, 54, and 121 ft/s. The purpose of this system was to modify the particulate size distribution prior to the candle and disc filter vessels. Standard guidelines were used to design the inlet areas, internal diameters, and exit diameters of the cyclones, but modifications were used to simplify the fabrication process. These modifications resulted in circular inlet cross-sections instead of the typical rectangular inlet cross-sections. The typical conical transitions were modified and resulted in straight outlets to the bottom solids exit. The three cyclones were fabricated from 304 ss pipe, tubing, and 125 lb flanges. Any combination of the three cyclones could be used within the cyclone system. The enclosure holding the three vessels was guard-heated to maintain the temperature of the sampled process stream.

3.5 Gas Stream Sampling With the Disc Filter Vessel

In order to compare filtration results obtained from the candle and disc filters, each filter required similar particulate size distributions and particulate loadings. To accomplish this, an isokinetic sampling probe was utilized. Figures 10 and 11 show the basic layout of the sampling probe. A 0.25-in. ss tube (ID drilled open to 0.187 in.) was slipped through the run length of a 1.0-in. ss tee-fitting, which sampled the gas and particulate to be sent to the disc filter. The 0.25-in. tube was flanged and welded to a 1.0-in. ss tube, which was held in the tee-fitting at the exit end, supplying gas to the disc filter. The other end of the tube extended through the tee, 5.375 in. into a 0.25-in. ss tube that was flared to the inlet end of the tee. The three positioning legs were used to center the 0.25-in. tube in the 1.0-in. tube. The gas stream was sampled 5.375 in. past the inlet to the tee.

The probe was designed to automatically sample isokinetically when both filters were operated at the same temperature, pressure, and filter face velocity. This principle of operation was possible since the volumetric flow rates through each vessel were independently controlled and the ratio of the inside area of the drilled-out 0.25-in. tube to the inside area of the 1.0-in. tube was equal to the ratio of the active disc filter area to the active candle filter area. The inherent problem with this approach was that the pressure drops between the sampling probe and filters were different, as were the pressure drops in the flow control legs between the filters and the atmosphere. While this made it difficult to maintain equal pressures in the two vessels, the error imparted to the isokinetic condition was not prohibitive.

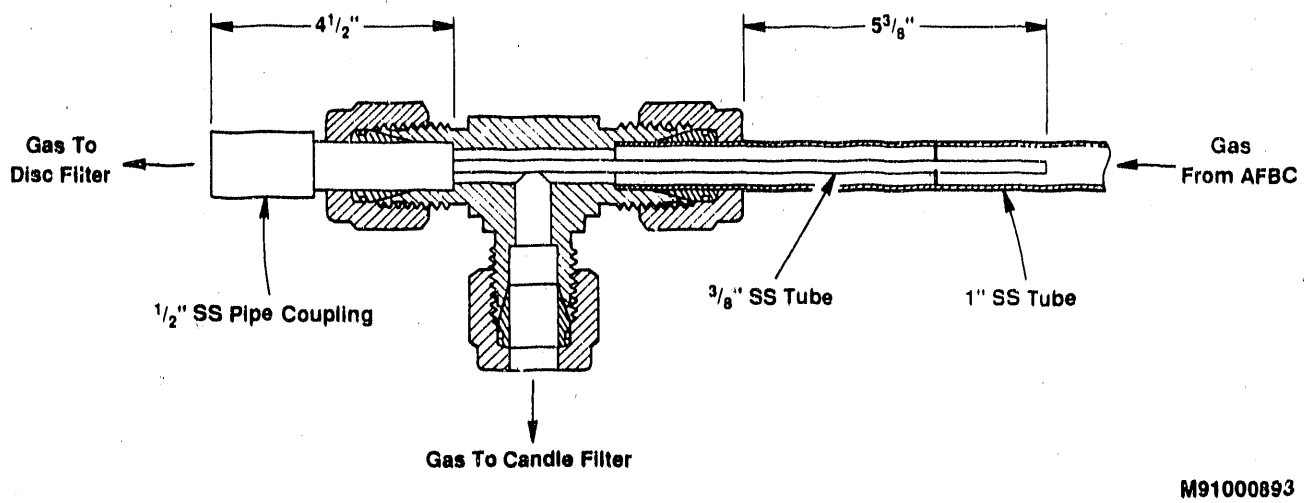

Figure 10. Isokinetic Sampling Probe for the Disc Filter

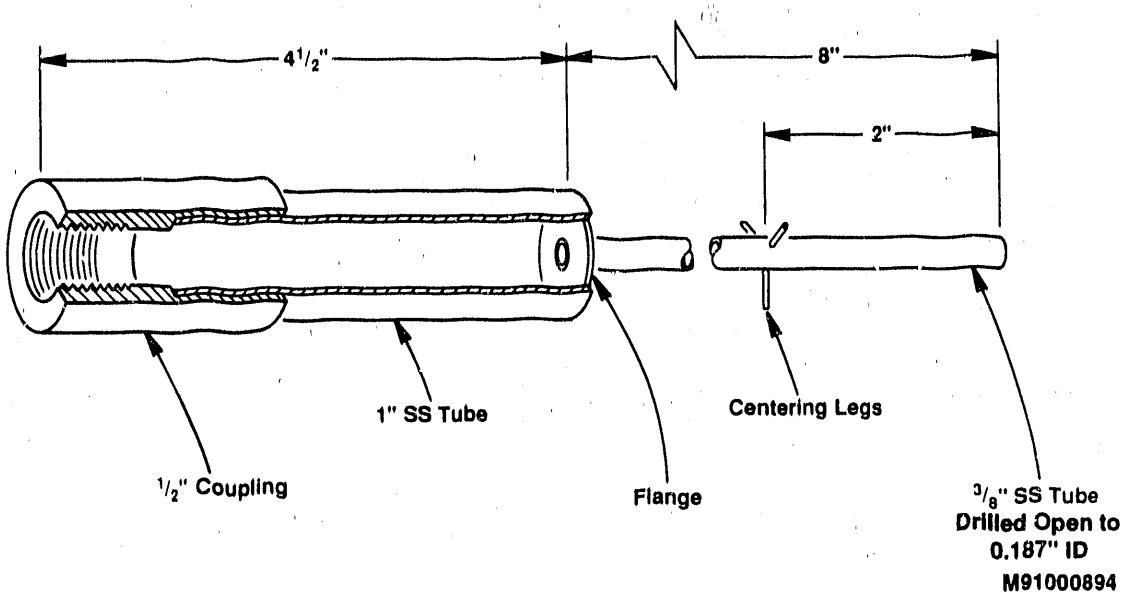

Figure 11. Insert for the Isokinetic Sampling Probe

4.0 CHARACTERISTICS AND OPERATION OF THE TEST FACILITY

This discussion includes a description of the general operation of the facility as well as performance traits that may have affected the interpretation of results or test conditions. A test facility shakedown period was held prior to the actual testing, and some hardware and procedural modifications were made. However, this discussion is mostly on the operational conditions and facility changes made during the test series.

4.1 Operational Characteristics of the Atmospheric Fluidized-Bed Combustor

Preheating the combustor began with 5,000 g of sand for bed material. The sand was used to provide a thermal mass, a flame arrester, and initial insulation of the screw feeders and distributor plate during preheating. Natural gas was introduced at a rate of 30 scf/h and was mixed in the plenum with 300 scf/h of air. The flame was manually lit on the top of the bubbling sand bed. With a flame established, air and natural gas inputs were increased at a 10:1 ratio until 70 scf/h of gas were introduced to the combustor. Fuel fed at this rate was sufficient to uniformly preheat the combustor to the desired temperature of 1,550 °F in approximately 4 to 5 hours. At this time, coal and sorbent were introduced to the combustor and the natural gas was shut off.

Following the light-off procedure, stable operation of the combustor was easily obtained. Table 1 lists the combustor operating conditions for all of

Table 1. Nominal Operating Conditions of the 6-Inch AFBC During the Test Series

AFBC Operating Parameter:	Value
Pressure:	25 psig
Bed Temperature:	1,575 °F
Excess Air:	100%
Coal Type:	Pittsburgh No. 8
Coal Size:	10 x 12 mesh
Sorbent:	Greer Limestone Sand
Sorbent Size:	10 x 10 mesh
Coal Feed Rate:	10 lb/h
Sorbent Feed Rate:	1.5 lb/h
Ca/S Molar Ratio:	1.6:1
Fluidizing Velocity:	5 ft/s
Air Flow Rate:	2,500 scf/h
Bed Depth:	21 in.
Bed Diameter:	6 in.
Particulate Emission:	7,725 ppmw

the tests. The basic operation methodology was to run the combustor with enough fluidizing air to provide a dirty gas stream to the filter vessels, to operate at a high enough combustor pressure to drive the gas flow to the filter vessels, and to provide enough excess combustor exhaust so that the back-pressure control valve on the main combustor exhaust leg would operate within the designed range. Having sufficient exhaust gas in the main exhaust leg also prevented condensate from forming and particulate from being deposited. When the combustor was operating with an internal bed temperature of 1,575 °F, the outside metal wall temperature of the vessel was typically less then 300 °F. A typical temperature profile through the combustor is shown in Figure 12.

The high temperature drop through the bed and freeboard of nearly 1,000 °F could be considered a problem that is characteristic of a small combustor size. The high thermal conductivity of the erosive resistant insulation in the freeboard caused further problems. The low exit temperature of the combustor exhaust eventually caused problems with condensate in the main combustor exhaust flow leg, and limited the maximum temperature attainable in the candle filter vessel.

During the initial shakedown, the combustor was found to operate reliably and with a reduced likelihood of clinkering if the bed were 21 inches deep. The deeper bed also produced a higher carbon utilization. Ash overflow drainage rates were typically 550 g/h with a standard deviation of 75 g/h. Appendix A is the mass weigh-back data from the combustor bed drain port and the main combustor exhaust cyclones. Appendix A also includes a typical chemical and physical analysis of these samples from the three locations.

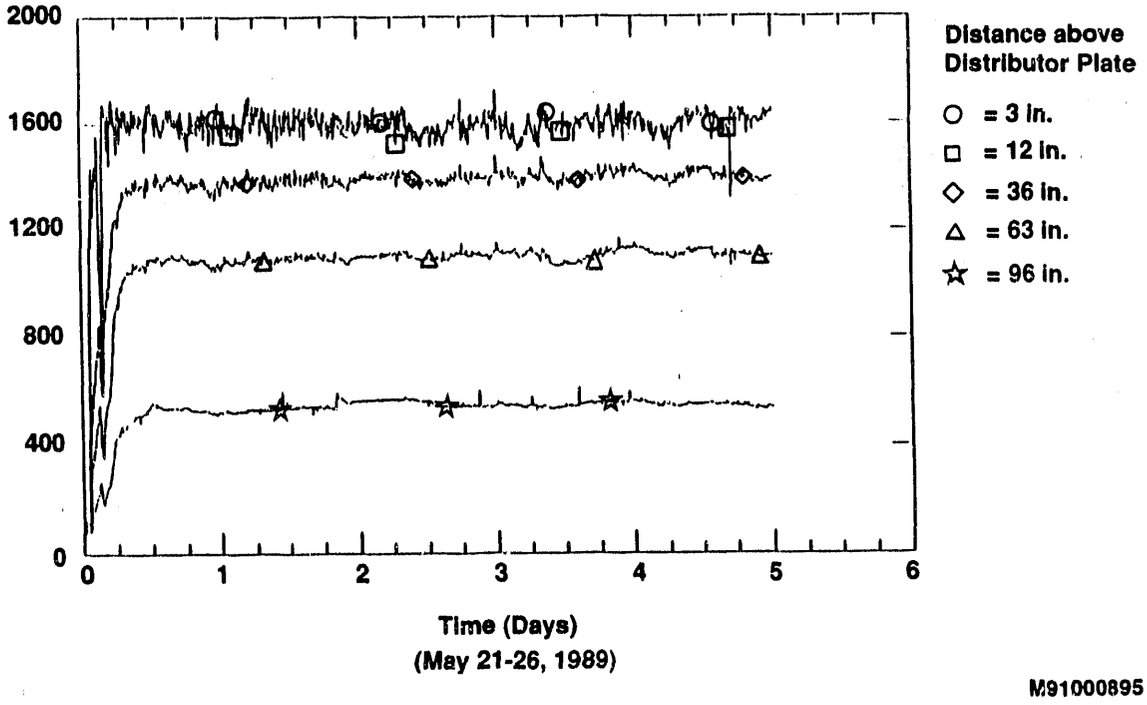

Figure 12. Vertical Temperature Profile Through the 6-Inch AFBC

The temperature at the freeboard sampling probe, which provided gas to the filter vessels, was typically 530 °F. Based on the freeboard gas temperature, combustor operating pressure, combustor flow rate, candle filter sampling rate, and the IDs of the freeboard and combustor sampling probe, deviations from isokinetic sampling conditions were determined. For the above conditions, the freeboard face velocity was 1.0 ft/s and the face velocity to the combustor sampling probe was 1.6 ft/s. Consequently, sampling occurred at 60% above the desired isokinetic conditions for all of the tests. While this seems high, the effects on the sample were believed to be small since the probe inlet was large and approximately half of the combustor process stream was extracted. The worst effect would have been to provide a sample that was not completely representative of the combustor. Such a skewed trend would have been an increase in the percentage of smaller particles per cubic foot of gas sampled. On the other hand, since the sampling conditions were generally the same for the three tests, there was no detrimental effect on the data analysis.

4.2 Operational Characteristics of the Cyclone System

Several deviations took place from the planned operation of the cyclone system. Originally, three cyclone configurations were planned: (1) a single primary cyclone (cyclone 1); (2) a primary and a secondary cyclone in series (cyclones 1 and 2); and (3) primary, secondary, and tertiary cyclone in series (cyclones 1, 2, and 3). The change in plans was motivated by the low anticipated particulate loading and the resultant time constraints if multiple cyclones in series were used. During the three tests, particulate size distributions were obtained by first using a single primary cyclone (cyclone 1); second, by using a straight unaltered combustor exhaust gas (no cyclone); and, finally, by using a secondary cyclone alone (cyclone 2). In application, the actual inlet velocities were 28 ft/s and 52 ft/s (based on inlet conditions of 1,210 scf/h at 25 psig and 600 °F) for cyclones 1 and 2, respectively. The average d_{50} cuts, based on a coulter-counter volume-percent measurement for the two cyclones, were 13.03 µm (cyclone 1), and 11.17 µm (cyclone 2). The large deviations from the theoretical d_{50} cut size could be from the simplifying modifications made when the cyclones were built and the high operating temperatures. The respective cyclone outlet dusts concentrations were 1,826 ppmw and 1,504 ppmw. The inlet dust loading was on the order of 7,500 ppmw. Appendix A includes the periodic weigh-backs from the respective cyclones.

Heaters on the cyclone system were designed to maintain the gas temperature. In practice, however, the gas stream was typically reheated. Inlet temperatures were typically about 550 °F; exit temperatures were about 800 °F.

4.3 Operational Characteristics of the Candle Filter Vessel

Presented in Table 2 are the nominal operating conditions for the candle filter test series. Details of the candle-filter vessel performance and test

series are in Appendix B, which includes process variable plots for all of the tests. Specific operational characteristics are presented below.

Table 2. Nominal Candle-Filter Operating Range During the Test Series

Operating Parameter:	Value
Inlet Temperature:	1,100 to 1,200 °F
Filter Face Temperature:	1,100 to 1,350 °F
Outlet Temperature:	1,100 to 1,350 °F
Pressure:	30 psig
Dust Loading:	1,504, 1,826, 7,725 ppmw
Time Cleaning:	1 s pulse every 1 h
Cleaning Reservoir Pressure:	200 and 225 psig
Flow Rates:	1,200 to 1,300 scf/h (up to 2,000 scf/h)
Face Velocity:	13 ft/min (up to 20 ft/min)
Run Time:	30 to 60 h (up to 100 h)

Candle filter gas temperatures were measured at three locations: one just at the inlet of the vessel, the second 0.5 inches from the candle filter surface mid-way along the longitudinal length, and finally as the gas left the candle filter just above the tubesheet. The inlet, mid-point, and exit temperatures, when averaged over time for all of the tests, were 1,280, 1,321, and 1,274 °F, respectively. While the vertical variation in temperature seen here would not be characteristic of an actual filtering system, the difference between any of the temperatures was never greater then 80 °F during any of the filtration tests (except during the preheat period at which time the middle candle filter temperature reached 1,725 °F). Not being able to operate the filter vessel at 1,500 to 1,600 °F as planned was primarily because of the low gas temperature in the combustor freeboard.

An additional problem encountered in the operation was the pressure drop downstream of the filter vessel in the flow control loop. This problem did not affect the operation of the filter or the test results. However, a 95% open valve position was an undesirable control position. This situation prevented higher filter face velocities from being reached. Smaller particulate size distributions could also complicate the situation because of the inherent higher pressure drop of the resulting dust cake. This problem was caused by the high pressure drop through the gas-stream heat exchanger (cooling coil) and the in-line total filter (TF on Figure 2). Changing the orifice size of the valve trim would have corrected this problem, but was not implemented during the short test period.

The dust cake thickness detector performed extremely well on the bench top and equally well during the first few hours of operation. With the candle

filter on line, the device was able to resolve dust cake build-up on the order of ten thousandths of an inch. Unfortunately, problems occurred in application: After a few cleaning cycles, the optical access ports became obscured with dust. This dust was predominately from the candle filter cleaning periods. The problem could be addressed with a shutter type arrangement attached to the access ports, which would only be opened for a short period of time just before and just after a cleaning cycle. A major limit to this laser-based system was the single point of resolution along the filter length. In this application, the dust cake was later found to be nonuniform along the length of the filter.

The candle filter blow-back cleaning system worked well for the duration of the tests. With the reservoir pressure at 225 psig, a 1-second pulse typically delivered 3.4 scf of nitrogen to the filter.

4.4 Operational Characteristics of the Disc Filter Vessel

Three procedures were conducted in the disc filter test series: (1) heated nitrogen was put through a clean disc filter to obtain baseline pressure drop measurements, (2) a particulate-laden gas was sampled isokinetically and sent to the disc filter for the formation of a dust cake, and (3) the established dust cake was subjected to clean heated nitrogen at 10 different flow rates. Table 3 lists the nominal operating conditions for the disc filter vessel. Two problems that occurred during these procedures are discussed below.

Table 3. Nominal Disc-Filter Operating Range

Operating Parameter:	Value
Filtration Temperature:	1,100 to 1,200 °F
Pressure:	Up to 30 psig
Run Time:	0.5 to 14 h
Flow Rates of Dirty Gas or Clean Heated N_2:	0 to 100 scf/h
Face Velocity:	0 to 20 ft/min

During the disc filter dust-loading tests, the pressure drop suddenly decreased across the filter for some of the tests. Appendix C shows this sudden decrease (e.g., DF8 and DF10). It was first thought that gasketing material had failed and formed a leak across the disc filter seal. However, upon inspection, signs of leaks were not obvious. In addition, the pressure drop after a sudden decrease never dropped below the pressure drop of the clean filter. If there were a leaking gasket, the leak was not enough to reduce the pressure drop to a value below that of a clean and intact filter

gasket assembly. Furthermore, this type of reducing pressure drop was not seen in any of the hot nitrogen flow tests. In an effort to further trouble-shoot this situation, a different gasketing material (Grafoil, Durametallic Corporation) was tried, but the same phenomenon occasionally occurred. It is assumed that this decrease occurred as a result of a collapsing or cracking dust cake.

A major problem encountered with the disc filter vessel was the spalling and flaking of the ss shroud (304 ss, 4-in. Schedule 5, pipe), which formed the flow passage from the dust inlet to the ceramic disc filter. When the vessel was cooled to facilitate removal of the disc filter, flakes of the shroud were found on the surface of the dust cake. Upon inspection, metal fragments were not found below the surface of the dust cake, which indicates that the flaking occurred only during the cool-down stage of the test. To solve this problem, the 4-in. ss pipe was replaced with a ceramic tube of appropriate length with a 3.5-in. OD and a 3.25-in. ID. All of the disc filter test results presented here were conducted with the ceramic tube in place.

The isokinetic sampling system provided particulate-laden gas stream to the disc filter. Unfortunately, deviations from isokinetic conditions existed (Table 4). The deviations shown in Table 4 were determined, based on the difference in filtration conditions between the disc and candle filters. Positive deviations from isokinetic sampling conditions imply a higher probe inlet gas velocity, which would tend to increase the number of smaller particles in the gas stream. Under some conditions, deviations of this magnitude can exist from isokinetic conditions without a significant effect on the sampled gas stream (Tine 1961).

Table 4. Deviations From Isokinetic Sampling for the Disc Filter Test Series

Disc Filter Test Identification	% Above Isokinetic Sampling Conditions
DF1	*
DF2	9.8
DF3	17.7
DF4	7.9
DF5	6.5
DF6	12.8
DF7	17.1
DF8	10.4
DF9	13.6
DF10	18.6
DF11	18.2
Average	13.2

* Operational data lost during computer failure.

5.0 EXPERIMENTAL PROCEDURE

Described here are the experimental procedures used for the three candle filter tests (CF1, CF2, and CF3) and the 11 disc filter tests (DF1 through DF11). The combustor was first preheated on natural gas until a bed temperature between 1,550 and 1,600 °F was reached. At that time, coal and limestone feeding was initiated. With the coal and limestone feed established, the combustor pressure was increased by closing the valve on the back-pressure controller. As the pressure increased, the flow rate to the combustor was raised proportionally to maintain a superficial fluidizing velocity of approximately 5 ft/s.

Combustor operating conditions for the tests were 2,500 scf/h of main fluidizing air, a bed temperature of 1,575 °F, and a pressure of 25 psig. During this time, the candle filter and disc filter vessels were preheated to 1,700 to 1,750 °F. During the preheat period, 100 scf/h of heated nitrogen was sent through the cyclone system and was split at the isokinetic sampling probe, thus sending 80 scf/h to the candle filter vessel and 20 scf/h to the disc filter vessel.

Flowing preheated nitrogen reduced temperatures at localized hot spots produced by guard heaters on the sampling lines between the combustor and filter vessels. Once the combustor was operating at the desired test conditions, the 100 scf/h of heated nitrogen was used to pressurize the cyclone system and candle filter vessel to 26 psig (1 to 2 psi above the combustor pressure). This pressure permitted a smooth transition when the sampling line from the combustor to candle filter vessel was opened.

During the test period, three different particle size distributions were generated and three candle filter tests were performed. The three size distributions were generated with the two different cyclone designs and the unaltered particulate-laden exhaust gas. The three candle filter tests (CF1, CF2, and CF3) were distinguished by the size distribution generated. The combustor freeboard gas stream was typically sampled at a rate of 1,210 scf/h. For this flow rate, temperature, and pressure, the candle filter face velocity was typically 13 ft/min. Once sampling was initiated, the blow-back cleaning system was energized. For all of the tests, cleaning occurred every hour with a 1-second pulse of high pressure nitrogen. During a candle filter test, all pressure, pressure drop, flow rate, and temperature measurements were made and recorded on the Automatic Data Acquisition and Control System (ADACS). The ADACS system was set to record data every 3 seconds during all tests. ADACS was also used to analyze the recorded data.

Following a test, flow to the candle filter was shut off just after a cleaning pulse, and the vessel was allowed to cool to the ambient temperature. With the vessel at a workable temperature, the candle filter and dust catch pan were removed. At that time, separate weigh-backs were made of the dust in the catch pan and the dust cake remaining on the candle filter (residual dust cake). Three samples were taken from the catch pan dust for coulter-counter size and chemical analyses. Once the candle filter vessel and connecting flow

lines were cleaned, modifications to the cyclone system were made to change the particulate size distribution reaching the filter vessels; then testing resumed.

When flow and temperatures in the candle filter vessel reached a steady state, isokinetic sampling for the disc filter test was started. With a disc filter installed prior to sending in the dirty process stream, heated nitrogen was passed through the filter in increments of 10 to 100 scf/h. At each flow increment, a steady-state pressure drop was reached and recorded. This information was later used to characterize the clean disc filter before dust loading. Following the initial procedure with heated nitrogen, the appropriate valves were opened to isokinetically sample the dirty gas stream en route to the candle filter.

During all of the disc filter tests, an effort was made to maintain the same gas temperature measured at the disc filter as that measured at the midpoint of the candle filter. Keeping these temperatures as close as possible helped to ensure isokinetic sampling conditions between the disc and candle filters. Depending on the desired cake thickness and particulate loading, the disc filter vessel was operated from 0.5 to 14 hours. Following the loading of a filter, ADACS data plots were made as a function of time for the dust loading process. These plots indicated pressure drop, flow rate, and filtration temperature. With a set dust loading (cake thickness) on the filter, the particulate-laden gas stream was shut off, and the last phase of the disc filter test was initiated.

In the last phase of the test, hot clean nitrogen was introduced to the filter and dust cake in 10 scf/h intervals, in a fashion similar to the procedure conducted on the clean disc filter. Following the flow of nitrogen in 10 scf/h increments, the filter assembly was cooled to approximately 600 °F and was removed from the vessel. The filter hold-down flange was then removed and the hot filter was placed in a Petri dish and stored in a large desiccator. The desiccator was stored in an oven at 400 °F for 12 hours and then was allowed to cool to room temperature. Once the filter and dust cake (still in the desiccator) cooled to room temperature, the dust cake thickness and mass were measured. Measurement of the dust cake thickness was made with a vernier calliper to the nearest 0.010 inch. The cake mass was then determined to within 0.1 grams. During the three candle filter tests, 11 disc filter tests were conducted.

6.0 TEST RESULTS

6.1 Candle Filter Test Results

Standard methods for analyzing the candle filter test results were employed. The main objective was to evaluate the specific flow resistance (K_2) of the dust cake for the three different tests. In the three candle filter tests (CF1, CF2, and CF3), the main objective was to evaluate the effect of particle size on K_2. Consequently, particle size was the only parameter varied.

Figure 13 illustrates a typical pressure drop versus time signature for barrier-filter dust-cake filtration with periodic blow-back cleaning. The cleaning cycle is triggered by either a preset time interval or a maximum pressure. P_0 represents the pressure drop associated with various system components present in the flow stream between the high and low side of the pressure measurement ports. Essentially, P_0 is the filter vessel's pressure drop without a candle filter in place. Depending on the location of pressure tap ports, the components of a filter vessel can include the dirty gas entrance nozzle, filter tubesheet, filter hold-down flange, and the clean gas exit nozzle. P_1 represents the same pressure drop as P_0 but with a clean virgin candle filter in place that is subjected to a dirty gas stream at time zero. The saw tooth appearance of the pressure drop line represents the increasing pressure drop with time as the dirty gas stream is filtered, a dust cake is formed, and the filter is periodically cleaned. Time T_1 is the time required

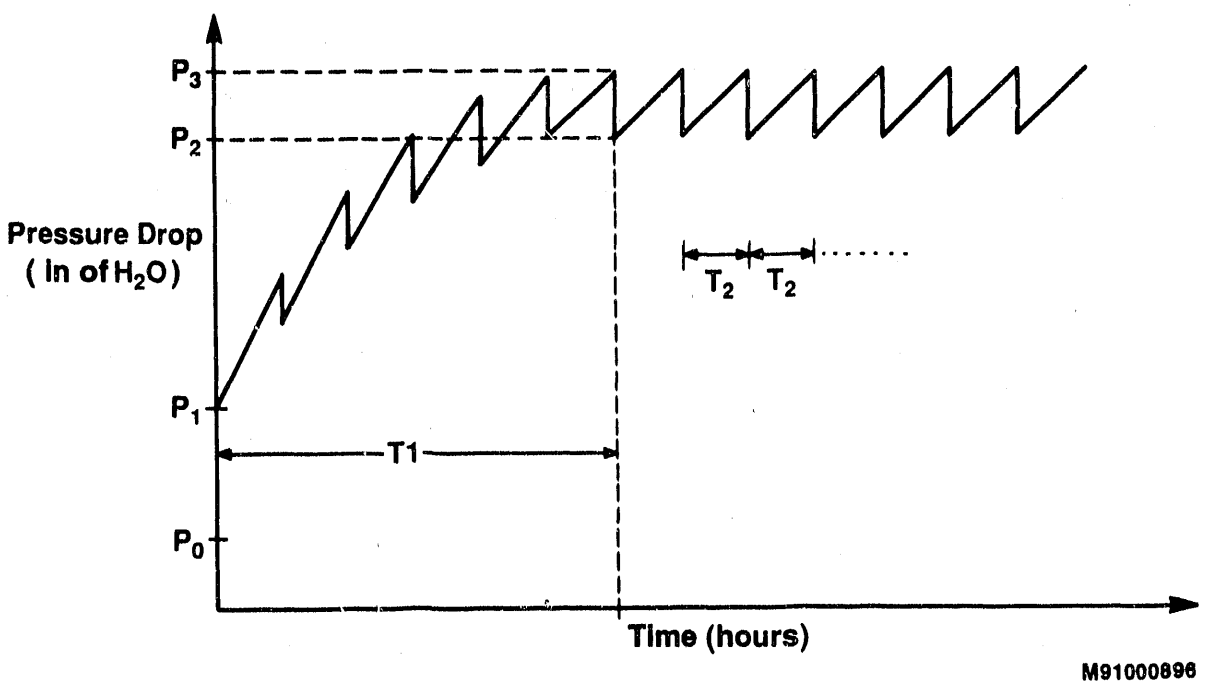

Figure 13. Characteristic Pressure Drop Versus Time for a Barrier Filter

for the formation of a steady-state residual dust cake on the filter. A residual dust cake is particulate that remains on the filter and is typically not removed during a cleaning cycle. P_2 is the low pressure drop just after the filter is cleaned, and P_3 is the pressure drop of the dirty filter just before cleaning.

Filter cleaning can be time initiated, in which case the filtration time interval T_2 will be set. If the dust concentration and filtration conditions remain constant, the rate of change in pressure drop between P_2 and P_3 will remain constant. Alternatively, if cleaning is triggered by a high pressure occurring when P_3 is reached, and if the filtration conditions and dust concentration remain constant, the filtration interval T_2 will be equal for all cycles.

Leith and Allen (1986) defined dust cake specific flow resistance, K_2, to be the pressure drop through the dust cake, P_d, divided by the quantity face velocity, V_f, times the areal density, W_c:

$$K_2 = P_d \; / \; [(V_f) \; (W_c)] \quad . \tag{1}$$

In this relationship, the areal density is the average dust cake mass per unit area. In Figure 13, P_d is the difference between P_3 and P_2. The value in Equation 1 that is difficult to determine, since the cleaning cycle periodically removes the accumulated dust, is the dust cake areal density. To determine the amount of dust added to the unit filter area per filtration cycle, the dust concentration must be determined and the filtration face velocity known. With these two quantities, the areal dust density can be written in terms of the filtration face velocity, dust loading, C_D, and filtration time, T_2:

$$W_c = (C_D) \; (V_f) \; (T_2) \quad . \tag{2}$$

By substituting Equation 2 into Equation 1, an expression for the specific flow resistance K_2 is developed, based on experimentally determined quantities:

$$K_2 = P_d \; / \; [(V_f^2) \; (C_D) \; (T_2)] \quad . \tag{3}$$

In the candle filter tests, the dust concentration, C_D, was determined by dividing the collected mass of dust by the total amount of gas passing through the filter. The total dust collected was determined by weighing the dust from the candle filter's catch-pan and the residual dust cake, which was still on the filter at the end of a test. A total gas volume sent through the filter for the period of the test was determined by multiplying the average candle filter flow rate by the length of the test period. This flow rate information was taken from the ADACS data, in a manner similar to the plots presented in Appendix B. The actual data used in calculating K_2 was taken from ADACS plots that were manipulated to remove the initial and final low points. (These low points were not part of the actual test time and would have tended to lower the actual statistics used in calculating the total flow.)

Figure 13 can also be used to illustrate how the mass of the residual dust cake can be calculated. The residual dust cake is dust that remains on the filter after repeated cleaning cycles. The residual dust cake typically forms in a finite period of time, T_1. The amount of dust involved in the residual dust cake can be estimated by first assuming that the specific flow resistance, K_2, calculated for the steady state cleaning cycles is the same for the residual cake. Then Equation 1 can be solved for the areal density of the dust cake, which is assumed to be equal to the mass of the residual dust cake divided by the filter area. The pressure drop used in this equation is now the difference between P_2 and P_1:

$$W_R = (P_2 - P_1) \; / \; [(V_f) \; (K_2)] \quad . \tag{4}$$

Appendix B presents the filter vessel's flow rates, filter face velocities, pressure drop signatures, and filter temperatures as a function of time for the three tests CF1, CF2, and CF3. Table 5 summarizes the results of the three candle filter tests.

Candle Filter Test One (CF1) was conducted for approximately 34 h with a single primary cyclone in-line. During the test, the filter vessel pressure averaged 23.7 psig with a standard deviation of 1.6 psi. The pressure in the blow-back cleaning reservoir averaged 207 psig. Filter inlet, mid-point, and outlet temperature profiles are shown in Appendix B. The temperature plots show that the filter vessel cavity was preheated to a temperature of 1,705 °F prior to introduction of the particulate-laden gas stream. When the dirty gas was introduced, the mid-point candle filter temperature cooled down to the incoming gas temperature. The apparent drop in the candle filter outlet temperature just before hour 30 of the test was caused by a momentary thermal couple failure.

Flow rate through the candle filter averaged 1,210.8 scf/h. Based on the flow rate, the vessel pressure, and the candle filter mid-point temperature, an average face velocity of 13.1 ft/min was calculated. The total gas passing the filter was measured to be 41,639.8 scf; the resulting dust collected was 5.7 lb. The residual dust cake was measured to have a mass of 0.21 lb. The pressure drop versus time signature for this test showed the characteristic increase in pressure drop for the freshly cleaned filter until the developing residual dust cake reached a steady state. Approximately 24 hours were required to form a steady-state residual dust cake.

Starting at hour 25, the subsequent nine cleaning cycles were used to determine an average K_2 value. The last filtration cycle was not used since it was cut short of a full hour. The average K_2 value was calculated, using Equation 3, to be 33.0 in H_2O ft min/lb, with a standard deviation of 9.5 in H_2O ft min/lb. The average particle diameter, based on the volume of collected dust, was 6.8 μm with an overall particulate concentration of 1,826 ppmw. The mass of the residual dust cake was determined, using Equation 4, to be 0.16 lb.

Candle Filter Test Two (CF2) was conducted without a cyclone in-line, allowing the unaltered AFBC particulate-laden gas stream to reach the candle

Table 5. Summary of Results From Candle-Filter Test Series

Test Parameter	CF1	CF2	CF3
Date	5/19-20/89	5/21-23/89	5/23-26/89
Run Time (h)	34	35.5	64
Cyclone Configuration	Cyclone 1	No Cyclone	Cyclone 2
Face Velocity (ft/min)	13.1	13.1	13.2
Particle Density (g/cm^3)	2.79	2.79	2.80
Average Particle Diameter by Volume (μm)	6.83	11.4	8.27
Average Particle Diameter by Population (μm)	2.75	4.01	2.95
Average Surface Area (BET* m^2/g)	5/38	11.0	7.5
Dust Concentration (ppmw)	1,826	7,725	1,504
Average Temperature (°F)	1,318	1,309	1,331
Average Vessel Pressure (psig)	23.7	23.8	23.5
K_2 (in H_2O ft min/lb)	33.0	7.4	40.7
Residual Dust Cake Mass Calculated (lb)	0.16	0.78	0.24
Total Pressure Drop Before Cleaning (psig)	4.4	4.0	5.0

* Brunauer, Emmitt, Teller

filter. This test was broken into two time periods because the candle filter vessel was taken off-line after a plug in the downstream flow control loop. Since the filter was down for a short period and the test at that time had only lasted 4.5 hours, the candle filter vessel was not cleaned out; the dust collected was averaged into the second part of the test.

The second part of CF2 lasted 31 hours with an average vessel pressure of 23.8 psig and a standard deviation of 1.8 psi. The second part of CF2 had an average flow rate of 1,222.6 scf/h with a standard deviation of 126.8 scf/h. Temperature, pressure, and flow rate conditions produced a candle filter face velocity of 13.1 ft/min with a standard deviation of 1.0 ft/min.

The total dust collected and the gas passing the filter were measured for the combined parts of CF2 and found to be 25.6 lb and 44,178.5 scf, respectively. Unfortunately, the residual dust cake mass in this test was not kept separate from the pan dust. At hour 22 of the second part of this test, the blow-back cleaning reservoir pressure was increased from 200 psig to 225 psig. Increasing the cleaning pressure effectively removed the residual dust cake, which had reached a steady state 17 hours into the test (when the blow-back reservoir was set at 200 psig).

Subsequent to the formation of the second residual dust cake, five filtration cycles were used to calculate K_2. The average K_2 value was determined to be 7.4 in H_2O ft min/lb with a standard deviation of 0.9 in H_2O ft min/lb. The average particle diameter based on volume was 11.4 μm for the collected dust, with an overall particulate concentration of 7,725 ppmw. The residual dust cake mass was calculated to be 0.78 lb/ft^2.

Candle Filter Test Three (CF3) was conducted for 64 hours (an ADACS failure 60 hours into the test prevented the last 4 hours of data from being recorded). The filter vessel pressure averaged 23.5 psig with a standard deviation of 1.3 psi. An average pressure of 227 psig was maintained in the blow-back reservoir during the entire test period. Dirty gas was filtered at a rate of 1,205 scf/h with a standard deviation of 94.5 scf/h. Using these conditions, a filter face velocity of 13.2 ft/min was calculated with a standard deviation 0.8 ft/min. During the 64-hour test, 77,548.8 scf of gas passed through the filter, depositing 8.75 lb of dust. The residual dust cake weighed 1.15 lb.

The stable residual dust cake was removed from the filter at hour 41. When this occurred, the candle filter pressure drop returned to its initial clean value. At this time there was no incident that could be associated with the detachment of the initial residual dust cake. Following the upset, a new residual dust cake formed, taking approximately 24 hours to reach a steady state.

The subsequent 18 filtration cycles were used to calculate an average K_2 value of 40.7 in H_2O ft min/lb with a standard deviation of 4.3 in H_2O ft min/lb. The average particle diameter based on volume was 8.2 μm for the collected dust, at a total dust concentration of 1,504 ppmw. The calculated residual dust cake mass was determined to be 0.20 lb for the first period and 0.24 lb for the second period.

The average particle size was measured for each test using coulter counter analysis of three grab samples taken from the dust catch pan following the test. Table 6 summarizes those samples averaged to determine a mean particle size. Appendix F contains chemical and morphological data on the three dust samples. Scanning electron micrographs presented in Appendix E show the random pore structure of the "cracker like" dust cakes found on the filter and in the catch pan. Appendix E also includes laboratory measurements[3] of the catch pan dust properties that can be used to compare these samples to other

[3] D. Pontius, Southern Research Institute. June 23, 1989. Personal Communication with C. Zeh, METC.

Table 6. Summary of Particulate Grab Samples From Candle-Filter Test Series

Sample Identification	Particle Diameter by Volume (μm)	Particle Diameter by Population (μm)	Particle Density (g/cm^3)	BET Surface Area (M^2/g)
CF1				
R11-1	6.66	2.57	2.78	6.43
R11-2	8.51	3.02	2.80	8.15
R11-3	5.32	2.66	2.80	1.57
Average	6.83	2.75	2.79	5.38
CF2				
R12-1	15.06	4.92	2.84	27.66
R12-2	10.60	3.98	2.75	3.79
R12-3	8.64	3.65	2.80	1.55
Average	11.40	4.01	2.79	11.00
CF3				
R13-1	9.80	3.45	2.86	17.91
R13-2	8.21	3.23	2.68	3.22
R13-3	6.80	2.17	2.87	1.55
Average	8.27	2.95	2.80	7.50

combustor dust effluents (Vann Bush, Snyder, and Chang 1987; Vann Bush, Snyder, and Smith 1989; Pruce 1981). Laboratory properties of the AFBC dust appeared to be similar to that of other combustors, except for the high carbon content of some samples.

6.2 Disc Filter Test Results

The main objective of the disc filter test series was to generate fundamental dust cake filtration data in a small-scale test facility. Test results were used to evaluate the effects of particle size on K_2, to compare small-scale disc filtration data with full-size candle filter data, and to examine additional aspects of dust cake filtration phenomena.

For each of the 11 disc filter tests (DF1 through DF11), three separate procedures were conducted. These procedures included passing hot clean nitrogen in increments of 10 to 100 scf/h through a clean disc filter to record a baseline pressure drop. Then the dirty gas stream was sampled for the formation of a dust cake on the disc filter. Finally, the dirty gas stream was shut off and hot clean nitrogen was passed through the disc filter in increments of 10 to 100 scf/h with a dust cake formed on the filter.

Results of the dust loading portion of the disc filter test series are summarized in Table 7. Appendix C presents ADACS data plots of the actual dust loading period; Appendix C also includes plots of the filter face velocity, filter exit temperature, vessel pressure, flow rate, and pressure drop. The plots of the dust loading period were used to calculate a K_2 value based on the maximum pressure drop reached during the loading period, the measured face velocity, and the areal density of the weighed-back dust. Appendix D contains the tabulated data from passing clean heated nitrogen through the formed dust cake and the chemical and physical analysis of the resulting dust cake. Appendix D also includes graphs of hot clean nitrogen being passed through the formed dust cake in increments of 10 scf/h as plots of face velocity versus pressure drop and specific flow resistance (K_2) versus face velocity.

6.3 Discussion of Results

The most significant result from this test series is the quantification of the effect of particle size on specific flow resistance (K_2) for various dust cakes. This effect is exhibited in both candle filter and disc filter dust cakes when results are compared within each test block. In the candle filter test block, when the effect of particle size on K_2 is compared between tests CF1 and CF2, a 40% reduction in mean particle diameter by volume produced a 346% increase in K_2. Likewise, when CF2 is compared to CF3, a 26% reduction in particle size produced an increase in K_2 of 450%. While the exact K_2 values cannot be compared between the disc and candle filter tests, a similar trend is seen in the disc filtration data. Caution must be used when comparing the disc filter data directly with the candle filter data, since particle size, dust cake thickness, and face velocity may be different.

There is some variability in the candle filter test data, and this is evident for the measurements of both particle size and K_2. The variability in K_2, quantified with standard deviations, is produced by the variation in pressure drop during each cleaning cycle for the period in which K_2 is calculated. The fluctuation in pressure drop could be caused by variations in dust concentrations exiting the fluidized-bed combustor, carried over through the cyclone system, and delivered to the candle filter. Higher dust loadings will produce higher pressure drops within equal filtration periods.

An alternate theory for this variation is that the residual dust cake changes after a quasi-steady state has been reached. This theory is supported by the somewhat similar slopes of the pressure drop versus time cycles while

Table 7. Summary of Results From Disc-Filter Test Series

Test Parameter	DF1	DF2	DF3	DF4	DF5	DF6	DF7	DF8	DF9	DF10	DF11
Date	5/16/89	5/19/89	5/20/89	5/21/89	5/21/89	5/22/89	5/22/89	5/23/89	5/24/89	5/24/89	5/25/89
Run Time (hr)	8	4	12	0.5	0.5	2	4	8	7	14	16
Face Velocity (ft/min)	(1)	12.5	14.1	12.6	12.8	13.6	14.0	13.7	13.5	14.3	14.3
Cake Thickness (in)	.145	(2)	.33	.02	.05	0.09	.175	.10	.08	.165	.23
Cake Mass (g)	21.7	5.2	40.4	4.6	6.2	12.0	27.8	11.9	8.2	17.2	30.2
Maximum ΔP of H_2O	(1)	15.7	75.5	4.6	2.9	14.4	22.6	25.4	15.3	39.9	89.5
Particle Density (g/cm^3)	2.71	2.68	2.72	2.81	2.80	2.76	(3)	2.74	2.74	2.66	2.69
Particle Diameter by volume (μm)	7.07	4.30	6.58	6.44	9.62	8.89	(3)	5.18	4.99	4.75	5.12
Particle Diameter by population (μm)	3.58	2.05	2.11	2.18	3.31	3.25	(3)	2.50	2.44	2.41	2.51
Surface Area (BET m^2/g)	2.37	2.94	4.84	2.65	2.28	3.15	(3)	3.20	2.86	3.36	3.15
Areal Density (lb/ft^2)	.48	.11	.90	.10	.13	.26	.62	.26	.18	.38	.67
Average Temperature (°F)	(1)	1,258	1,242	1,200	1,156	1,259	1,164	1,185	1,179	1,187	1,151
Average Pressure (psig)	(1)	23.8	23.3	23.5	23.6	23.7	23.8	23.3	23.5	23.7	23.5
K_2 (H_2O ft min/lb)	(1)	10.8	5.9	3.5	1.7	3.9	2.6	7.1	6.3	7.3	9.3
Test Conducted During Candle Filter Test	CF1	CF1	CF1	CF2	CF2	CF2	CF2	CF3	CF3	CF3	CF3

(1) Data lost during computer failure.
(2) Dust cake sample disturbed during handling.
(3) Dust sample lost.

the residual dust cake is forming (indicating uniform dust loading). Once the residual dust cake appears to have reached a steady state, it then begins to outgrow its own supporting mechanisms and decay. This reforming and decaying procedure could produce filter-flow pressure-drop characteristics that would produce different pressure drop versus time slopes. The variation (as measured with standard deviation) in pressure drop for the three candle filter tests was similar to the variation in K_2 for a particular test. The exact variation in pressure drop can be quantified from the ADACS plots of pressure drop versus time for each test.

An additional source of error that affects the strength and confidence of this particle size versus K_2 trend is associated with the particle size measurement. While the size distributions from cyclone 1 (CF1) and cyclone 2 (CF3) were expected to be close, it was assumed that, based on the cyclone design, the particulate size distribution leaving cyclone 2 would be smaller than that leaving cyclone 1. However, the coulter counter measurements in Table 5 indicate that this was not the case. This could be because the three grab samples taken from the candle filter's catch pan for either CF1 or CF3 did not represent the actual mean particle size distribution. Also, high temperature effects on gas viscosity have been known to foul cyclone performance, altering the predicted d_{50} size. All other indicators, such as the calculation of K_2, the dust concentration, and the designed d_{50} cut size of cyclone 2, indicate that a smaller particle size should have been delivered and measured from cyclone 2.

Theory can be used to examine the particle size versus K_2 trend. If a simple expression is used for the areal density of the dust cake (Leith and Allen 1986), and if Equation 5 is substituted into Equation 1, the resulting Equation 6 can be solved for K_2. Equation 6 shows that K_2 will vary by the inverse cubed power of the particle diameter. The magnitude of the trend produced from the experimental data is similar.

$$W_c = [(N)\ (Ro)\ (\pi)\ (D^3)]\ /\ 6\ , \text{ and} \tag{5}$$

$$K_2 = (6\ P_d)\ /\ [(V_f)\ (Ro)\ (\pi)\ (D^3)\ (N)]\ . \tag{6}$$

In calculating the residual dust cake, two assumptions were made: (1) the K_2 value calculated during the filtration cycles was assumed to be applicable to the residual dust cake, and (2) the residual dust cake was assumed to be uniform over the length of the candle filter. The distribution of the dust cake was clearly not uniform over the length of the candle filter. Typically, a bulbous dust cake was found at the end of the filter and a short cylindrical segment was found midway along the length of the filter. Between these two irregular sections and above the cylindrical section, there was typically a thin (approximately 0.125 to 0.25 in. thick) "cracker"-like cake (i.e., cracker-like in the sense that pieces of the dust cake could be hand held and snapped like a cracker).

The irregularity in the distribution of the residual dust cake was most likely caused by the vessel and filter configuration used in these tests. Specifically, the location of the dust inlet nozzle contributed to the bulbous

region developed on the end of the filter. The cylindrical section that developed along the middle section of the candle filter was probably related to the settling time for the collected dust as it was blown off the filter during a cleaning pulse. During the short 1-second cleaning pulse, the flow of filtrate was momentarily reversed as the dust cake was removed from the filter; then the normal flow of filtrate resumed. However, during this short 1-second period of time, the removed dust either fell into the vessel catch pan or was re-entrained into the incoming dirty gas. If this was indeed the case, and if the dust did not settle past the mid-point of the filter, then when the incoming gas stream resumed, the dust concentration at the filter mid-point was high. This causes a thicker dust cake and presumably a thicker residual dust cake to form. This same phenomenon could have contributed to the bulbous development on the end of the candle filter.

Another possible source of the cylindrical section of residual dust cake could have been from the nonheated section of the candle filter shroud directly across from the vessel viewing ports. The phenomenon would presumably be related to a local cool spot. The cylindrical section was typically 4 inches long (similar to the nonheated section needed for the viewing ports) and 2 inches higher then the elevation of the viewing ports.

During the dust loading period in the disc filter tests, it was difficult to ascertain the impact of cake thickness (areal density) on the value of K_2, except that they were directly related and that the areal density effect was probably an order of magnitude weaker then the effect of average particle diameter. Disc filter tests DF8 through DF11 illustrate this. In these tests dust was collected with the same cyclone configuration and had the smallest variation in average particle size. (The largest variation was 5.1%.) Assuming that the particle sizes were equal for this analysis, cake thickness had a weak but directly related effect on K_2. For instance, if DF8 is compared to DF10, a doubling of the cake thickness produced a 31% increase in the K_2 value. This effect was at least an order of magnitude weaker than the effect of particle size. The ratio of dust cake thickness to cake mass was not consistent for all disc filter tests, suggesting that compression and consolidation could have been occurring for the cakes with higher mass (higher areal density and cake thickness). That is, cakes of higher mass per unit area produced a higher pressure drop, resulting in additional consolidation and reduced cake thickness. Again, the overall effect on K_2 is not strong.

After the dust loading period, the formed dust cake was subjected to 10 different face velocities by increasing the flow of clean heated nitrogen through the cake from 0 to 100 scf/h in 10 scf/h increments. The objective of this test was to evaluate phenomenological behavior of dust cakes (preformed in this case) subjected to different face velocities. These data, graphically summarized in Appendix D, illustrate the effects of face velocity on K_2. While it was difficult to explain the large and sudden increases in K_2 in some of the tests, all tests showed an increase. The larger increases in K_2 tended to occur for the thinner cakes. This was probably caused by the more continuous nature of thin cakes, which allowed an increase in momentum (because of the increase in face velocity) to be transmitted; this compacted the entire cake. Conversely, a thick cake distributed the momentum force

through the cake structure, thereby sheltering the lower portions of the cake from consolidation forces. Similar trends seem to have been produced by other researchers (Rothwell 1976, 1985, 1986; Holland and Rothwell 1977a, 1977b). The dust cakes subjected to clean heated nitrogen in this portion of the test series were formed at face velocities ranging between 12.5 and 14.3 ft/min, and had an internal structure corresponding to the formation face velocity.

Using the range of face velocities produced by the heated nitrogen with an assumed average particle size of 7.0 μm and other properties calculated at 40 psia and 1,300 °F, the Reynolds number was found to vary from 0.0016 to 0.010 (flow dominated by viscous drag) for tests DF1 through DF11. It was then assumed for the disc filter tests that a change in the Reynolds number by an order of magnitude caused by an increase in the momentum forces would produce a small increase in K_2 (5 to 20%) for thick dust cakes and a moderate to large (50 to 400%) increase for thin dust cakes.

This analysis was semi-qualitative and the dust cakes were formed at fixed velocities. However, this reasoning can be extended to a HTHP filtration application. In such a case, the Reynolds number will still be low, or about 0.20 (assuming there is no effect of pressure on the viscosity), and will still be governed by viscous forces. Consequently, when the momentum forces are increased by an order of magnitude in a HTHP application, the K_2 value will rise by 5 to 20% for thick dust cakes and even higher for thin dust cakes.

In other words, if candle filter test CF2 (the candle filter test that had a thick dust cake per filtration cycle) were conducted at a pressure of 165 psig, then the consolidation effects on the candle filter would have been similar to a disc filter. Furthermore, if the particulate size and morphology of the effluent from a PFBC were the same as that from this AFBC, then the resulting K_2 might increase from 7.4 to 8.8 in H_2O ft min/lb.

Caution should be used in extending the disc filter results to a full-size candle filter test at high or low pressure since these tests were done with pre-formed dust cakes at a set face velocity. In addition, the consolidation phenomenon would be different for a dust cake that was continuously being formed. This would be opposite of that for the disc filter cakes, which were formed at a fixed face velocity to a set thickness and then were exposed to increasing face velocity without the addition of more dust.

Two types of pressure effects can be discussed in relation to high-temperature dust cake filtration: (1) effects of pressure on the filtration fluid mechanics, and (2) effects of pressure on dust cake consolidation properties. An increase in the gas pressure will proportionally increase the gas density, momentum, and consequently, the mass flux of filtrate through the filter. Furthermore, the effect of an increase in pressure on the gas viscosity will be less than 5% at ambient temperature and probably less than 1% at elevated temperatures (Miller 1983). It has been shown that for operating conditions of about 177 psia and 1,550 °F and for porosities expected from PFBC-derived dust cakes, the filtrate Reynolds number will be less then 1.0 (Seville et al. 1989) and will probably be 0.1 to 0.3. This range in Reynolds

number yields a laminar flow regime, governed by viscous forces (Collins 1961; Hillel 1980). Consequently, for a fixed face velocity and operating temperature and an incompressible dust cake, an increase in absolute pressure by an order of magnitude will not increase the pressure drop through the filter. A similar type of pressure effect on pressure drop has been empirically shown for flow through fixed packed beds with the Ergun equation (Kunii and Levenspiel 1969).

The pressure increase and resulting increase in gas momentum will have an effect on the structure, formation, and resulting K_2 values of the dust cake. The dust cake structure will show a change in porosity, which is characterized by the value of K_2. This increase in momentum will be similar to the effect seen when the clean heated nitrogen was passed through the pre-formed dust cake in the disc-filter test series. In the test series, the flow Reynolds number and resulting momentum were increased by an order of magnitude, producing a small increase in K_2 for thick cakes and a large increase for thin cakes. It is difficult to predict how strong this effect will be in large-scale pressurized filter applications with continuously forming dust cakes. However, we hypothesize that the increase in K_2 will be about 10 to 20% if thick cakes are established.

Another phenomenon that may be affected by the pressure increase is the supporting function of the fluid as it passes through the cake structure. This fluid will have a higher density because of an increase in pressure. Thus, it may support the dust cake better than a less dense fluid. However, it is difficult to predict how strong this effect will be. This effect may counteract dust cake consolidation tendencies caused by an increase in pressure.

The difference in K_2 values between the disc and candle filter is to be expected. The difference can be caused by many factors, including particle size distribution, particulate morphology, cake thickness, face velocity, filtrate properties, and filter configuration. The isokinetic sampling in the disc filter tests was designed to maintain equal particulate size distributions on both filters; however, there were substantial variations. These variations and the difference in K_2 values reaffirm the care that must be taken when trying to characterize the particulate from small-scale test facilities and to then extend these characteristics to a full-scale application. Care should also be taken when K_2 values for one or two candle filter systems are extended to larger commercial-scale systems. In general, the K_2 value measured in a small-scale system will not be directly indicative of full-scale values. Helfritch (1972) presented a similar result. This caution will be true even if the particulate size distributions are equal, since other factors such as filter geometry affect the consolidation tendencies and the resulting K_2 value. However, key parameters (particulate size distribution in this case) showed the same trend and similar magnitudes in both the full-size candle-filter test block and in the small-scale disc-filter test block.

The candle filter and cleaning system operated well for these test conditions. This was typified by the moderate pressure drop through the filtering

system of 4 to 5 psi. This pressure drop was associated with a face velocity of 13 ft/min and two different dust loadings on the order of 7,700 to 1,500 ppmw. Caution must be used when comparing total pressure drops before cleaning as shown in Table 5 since permeability is known to decline with use, leading to higher filtration pressure drops. Permeability reduction was generally attributed to infiltration of the porous ceramic structure by fine particulate, which accumulate and remain in the filter structure throughout the cleaning cycles. While an on-line reduction in filter permeability was recorded in the test program that paralleled this effort (Zeh, Chiang, and Ayers 1990), this phenomenon was not particularly evident here because of the relatively short test periods. Post-test evaluation of the candle filter used in this test series revealed a 9% reduction in permeability and a shift in large pore size to 53.95 μm and in mean pore size to 39.66 μm.[4]

[4] P. Eggerstedt, Industrial Filter and Pump Manufacturing Company. January 20, 1989. Personal Communication with C. Zeh, METC.

7.0 CONCLUSIONS AND RECOMMENDATIONS

Based on the results of this testing, the following conclusions can be made:

- On average a 33% reduction in mean particle size by volume will produce a 498% increase in the dust-cake specific flow resistance, K_2.
- The magnitude of trends, particularly the effect of particle size on K_2, that will be seen in full-size filter applications can be predicted with a small-scale disc-filter test facility.
- The specific flow resistance of a specified dust cannot be absolutely predicted with a small-scale disc test facility.
- At least 24 hours are needed to condition a candle filter and form a residual dust cake.
- Thicker dust cakes can produce a higher specific flow resistance, K_2, most likely because of cake consolidation. This trend is much weaker than the effect of particle size on K_2.
- Increasing the face velocity will increase the K_2 value. This trend is seen to be much stronger for thin dust cakes than for thick cakes because thicker cakes may distribute the consolidation forces created by an increase in filtrate momentum.
- A reduction in particulate loading by a factor of five using cyclonic separation devices, accompanied by a corresponding reduction in particulate size distribution, will have a marginal effect (increased by 10 to 20 in. H_2O) on the overall pressure drop of the filtration system.

In conclusion, the following recommendations can be made for the particulate removal system to be utilized at the Tidd PFBC. Cyclones should be removed from the flow stream, or the operational performance should be reduced, so that particulate with a larger mean size distribution is received at the filter. This design philosophy has been supported by others (First 1984). The larger mean size reaching the filter will help reduce the K_2 value, produce a more desirable dust cake for cleaning purposes, and possibly reduce the overall pressure drop through the filter system.

An increase in pressure will not substantially affect the overall pressure drop through the filter system. This is true since even at higher pressure and mass flux, the Reynolds number is still less than 1.0 and the pressure drop is therefore, governed by viscous drag. While the higher operating pressure envisioned for the Tidd plant (177 psia) will increase the gas density and associated momentum, the overall effect should only be a 10 to 20% increase in K_2 because of the consolidation of the dust cake. Therefore, if a similar particulate morphology exists, and if a candle filter system is used without an excessive long-term reduction in filter permeability, we predict that the gas filtration system could be operated at a face velocity of 13 ft/min, without upstream cyclones, and an approximate overall pressure drop of 4.5 psig.

8.0 NOMENCLATURE

C_D	Dust loading, lb/ft^3
D	Particle diameter in Equations 5 and 6, ft
K_2	Dust cake specific resistance, in. $H_2O \cdot ft \cdot min/lb$
N	Number of particles per unit area, $No./ft^2$
P_d	Pressure drop through dust cake (P_3-P_2), in. H_2O
P_0	Pressure drop through filter vessel without filter, in. H_2O
P_1	Same as P_0 but now with clean virgin filter in place, in. H_2O
P_2	Pressure drop just after the filter has been cleaned, in. H_2O
P_3	Pressure drop just before the filter has been cleaned, in. H_2O
Ro	Particle density in Equations 5 and 6, lb/ft^3
T_1	Time to form residual dust cake, h
T_2	Length of filtration cycle, h
V_f	Superficial face velocity at filter, ft/min.
W_c	Areal density of dust cake, lb/ft^2
W_R	Weight of residual dust cake, lb

9.0 ABBREVIATIONS AND ACRONYMS

ADACS	Automatic Data Acquisition and Control System
AFBC	Atmospheric fluidized-bed combustor
ASTM	American Society for Testing and Materials
BET	Brunauer, Emmitt, Teller
CF	Candle filter
DF	Disc filter
DOE	U.S. Department of Energy
FI	Flow indicator
FT	Fluid temperatures
HT	Hemispherical temperature
HTHP	High-temperature, high-pressure
ID	Inside diameter
IT	Initial deformation temperature
IGT	Institute of Gas Technology
M	Motor
METC	Morgantown Energy Technology Center
OD	Outside diameter
PDT	Differential pressure indicator
PFBC	Pressurized fluidized-bed combustor
PI	Pressure indicator
SEM	Scanning electron microscope
SS	Stainless steel
ST	Softening temperature
TF	Total filter
TI	Temperature indicator

10.0 REFERENCES

Collins, R.E. 1961. Flow of Fluids Through Porous Materials. New York: Reinhold Publishing Co.

First, M.W. April 1984. High-Temperature Gas Filtration Research Needs. DE-AC01-83FE60365, 89 p.

Helfritch, D.J. 1972. The Prediction of Baghouse Performance By Means of a Small Field Test Instrument. Buffalo, New York: Dustex Co.

Hillel, D. 1980. Fundamentals of Soil Physics. New York: Academic Press.

Holland, C.R., and E. Rothwell. 1977a. Model Studies of Fabric Dust Filtration. 1. Flow Characteristics of Dust Cakes Uniformly Distributed on Filter Fabrics. Filtration & Separation January/February: 30-36.

Holland, C.R., and E. Rothwell. 1977b. Model Studies of Fabric Dust Filtration, 2. A Study of the Phenomena of Cake Collapse. Filtration & Separation May/June: 224-231.

Institute of Gas Technology. February 1987. Institute of Gas Technology Hot Gas Cleanup Bench-Scale Unit. Unpublished report for METC under Contract No. DE-AC21-85UC22144.

Kunii, D., and O. Levenspiel. 1969. Fluidization Engineering. Malabar, Florida: Robert E. Krieger Publishing Co.

Leith, D., and R.W.K. Allen. 1986. Dust Filtration By Fabric Filters, In Progress in Filtration & Separation 4, R.J. Wakeman, ed., Amsterdam: Elsevier Publishing Co., p. 1-51.

Miller, R.W. 1983. Flow Measurement Engineering Handbook. New York: McGraw Hill Co.

Pruce, L. 1981. Evaluating the Use of Coal, Ash Analyses For Predicting Fabric-Filter Performance, Power February: 80-83.

Rothwell, E. 1976. Concepts of Fabric Dust Filtration. Filtration & Separation September/October: 477-484.

Rothwell, E. 1985. An Analysis of Fabric Dust Filtration I: Model Observations of Dust Cake Formation. Filtration & Separation September/October: 317-324.

Rothwell, E. 1986. An Analysis of Fabric Dust Filtration II: Computation of Constant Pressure-Drop Filtration. Filtration & Separation March/April: 113-118.

Seville, J.P.K., R. Clift, C.J. Withers, and W. Keidel. 1989. Rigid Ceramic Media for Filtering Hot Gases. Filtration & Separation July/August: 265-271.

Tine, G. 1961. Gas Sampling and Chemical Analysis in Combustion Processes. New York: Pergamon Press.

Vann Bush, P., T.R. Snyder, and R.L. Chang. 1989. Determination of Baghouse Performance From Coal and Ash Properties: Part 1, JAPCA 39: 228-237.

Vann Bush, P., T.R. Snyder, and W.B. Smith. 1987. Filtration Properties of Fly Ash From Fluidized-Bed Combustion, JAPCA 37: 1292-1297.

Zeh, C.M., T.K. Chiang, and W.J. Ayers. May 1990. Evaluation of Ceramic Candle Filter Performance in a Hot Particulate Laden Stream, Technical Note. DOE/METC-90/4099. NTIS/DE90000483. 59 p.

APPENDICES

Appendix A: Dust and Bed Material Data

Appendix A includes the periodic mass measurements of dust and bed material from cyclones 1 and 2 on the combustor exhaust (Cyc. 1 and Cyc. 2, respectively), the mass measurements of dust from the cyclone system for the two configurations (Cyc. Sys. 1 and 2), and material removed from the overflow bed drain. All masses are recorded in grams and the time of day in hours. Most measurements were made every 2 hours, but some deviations exist. Footnotes to the data are listed below. Also included is a laboratory analysis of these samples.

(1) Testing started with a single primary cyclone in-line in the cyclone system. Candle filter test CF1 and disc filter tests DF1, DF2, and DF3 were conducted with this cyclone configuration (5/16/89 - 5/20/89).

(2) The cyclone system was off-line for several hours while repairs were made to the candle filter flow control loop; consequently gas was not taken through the cyclone system.

(3) Testing started without a cyclone in the cyclone system; consequently the unaltered combustor effluent was sent to the filter vessels. Candle filter test CF2 and disc filter tests DF4, DF5, DF6, and DF7 were conducted with this configuration (5/16/89 - 5/20/89).

(4) Testing started with the single secondary cyclone in-line in the cyclone system. Candle filter test CF3 and disc filter tests DF8, DF9, DF10, and DF11 were conducted with this cyclone configuration (5/23/89 - 5/26/89).

Table 8. Material Removed from Cyclone System, AFBC Exhaust Cyclones, and Bed Overflow Drain

Date	Time (h)	Periodic Discharge: Cyclone 1 (g)	Periodic Discharge: Cyclone 2 (g)	Periodic Discharge: Cyclone System (g)	Periodic Discharge: Overflow Bed Drain (g)	Discharge Rates: Cyclone 1 (g/h)	Discharge Rates: Cyclone 2 (g/h)	Discharge Rates: Cyclone System (g/h)	Discharge Rates: Overflow Bed Drain (g/h)	Notes
05/16/89	100	580.5	27.5	596.1	1247.1	290.3	13.8	298.1	623.6	(1)
	300	599.6	21.8	468.9	1327.4	299.8	10.9	234.5	663.7	
	500	626.5	10.1	414.7	1205.1	313.3	5.1	207.4	602.6	
	700	592.4	71	715.1	1267.2	296.2	35.5	357.6	633.6	
	900	596.7	31.6	657.3	1184.5	298.4	15.8	328.7	592.3	
	1100	595.2	53.2	525.2	1282.3	297.6	26.6	262.6	641.2	
	1300	584	39.7	686.4	1185.1	292.0	19.9	343.2	592.6	
	1500	569.2	39.6	545.1	1137.7	284.6	19.8	272.6	568.9	
	1700	629.4	37.2	631.5	1254.4	314.7	18.6	315.8	627.2	
	1900	646.6	30.2	556.8	1390.3	323.3	15.1	278.4	695.2	
	2100	798.3	53.5	372.8	1317.8	399.2	26.8	186.4	658.9	
	2400	623.2	39.5	303.3	1337.1	207.7	13.2	101.1	445.7	
05/17/89	200	635.1	60.3	548.1	1567.3	317.6	30.2	274.1	783.7	
	400	503.3	33.7	702.6	1270.8	251.7	16.9	351.3	635.4	
	600	613.5	20.1	370.7	1445.9	306.8	10.1	185.4	723.0	
	800	711.5	40	637.2	1347.3	355.8	20.0	318.6	673.7	
	1000	703	29.1	573.5	1251.1	351.5	14.6	286.8	625.6	
	1200	703.6	33.7	25.4	1211.4	351.8	16.9	12.7	605.7	
	1400	598.9	25.5	295.1	1231.9	299.5	12.8	147.6	616.0	
	1600	606.6	35.4	739.4	1340.7	303.3	17.7	369.7	670.4	
	1800	633	35.6	664.2	1403.2	316.5	17.8	332.1	701.6	
	2000	655.2	29	776.3	1605.8	327.6	14.5	388.2	802.9	
	2200	602.5	52.1	662	946.9	301.3	26.1	331.0	473.5	
	2400	199.7	21.6	634.8	1359.5	99.9	10.8	317.4	679.8	
05/18/89	200	992.6	21.6	645.5	1271.8	496.3	10.8	322.8	635.9	
	400	613.8	49.4	321.4	1306.1	306.9	24.7	160.7	653.1	
	600	680.5	29.6	430	1259.5	340.3	14.8	215.0	629.8	
	800	772.3	48.3	224.7	1494.3	386.2	24.2	112.4	747.2	
	1000	597.8	47.4	584.6	1358.3	298.9	23.7	292.3	679.2	
	1200	618.8	25.4	493.6	1506.3	309.4	12.7	246.8	753.2	
	1400	528	49.7	417.3	878.7	264.0	24.9	208.7	439.4	
05/19/89	400	1297.2	58.8		2544.7	648.6	29.4	0.0	1272.4	(2)
	600	757.5	48		664.7	378.8	24.0	0.0	332.4	
	700	741.6	43.7		489.9	741.6	43.7	0.0	489.9	
	900	918.9	38		1325.1	459.5	19.0	0.0	662.6	
	1100	306.7	41.6	663.8	1439.5	153.4	20.8	331.9	719.8	
	1300	484.9	28.8	607.1	1398.5	242.5	14.4	343.6	699.3	
	1500	400.9	32.1	603.5	1316.1	200.5	16.1	301.8	658.1	
	1700	480.1	23.4	647.4	1617.2	240.1	11.7	323.7	808.6	
	1900	1250	19.5	343.4	1537.3	625.0	9.8	171.7	768.7	
	2100	685.3	43.6	694.7	1389.7	342.7	21.8	347.4	694.9	
	2300	699	41.7	464.5	1428.4	349.5	20.9	232.3	714.2	
05/20/89	100	713.7	67.6	756	1414.5	356.9	33.8	378.0	707.3	
	300	922	13.9	506.2	1112.2	461.0	7.0	253.1	556.1	
	500	612.4	42.9	762.9	1540.2	306.2	21.5	381.5	770.1	
	700	529.7	38.6	510	1238.9	264.9	19.3	255.0	619.5	
	900	576.7	23.8	450	1348.1	288.4	11.9	225.0	674.1	
	1100	577.2	35.8	632	1285.6	288.6	17.9	316.0	642.8	
	1300	602.4	20.9	588.6	1168.5	301.2	10.5	294.3	584.3	
	1500	642.4	34.8	243.5	1193.8	321.2	17.4	121.8	596.9	
	1700	564.3	28.4	737.5	1343.6	282.2	14.2	368.8	671.8	
	1900	1054.1	12.3	426.7	1161.6	527.1	6.2	213.4	580.8	
05/21/89	1200	1845.7	117.1		5012.8	922.9	58.6	0.0	2506.4	(3)
	1400	539.2	20.1		1248.2	269.6	10.1	0.0	624.1	
	1600	890.8	71.7		1112.6	445.4	35.9	0.0	556.3	
	1800	1250.5	32.1		1119.5	625.3	16.1	0.0	559.8	
	1900	121	101.1		765.5	121.0	101.1	0.0	765.5	
	2100	382	17.9		988.2	191.0	9.0	0.0	494.1	
	2300	501	24.7		1037.9	250.5	12.4	0.0	519.0	

Table 8. Material Removed from Cyclone System, AFBC Exhaust Cyclones, and Bed Overflow Drain

(Continued)

Date	Time (h)	Periodic Discharge				Discharge Rates				Notes
		Cyclone 1 (g)	Cyclone 2 (g)	Cyclone System (g)	Overflow Bed Drain (g)	Cyclone 1 (g/h)	Cyclone 2 (g/h)	Cyclone System (g/h)	Overflow Bed Drain (g/h)	
05/22/89	130	637.6	22.1		1359	255.0	8.8	0.0	543.6	
	330	541.8	23.3		1124.5	270.9	11.7	0.0	562.3	
	500	521.4	28.5		1045.1	347.6	19.0	0.0	696.7	
	700	743.7	48.9		1192.9	371.9	24.5	0.0	596.5	
	900	655.1	52.1		1131.1	327.6	26.1	0.0	565.6	
	1000	326.1	22.4		605.5	326.1	22.4	0.0	605.5	
	1200	564.1	28.2		1046.2	282.1	14.1	0.0	523.1	
	1600	672.1	71.2		1042.8	168.0	17.8	0.0	260.7	
	1800	648.1	28.8		1191.2	324.1	14.4	0.0	595.6	
	2000	659.1	41.7		1105.1	329.6	20.9	0.0	552.6	
	2200	709.3	48.3		1218.7	354.7	24.2	0.0	609.4	
	2400	947.1	104.7		1274	473.6	52.4	0.0	637.0	
05/23/89	200	1297.2	65.3		976.2	648.6	32.7	0.0	488.1	
	400	1373.2	30.8		1099	686.6	15.4	0.0	549.5	
	600	1442.4	106.5		1179.8	721.2	53.3	0.0	589.9	
	800	1458.2	68.4		1167	729.1	34.2	0.0	583.5	
	1000	1504.5	59.6		1269.1	752.3	29.8	0.0	634.6	
	1200	1204.7	44.5		973.9	602.4	22.3	0.0	487.0	
	1400	970.5	510.2		1034.3	485.3	255.1	0.0	517.2	
	1600	1373.7	24.3		1183.4	686.9	12.2	0.0	591.7	
	1800	651	76		1175	325.5	38.0	0.0	587.5	
	2000	392.1	21	408.8	1322.8	196.1	10.5	204.4	661.4	(4)
	2200	429.5	32.4	737.4	1232.4	214.8	16.2	368.7	616.2	
	2400	515.7	29.7	704	1066.5	257.9	14.9	352.0	533.3	
05/24/89	200	550.7	30.9	732.3	1268.9	275.4	15.5	366.2	634.5	
	400	636	49	704	1208.2	318.0	24.5	352.0	604.1	
	600	604.8	36.6	335.5	981.2	302.4	18.3	167.8	490.6	
	800	698.8	38.3	684.9	1085.1	349.4	19.2	342.5	542.6	
	1000	724.9	30.8	653.5	995.7	362.5	15.4	326.8	497.9	
	1200	494.3	210.8	703.5	789.3	247.2	105.4	351.8	394.7	
	1400	615.6	11.9	695	2096.1	307.8	6.0	347.5	1048.1	
	1600	635.3	34.5	520.3	1018.9	317.7	17.3	260.2	509.5	
	1800	661.1	36	677	1195.2	330.6	18.0	338.5	597.6	
	1900	450.5	54.5	396.7	672.9	450.5	54.5	396.7	672.9	
	2100	590.2	18.4	735.4	1111.8	295.1	9.2	367.7	555.9	
	2300	670.4	28.5	759.1	650.7	335.2	14.3	379.6	325.4	
05/25/89	100	700.9	25.9	725.7	1610.7	350.5	13.0	362.9	805.4	
	300	403.2	28.5	672.1	1037	201.6	14.3	336.1	518.5	
	500	774.1	21.2	637	1133.8	387.1	10.6	318.5	566.9	
	700	713.1	40.5	695.5	1121.5	356.6	20.3	347.8	560.8	
	900	669.3	29.3	695.8	1078.1	334.7	14.7	347.9	539.1	
	1100	765.1	47.6	699.5	1197.9	382.6	23.8	349.8	599.0	
	1300	649.1	38.8	613.5	1325.3	324.6	19.4	306.8	662.7	
	1500	672.4	32.3	752.3	1151.5	336.2	16.2	376.2	575.8	
	1700	504.4	38.6	580.9	1060.8	252.2	19.3	290.5	530.4	
	1900	608.2	5.2	735.5	1109.3	304.1	2.6	367.8	554.7	
	2100	670.7	204.6	846.7	1121.5	335.4	102.3	423.4	560.8	
	2300	502.7	26.8	634.6	1096.3	251.4	13.4	317.3	548.2	
05/26/89	100	628.8	36.5	588.6	1009.1	314.4	18.3	294.3	504.6	
	300	603.4	28.3	629.4	1064.1	301.7	14.2	314.7	532.1	
	500	630.6	26.7	677.8	1230.8	315.3	13.4	338.9	615.4	
	700	671.1	16.8	735.3	1151.4	335.6	8.4	367.7	575.7	
	900	751.1	95.8	393.7	884.6	375.6	47.9	196.9	442.3	

Table 9. Laboratory Analysis of Combustor Discharge Material, Samples R20, R15, R16, R7-6, and R17

Parameter	Sample Identification				
	Bed Drain	Cyclone 1	Cyclone 2	Cyclone System 1	Cyclone System 2
Mean Particle Size (by volume) (μm)	17.37	10.94	4.19	11.33	11.17
Mean Particle Size (by population (μm)	4.76	3.72	1.90	3.76	3.65
Density (by helium) (g/cc)	3.02	2.78	2.91	2.75	2.64
BET[1] Surface Area (via nitrogen (m^2/g)	1.26	15.02	7.35	13.50	13.73
Pore Volume, Adsorption (via N_2) (cm^3/g)	0.0023	0.0086	0.0111	0.0080	0.0074
Ash (%)	99.05	71.08	91.64	73.83	74.85
Carbon (%)	0.52	25.57	4.82	21.10	22.09
Nitrogen (%)	0.01	0.45	0.11	< 0.01	0.36
Total Sulfur (%)	11.75	3.738	6.829	4.707	4.597
Sulfur (%)	8.08	1.91	2.55	2.52	2.42
Hydrogen (%)	0.24	0.26	< 0.01	0.15	0.22
Moisture (%)	0.00	1.19	1.78	0.35	0.49
K_2O (%)	0.02	1.623	2.365	1.261	1.188
SiO_2 (%)	27.8	42.3	38.9	40.5	40.9
Fe_2O_3 (%)	1.08	7.10	4.97	5.79	6.68
MgO (%)	--	2.675	2.130	3.422	3.439
ZnO (%)	0.008	0.0061	0.0079	0.0104	0.0061
SrO (%)	--	0.087	0.129	0.058	0.069
CaO (%)	45.27	20.683	15.450	28.873	27.336
P_2O_5 (%)	< 0.57	0.331	0.285	0.405	0.391
Al_2O_3 (%)	5.04	17.89	19.13	15.88	14.97
TiO_2 (%)	--	0.68	0.90	0.45	0.48
MnO (%)	0.00	0.002	0.000	0.005	0.004

[1] Brunauer, Emmit, Teller

Appendix B: Process Variable Plots for Candle Filter Tests CF1, CF2, and CF3

Appendix B is a series of plots of the process variables made with ADACS. Similar plots were used to calculate experimental parameters needed to analyze the results. These particular plots were not used for the calculations because they include initial and final process values. Including the initial and final points (time before or after the actual test started or ended) would have lowered the mean value and increased the frequency of the minimum values. In other words, the statistics given on the top of each plot presented in Appendix B may be slightly different than the values used in calculating K_2 and face velocity.

The bottom header in each figure details the start and stop time of the plot, which is generally slightly longer then the actual test time so that end points could be included, and the skip factor, which indicates the number of raw data points skipped when collecting data for the plot. For instance, the ADACS system recorded data every 3 seconds, and if the skip factor was 05, then a real-time data point was plotted every 15 seconds. The abscissa is a time line and is plotted in hours. The ordinate is a line of magnitude and has units that are associated with each slot. The top header provides the slot number, units for that slot, and a slot description. Statistics are also provided that give the number of samples during the time of the plot, the mean, a standard deviation, and a minimum and maximum frequency of occurrence for the high and low values.

Slot descriptions are as follows:

- CANDLE FILTER HI FLOW -- Total flow rate of filtrate through the candle filter.
- CANDLE FILTER DP -- Pressure drop across the candle filter.
- CANDLE FILTER INLET -- Gas temperature in the pipe as gas enters the filter vessel.
- CANDLE FILTER TEMPERATURE -- Gas temperature 0.5 inches from the filter surface midway along the length.
- CANDLE FILTER OUTLET -- Gas temperature as gas exits the filter just above the tubesheet. (Note: In Figures 17, 22, and 27, candle-filter outlet temperature is mistakenly referred to as patch-filter outlet temperature.)
- CANDLE FILTER FACE VELOCITY -- Superficial gas velocity, based on the total filtrate flow, candle filter temperature, pressure in candle filter vessel, and the surface area of filter.
- ISO #1 PRESSURE -- Candle filter vessel pressure.

SLOT	UNITS	DESCRIPTION	# SAMPLES	MEAN	ST DEV	MIN - FREQ	MAX - FREQ
985	"H2O	CANDLE FILTER DP	914	71.435	21.769	0.614 01	128.363 01

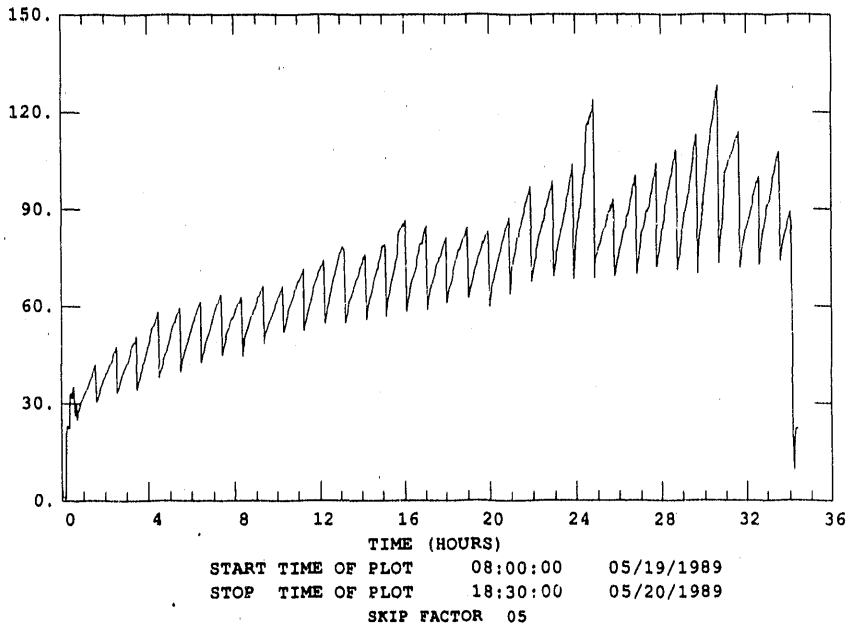

Figure 14. Pressure Drop Versus Time Signature for Candle Filter Test CF1

SLOT	UNITS	DESCRIPTION	# SAMPLES	MEAN	ST DEV	MIN - FREQ	MAX - FREQ
3103	SCFH	CANDLE FILTER HI FLOW	914	1204.514	155.469	0.000 09	1385.268 01

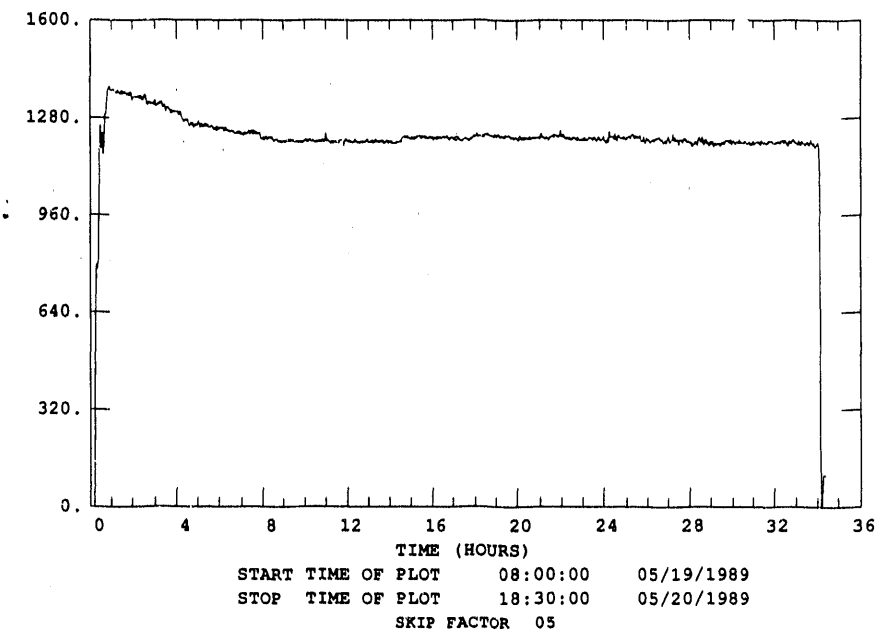

Figure 15. Filter Flow Rate Versus Time for Candle Filter Test CF1

SLOT	UNITS	DESCRIPTION	# SAMPLES	MEAN	ST DEV	MIN - FREQ	MAX - FREQ
3113	FT/M	CANDLE FILTER FACE VELOCITY	914	13.063	1.492	0.336 01	15.885 01

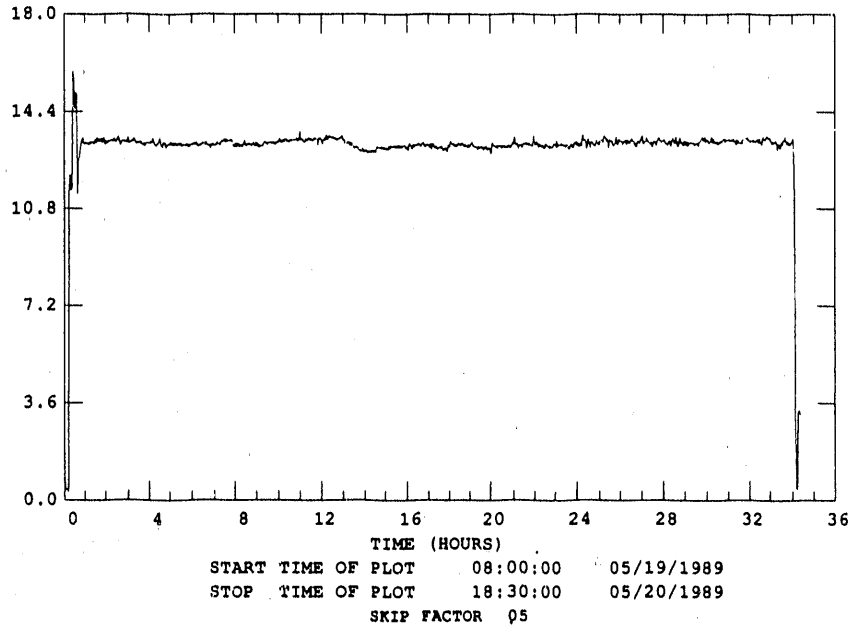

Figure 16. Filter Face Velocity Versus Time for Candle Filter Test CF1

	SLOT	UNITS	DESCRIPTION	# SAMPLES	MEAN	ST DEV	MIN - FREQ	MAX - FREQ
○	929	DEGF	CANDLE FILTER INLET	914	1293.414	45.478	1124.564 01	1355.734 01
□	930	DEGF	CANDLE FILTER TEMP.	914	1318.504	69.339	1113.660 01	1705.689 01
	958	DEGF	PATCH FILTER OUTLET	914	1242.998	279.011	-5332.644 01	1457.911 01

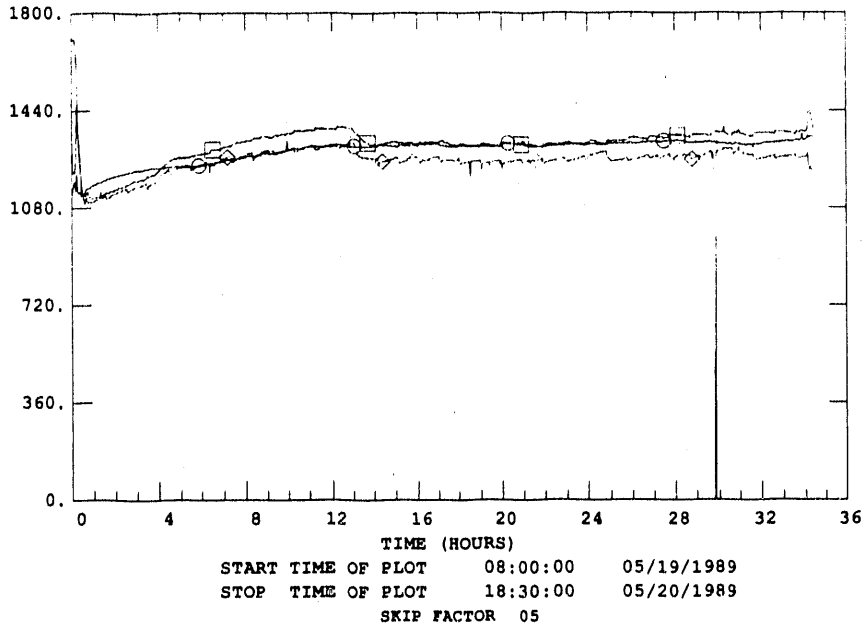

Figure 17. Filtrate Temperatures Versus Time for Candle Filter Test CF1

SLOT	UNITS	DESCRIPTION	# SAMPLES	MEAN	ST DEV	MIN - FREQ	MAX - FREQ
1004	PSIG	ISO #1 PRESS.	914	23.604	1.996	0.519 01	25.419 01

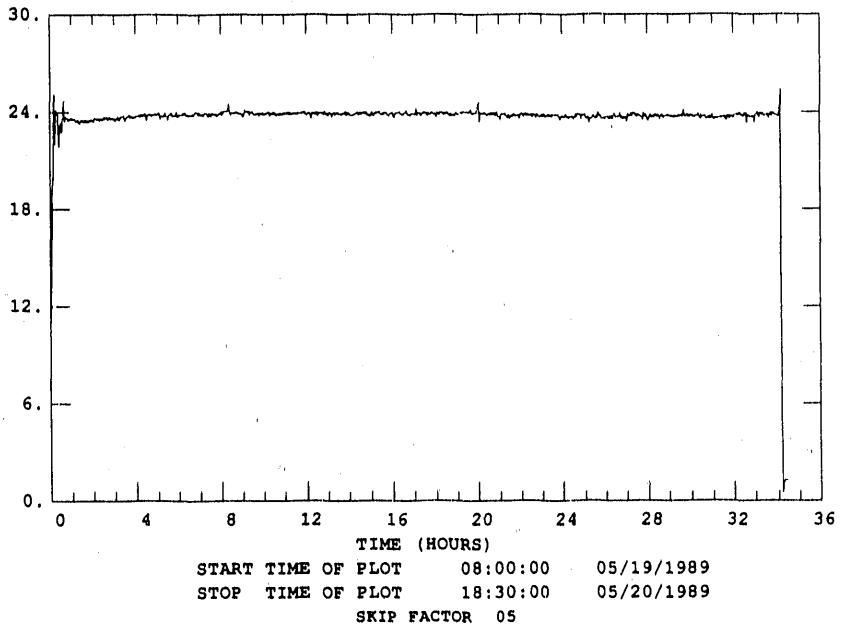

Figure 18. Candle Filter Vessel Pressure for Candle Filter Test CF1

SLOT	UNITS	DESCRIPTION	# SAMPLES	MEAN	ST DEV	MIN - FREQ	MAX - FREQ
985	"H2O	CANDLE FILTER DP	128	39.586	12.926	0.347 01	61.542 01

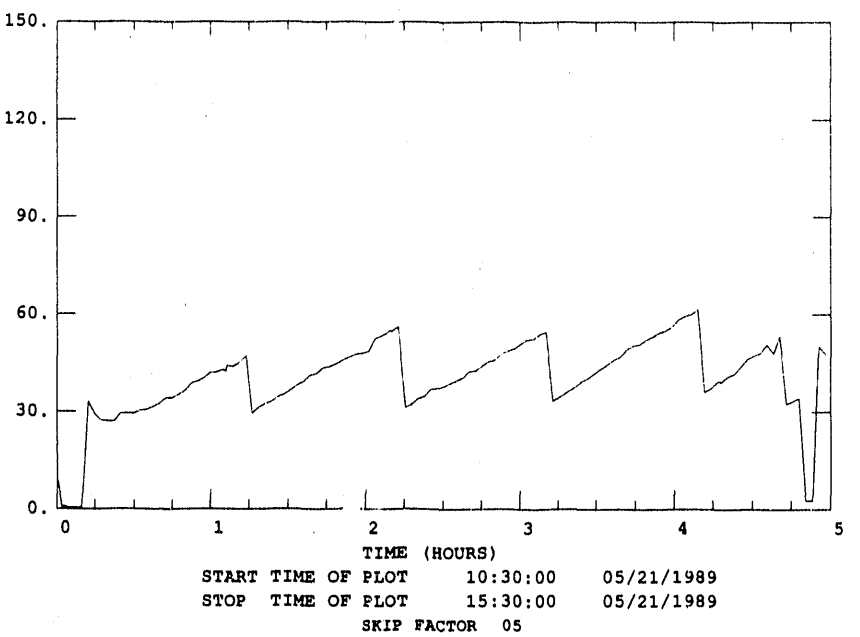

Figure 19. Pressure Drop Versus Time Signature for Candle Filter Test CF2

SLOT	UNITS	DESCRIPTION	# SAMPLES	MEAN	ST DEV	MIN - FREQ	MAX - FREQ
3103	SCFH	CANDLE FILTER HI FLOW	128	1204.772	342.416	0.000 08	1370.683 01

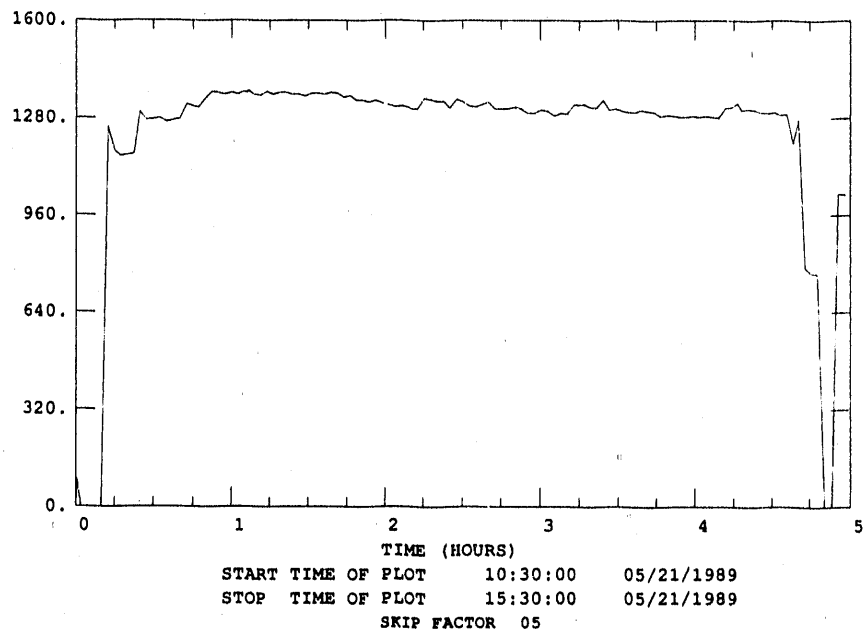

Figure 20. Filter Flow Rate Versus Time for Candle Filter Test CF2

SLOT	UNITS	DESCRIPTION	# SAMPLES	MEAN	ST DEV	MIN - FREQ	MAX - FREQ
3113	FT/M	CANDLE FILTER FACE VELOCITY	128	11.863	3.160	0.150 01	14.804 01

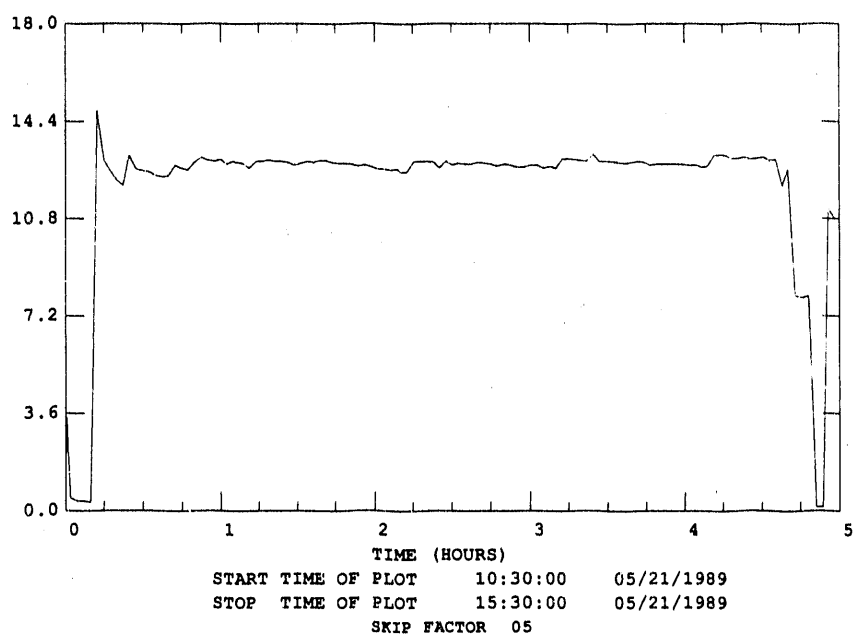

Figure 21. Filter Face Velocity Versus Time for Candle Filter Test CF2

	SLOT	UNITS	DESCRIPTION	# SAMPLES	MEAN	ST DEV	MIN - FREQ	MAX - FREQ
○	929	DEGF	CANDLE FILTER INLET	128	1207.024	34.334	1147.572 02	1311.083 01
□	930	DEGF	CANDLE FILTER TEMP.	128	1191.092	140.834	1092.260 03	1734.313 01
◇	958	DEGF	PATCH FILTER OUTLET	128	1185.025	54.356	969.749 01	1365.024 01

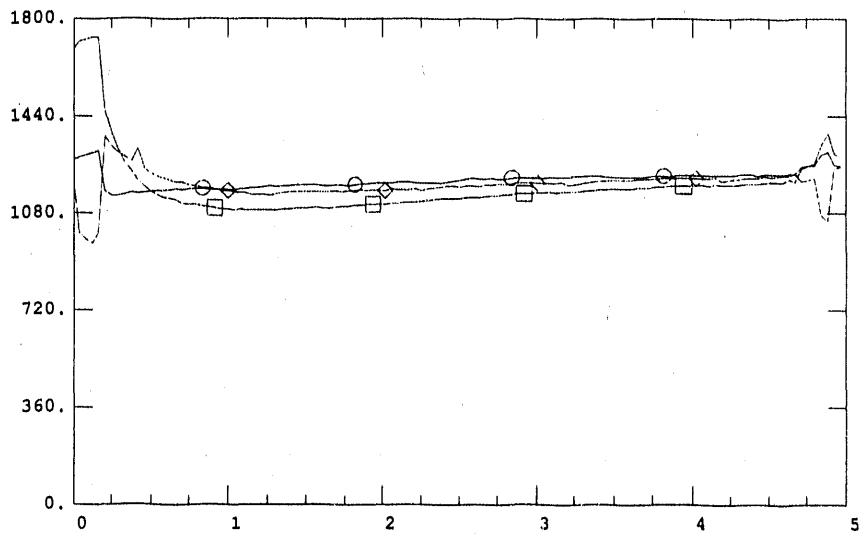

Figure 22. Filtrate Temperatures Versus Time for Candle Filter Test CF2

SLOT	UNITS	DESCRIPTION	# SAMPLES	MEAN	ST DEV	MIN - FREQ	MAX - FREQ
1004	PSIG	ISO #1 PRESS.	128	23.169	3.723	0.709 02	27.106 01

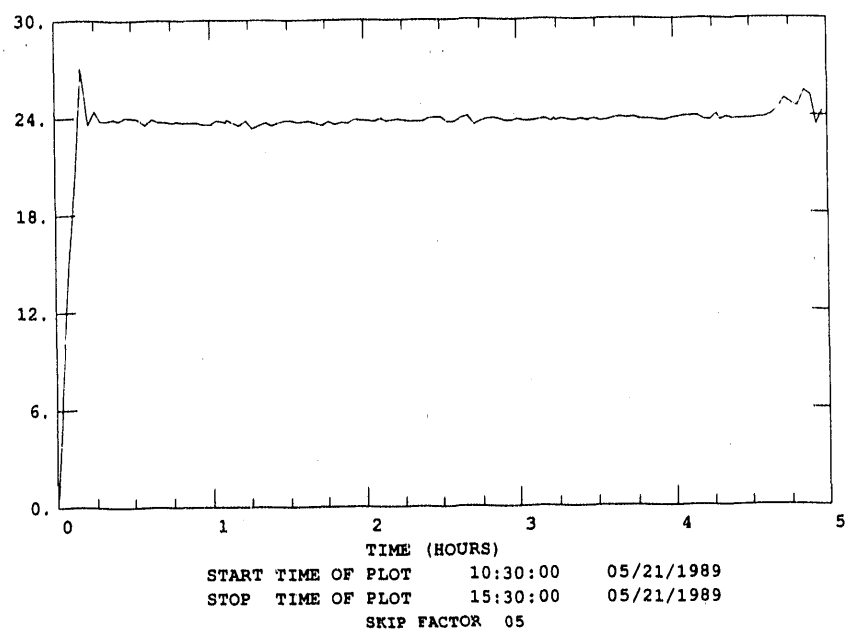

Figure 23. Candle Filter Vessel Pressure for Candle Filter Test CF2

SLOT	UNITS	DESCRIPTION	# SAMPLES	MEAN	ST DEV	MIN - FREQ	MAX - FREQ
985	"H2O	CANDLE FILTER DP	807	64.248	20.542	-2.033 01	109.432 01

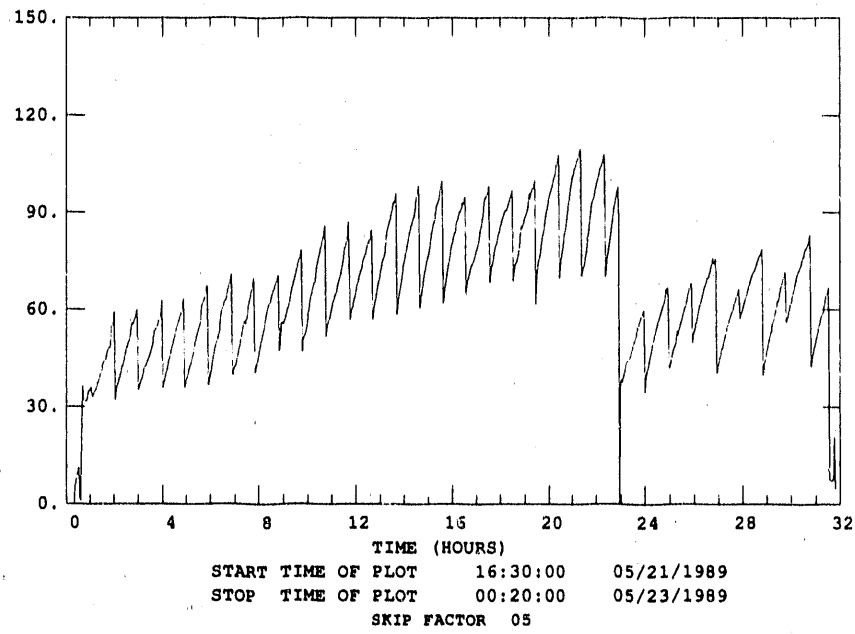

Figure 24. Pressure Drop Versus Time Signature for the Second Part of Candle Filter Test CF2

SLOT	UNITS	DESCRIPTION	# SAMPLES	MEAN	ST DEV	MIN - FREQ	MAX - FREQ
3103	SCFH	CANDLE FILTER HI FLOW	807	1197.816	213.888	0.000 22	1453.338 01

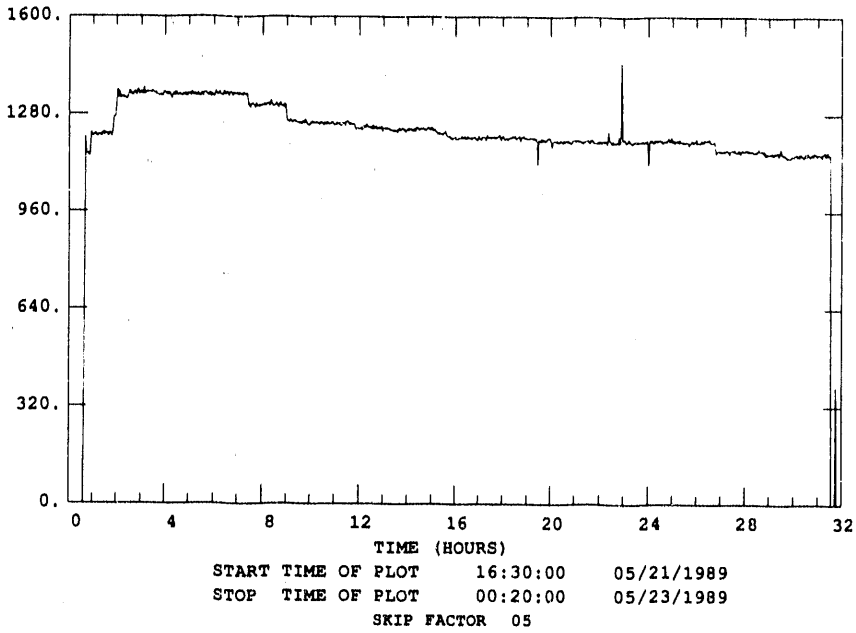

Figure 25. Filter Flow Rate Versus Time for the Second Part of Candle Filter Test CF2

SLOT	UNITS	DESCRIPTION	# SAMPLES	MEAN	ST DEV	MIN - FREQ	MAX - FREQ
3113	FT/M	CANDLE FILTER FACE VELOCITY	807	12.853	2.078	0.217 01	14.977 01

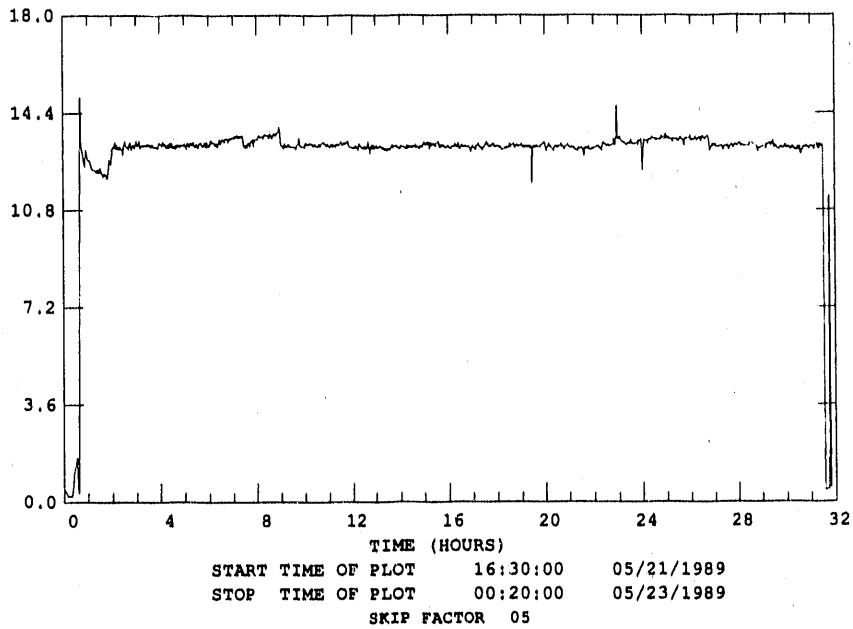

Figure 26. Filter Face Velocity Versus Time for the Second Part of Candle Filter Test CF2

	SLOT	UNITS	DESCRIPTION	# SAMPLES	MEAN	ST DEV	MIN - FREQ	MAX - FREQ
○	929	DEGF	CANDLE FILTER INLET	807	1264.925	23.571	1138.987 01	1402.784 01
□	930	DEGF	CANDLE FILTER TEMP.	807	1316.776	111.843	1137.665 01	1759.555 01
◇	958	DEGF	PATCH FILTER OUTLET	907	1267.408	83.249	907.775 01	1365.750 01

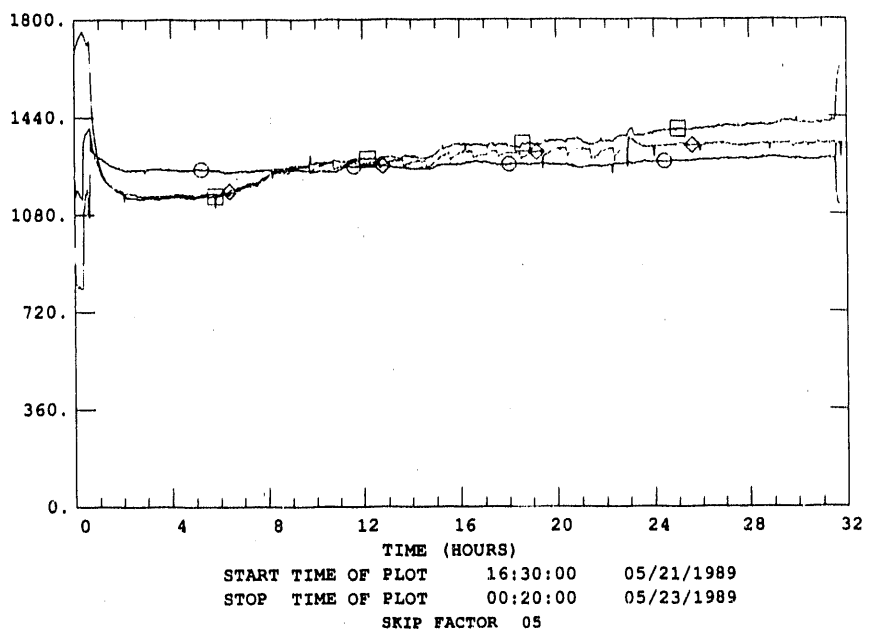

Figure 27. Filtrate Temperature Versus Time for the Second Part of Candle Filter Test CF2

SLOT	UNITS	DESCRIPTION	# SAMPLES	MEAN	ST DEV	MIN - FREQ	MAX - FREQ
1004	PSIG	ISO #1 PRESS.	807	23.442	3.196	0.302 01	27.793 01

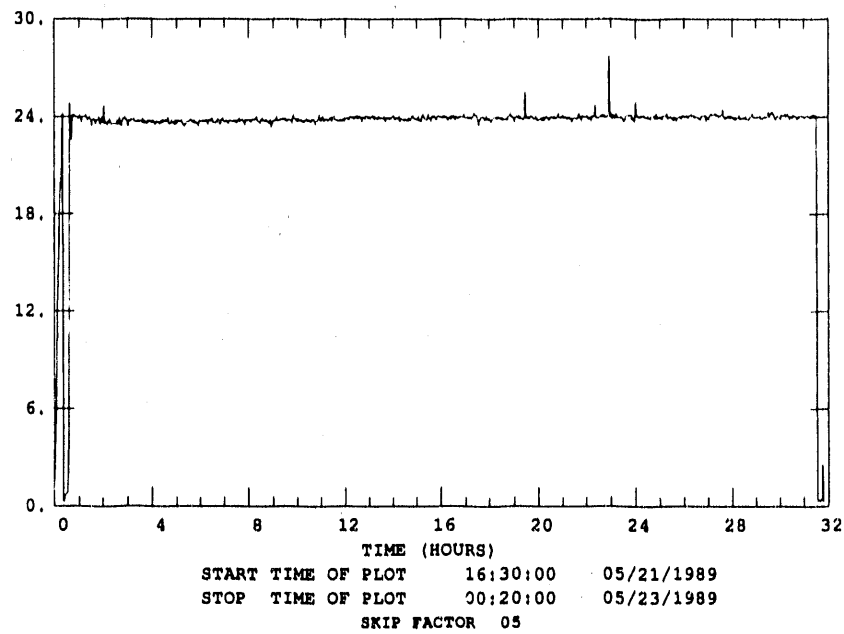

Figure 28. Candle Filter Vessel Pressure for the Second Part of Candle Filter Test CF2

SLOT	UNITS	DESCRIPTION	# SAMPLES	MEAN	ST DEV	MIN - FREQ	MAX - FREQ
985	"H2O	CANDLE FILTER DP	1490	90.042	22.069	0.624 01	133.611 01

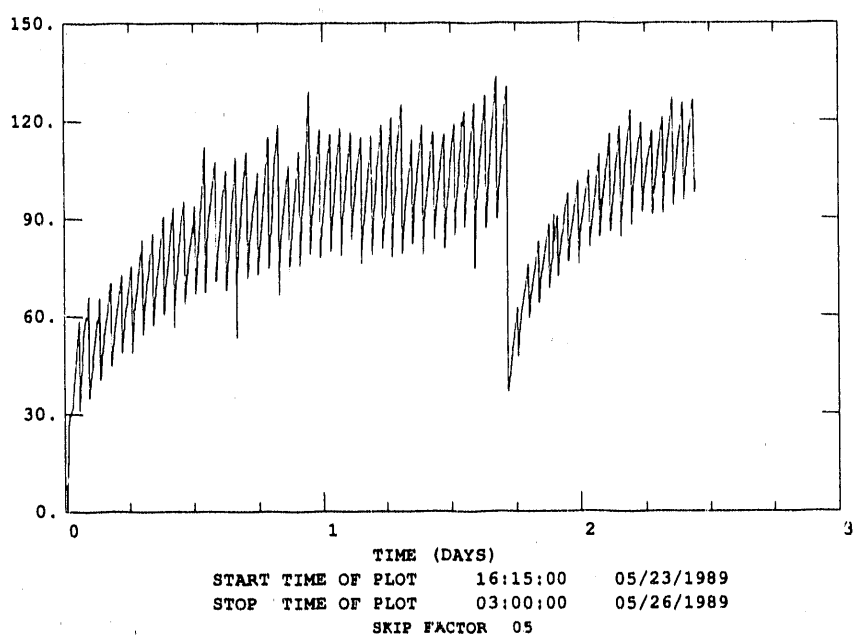

Figure 29. Pressure Drop Versus Time Signature for Candle Filter Test CF3

SLOT	UNITS	DESCRIPTION	# SAMPLES	MEAN	ST DEV	MIN - FREQ	MAX - FREQ
3103	SCFH	CANDLE FILTER HI FLOW	1490	1203.245	107.547	0.000 09	1412.323 01

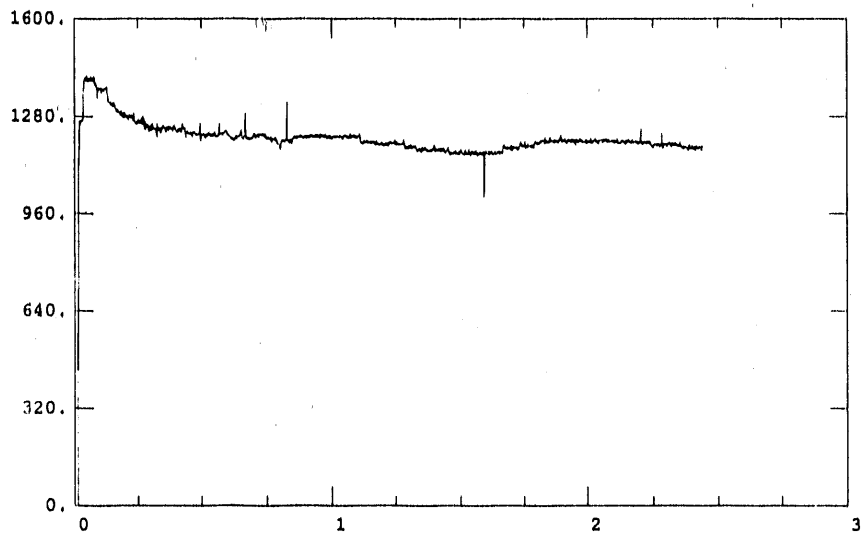

Figure 30. Filter Flow Rate Versus Time for Candle Filter Test CF3

SLOT	UNITS	DESCRIPTION	# SAMPLES	MEAN	ST DEV	MIN - FREQ	MAX - FREQ
3113	FT/M	CANDLE FILTER FACE VELOCITY	1490	13.198	0.965	0.328 01	13.889 01

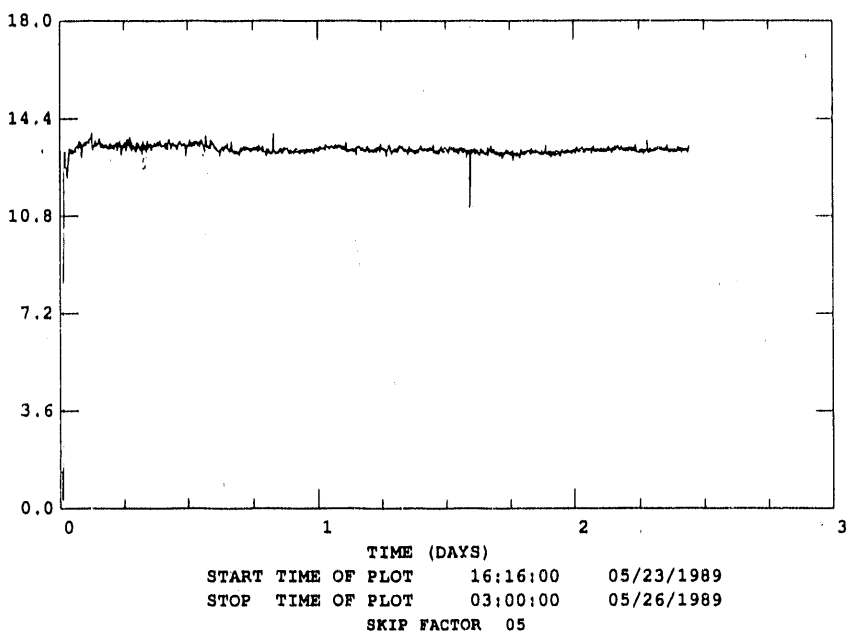

Figure 31. Filter Face Velocity Versus Time for Candle Filter Test CF3

SLOT	UNITS	DESCRIPTION	# SAMPLES	MEAN	ST DEV	MIN - FREQ	MAX - FREQ
929	DEGF	CANDLE FILTER INLET	1490	1292.734	35.272	1095.724 01	1347.256 01
930	DEGF	CANDLE FILTER TEMP.	1490	1335.443	70.167	1056.988 02	1697.098 01
959	DEGF	CANDLE FILTER OUTLET	1490	1307.270	42.761	1106.201 01	1478.036 01

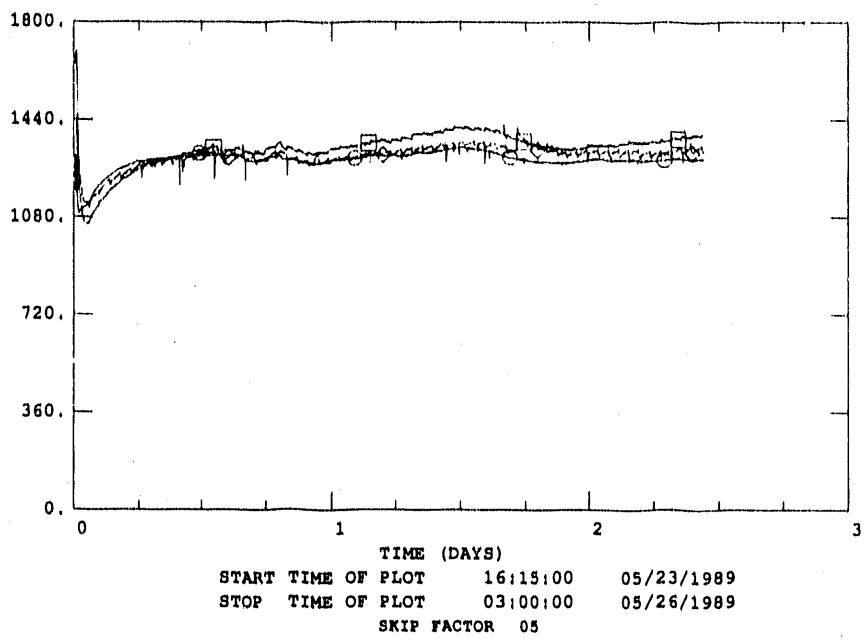

Figure 32. Filtrate Temperatures Versus Time for Candle Filter Test CF3

SLOT	UNITS	DESCRIPTION	# SAMPLES	MEAN	ST DEV	MIN - FREQ	MAX - FREQ
1004	PSIG	ISO #1 PRESS.	1490	23.525	1.604	0.552 01	26.294 01

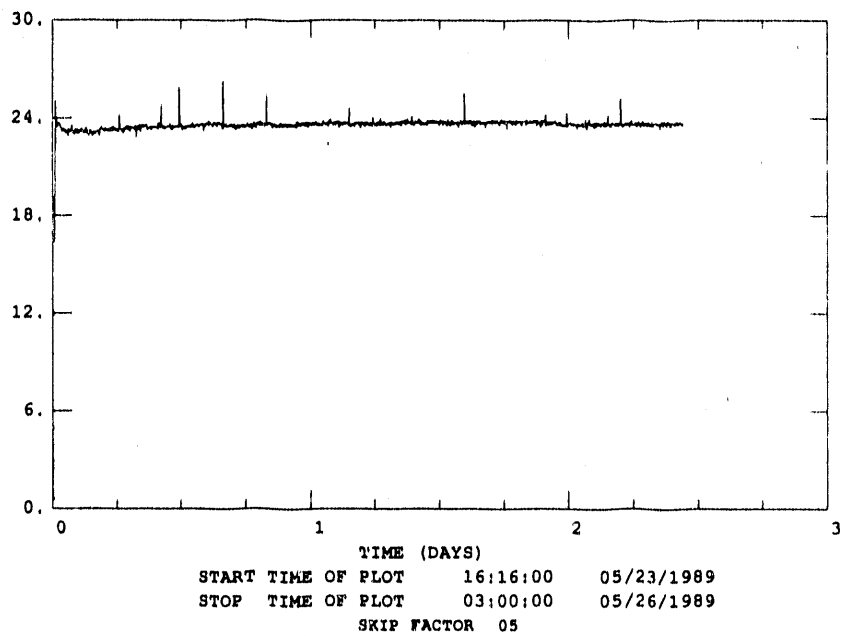

Figure 33. Candle Filter Vessel Pressure for Candle Filter Test CF3

Appendix C: Process Variable Plots for Disc-Filter Dust-Loading Tests DF2 Through DF11

Appendix C is the series of ADACS plots that illustrate process parameters during the dust loading period of the disc filter test series. The meaning of the top and bottom headers are the same as in Appendix B. The slot numbers are different; however, the same approach was used to analyze the data and evaluate K_2. The data for Disc Filter Test 1 (DF1) was lost because of a computer hardware problem. Also included here is Table 10 containing a laboratory analysis of the disc filter dust cakes.

Slot descriptions are as follows:

- PATCH FILTER DP -- Pressure drop across the disc filter.
- PATCH FILTER HIGH FLOW -- Total flow rate through the disc filter.
- PATCH FILTER FACE VELOCITY -- Filter face velocity, based on the vessel pressure, candle filter outlet temperature, flow rate, and filter area.
- PATCH FILTER OUTLET -- Temperature of the filtrate on the back side of the disc filter. (Note: In Figures 35, 38, 41, 44, 47, and 50, patch-filter outlet temperature is mistakenly referred to as candle-filter outlet temperature.)
- ISO #2 PRESSURE -- Disc filter vessel pressure.

Table 10. Laboratory Analysis of Disc-Filter Dust Cakes

Parameter	Sample Identification										
	DF1	DF2	DF3	DF4	DF5	DF6	DF7*	DF8	DF9	DF10	DF11
Mean Particle Size (by volume) (μm)	7.07	4.30	6.58	6.44	9.62	8.89		5.18	4.99	4.75	5.12
Mean Particle Size (by population) (μm)	3.58	2.05	2.11	2.18	3.31	3.25		2.50	2.44	2.41	2.51
Density (by helium) (g/cm^3)	2.71	2.68	2.72	2.81	2.80	2.76		2.74	2.74	2.66	2.69
BET** Surface Area (via nitrogen) (m^2/g)	2.37	2.94	4.84	2.65	2.28	3.15		3.20	2.86	3.36	3.15
Pore Volume, Adsorption (via nitrogen) (cm^3/g)	0.0053	0.0056	0.0090	0.0056	0.0046	0.0069		0.0063	0.0081	0.0061	0.0048
Ash (%)	97.38	98.63	96.00	96.78	96.42	95.64		97.50	98.48	99.37	96.54
Carbon (%)	0.65	0.57	1.36	1.24	1.65	1.45		0.57	0.57	0.22	1.55
Nitrogen (%)	0.09	< 0.01	< 0.01	< 0.01	0.01	0.03		< 0.01	0.02	< 0.01	0.03
Total Sulfur (%)	8.809	8.751	8.314	6.922	5.956	6.059		10.096	8.48	9.599	9.69
Sulfur (%)	5.83	5.79	5.85	5.24	4.99	4.37		6.70	5.60	6.48	6.17
Hydrogen (%)	0.03	0.18	0.04	0.06	0.02	0.12		0.01	0.01	0.09	0.06
Moisture (%)	0.12	0.18	0.08	0.24	0.14	0.11		0.48	0.24	0.22	0.18
K_2O (%)	2.165	2.362	2.079	1.815	1.781	1.820		2.105	2.13	2.197	2.06
SiO_2 (%)	38.0	37.1	38.5	39.0	39.5	40.1		34.9	35.0	35.2	35.6
Fe_2O_3 (%)	5.34	4.85	5.0	5.76	5.98	5.53		5.08	4.92	4.17	4.53
MgO (%)	2.107	2.132	2.191	2.298	2.327	2.459		1.512	--	1.594	--
ZnO (%)	0.0110	0.0153	0.0093	0.0086	0.0065	0.0100		0.0065	0.008	0.0085	0.008
SrO (%)	0.084	0.098	0.075	0.059	0.055	0.066		0.126	--	0.145	--
CaO (%)	15.368	15.095	16.514	19.045	18.840	19.501		12.516	13.07	12.407	14.86
P_2O_5 (%)	0.275	0.268	0.290	0.314	0.310	0.321		0.253	0.26	0.257	--
Al_2O_3 (%)	18.97	18.56	19.06	18.35	18.90	18.98		18.97	18.79	19.31	18.40
TiO_2 (%)	0.84	0.93	0.80	0.69	0.70	0.72		1.01	--	1.01	--
MnO (%)	0.014	0.010	0.002	0.017	0.017	0.000		0.007	0.00	0.000	0.005
Ash Fusion IT (°F)	2,145	--	2,150	2,280	2,305	2,190		2,175	2,245	2,190	2,195
Ash Fusion ST (°F)	2,210	--	2,310	2,375	2,380	2,290		2,260	2,340	2,350	2,295
Ash Fusion HT (°F)	2,230	--	2,330	2,420	2,400	2,310		2,285	2,380	2,390	2,315
Ash Fusion FT (°F)	2,290	--	2,375	2,485	2,475	2,405		2,390	2,500	2,460	2,410

* Sample DF7 lost.
** BET = Brunauer, Emmitt, Teller.

	SLOT	UNITS	DESCRIPTION	# SAMPLES	MEAN	ST DEV	MIN - FREQ	MAX - FREQ
○	994	"H2O	PATCH FILTER DP	114	24.534	6.445	4.002 01	33.814 01
□	3106	SCFH	PATCH FILTER HI FLOW	114	58.317	12.998	9.501 01	101.600 01
◇	3114	FT/M	PATCH FILTER FACE VELOCITY	114	6.191	5.411	1.104 01	12.947 01

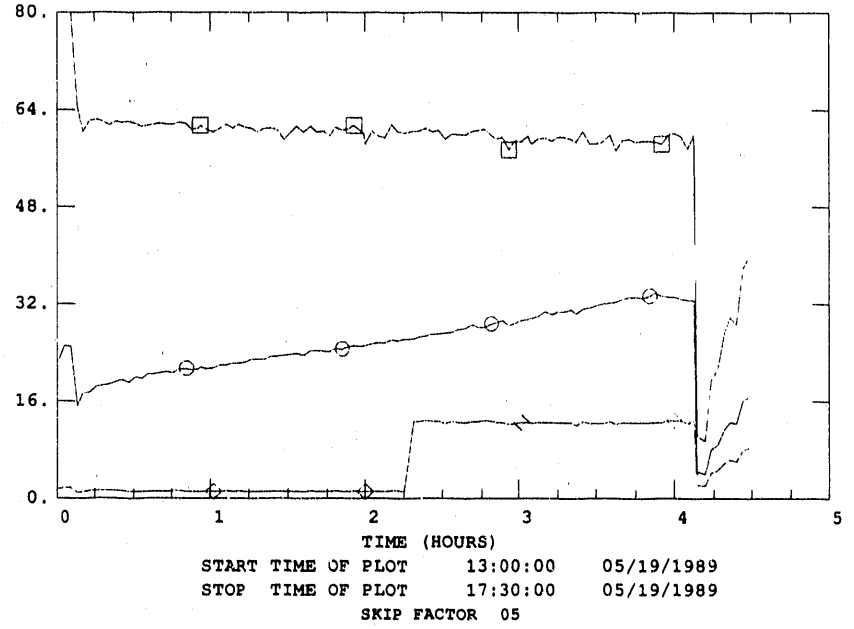

Figure 34. Pressure Drop, Flow Rate, and Face Velocity During Disc Filter Test DF2

SLOT	UNITS	DESCRIPTION	# SAMPLES	MEAN	ST DEV	MIN - FREQ	MAX - FREQ
957	DEGF	CANDLE FILTER OUTLET	114	1313.072	26.089	1237.951 01	1345.288 01

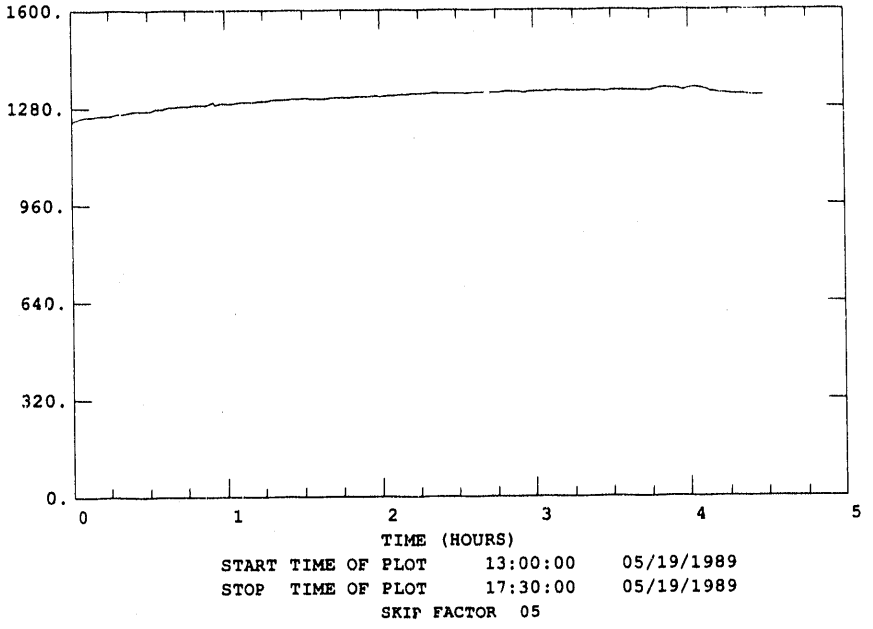

Figure 35. Disc Filter Outlet Temperature During Disc Filter Test DF2

SLOT	UNITS	DESCRIPTION	# SAMPLES	MEAN	ST DEV	MIN - FREQ	MAX - FREQ
1005	PSIG	ISO #2 PRESS.	114	24.068	1.153	22.420 01	32.167 01

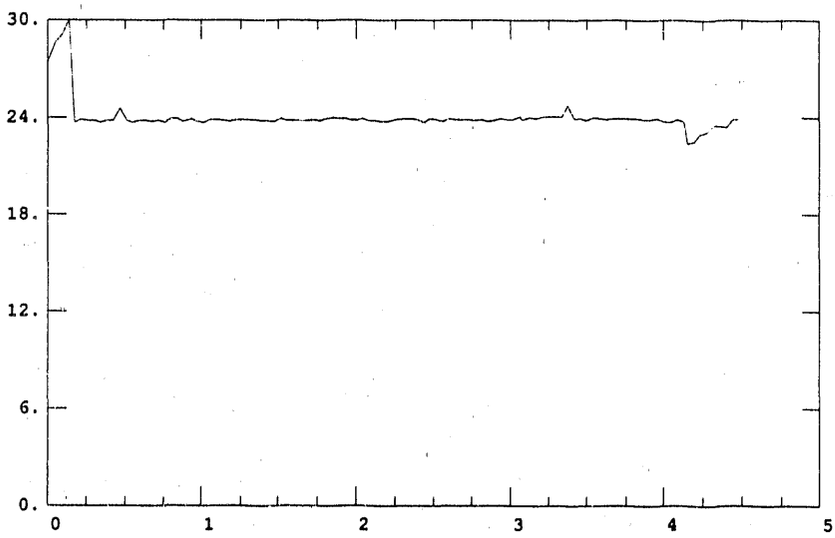

Figure 36. Disc Filter Vessel Pressure During Disc Filter Test DF2

SLOT	UNITS	DESCRIPTION	# SAMPLES	MEAN	ST DEV	MIN - FREQ	MAX - FREQ
994	"H2O	PATCH FILTER DP	362	47.478	21.181	1.083 01	94.250 01
3106	SCFH	PATCH FILTER HI FLOW	362	64.901	8.000	6.124 01	92.016 01
3114	FT/M	PATCH FILTER FACE VELOCITY	362	13.753	4.245	-38.500 01	29.999 01

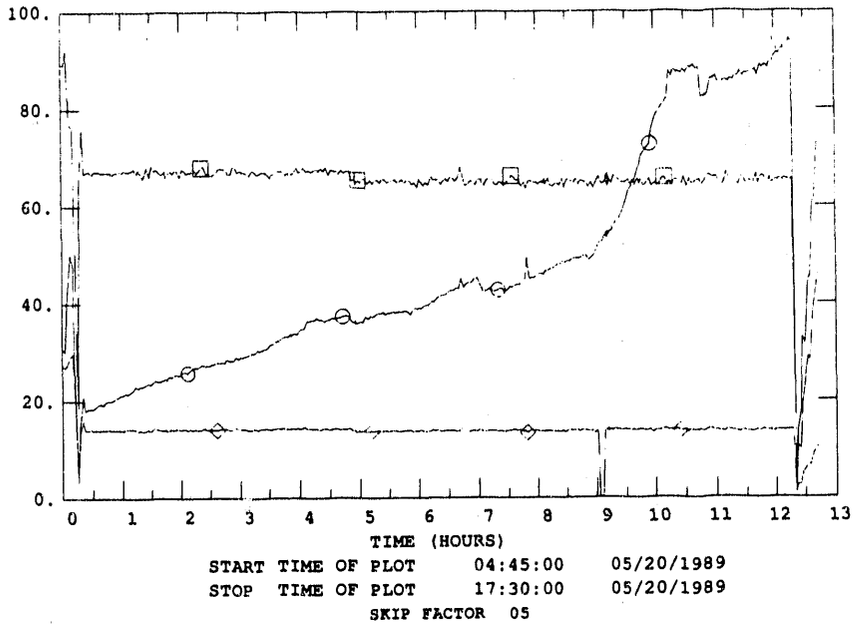

Figure 37. Pressure Drop, Flow Rate, and Face Velocity During Disc Filter Test DF3

SLOT	UNITS	DESCRIPTION	# SAMPLES	MEAN	ST DEV	MIN - FREQ	MAX - FREQ
957	DEGF	CANDLE FILTER OUTLET	362	1180.005	9.875	1147.687 01	1193.370 01

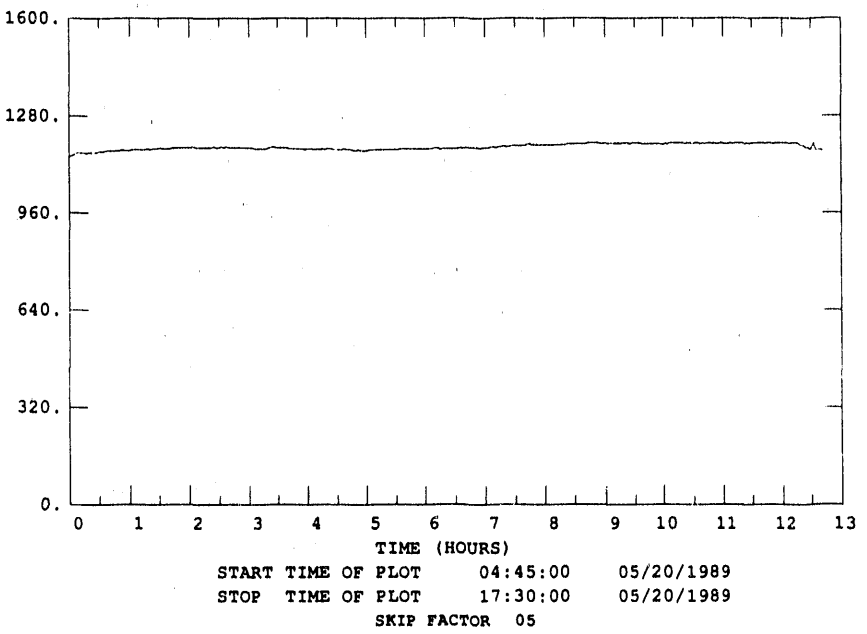

Figure 38. Disc Filter Outlet Temperature During Disc Filter Test DF3

SLOT	UNITS	DESCRIPTION	# SAMPLES	MEAN	ST DEV	MIN - FREQ	MAX - FREQ
1005	PSIG	ISO #2 PRESS.	362	23.317	2.105	5.955 01	29.480 01

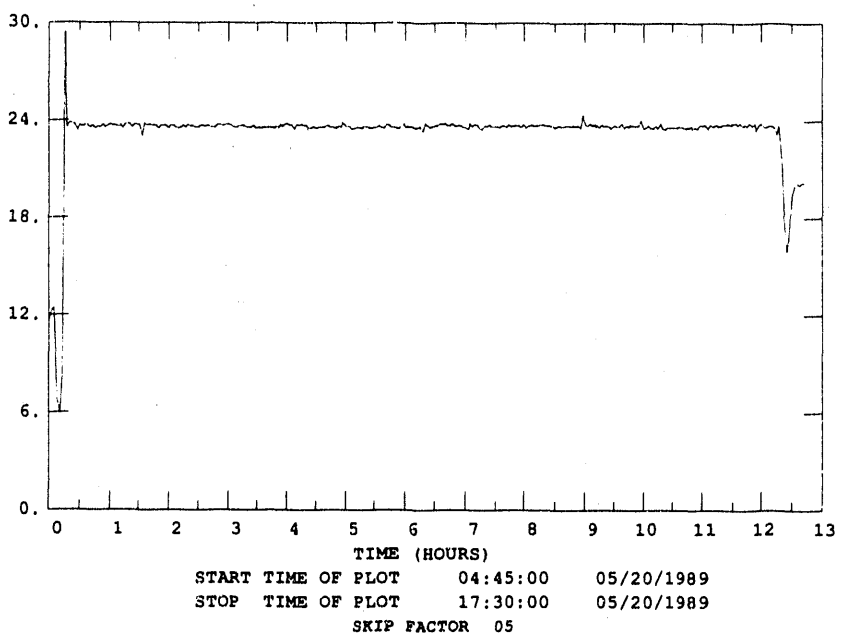

Figure 39. Disc Filter Pressure During Disc Filter Test DF3

SLOT	UNITS	DESCRIPTION	# SAMPLES	MEAN	ST DEV	MIN - FREQ	MAX - FREQ
994	"H2O	PATCH FILTER DP	19	12.570	8.393	-0.965 01	20.489 01
3106	SCFH	PATCH FILTER HI FLOW	19	43.114	25.833	6.863 01	63.732 01
3114	FT/M	PATCH FILTER FACE VELOCITY	19	8.743	5.155	1.204 01	12.831 01

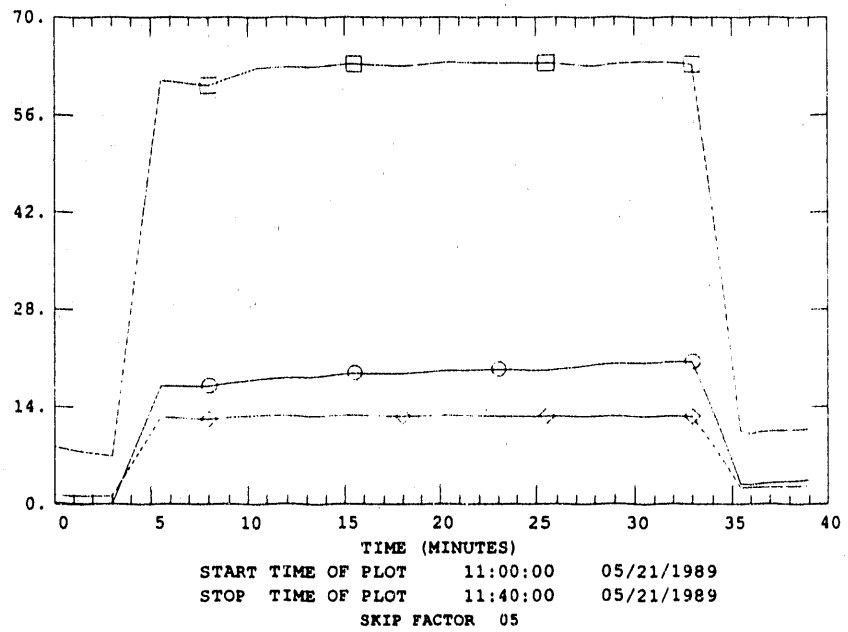

Figure 40. Pressure Drop, Flow Rate, and Face Velocity During Disc Filter Test DF4

SLOT	UNITS	DESCRIPTION	# SAMPLES	MEAN	ST DEV	MIN - FREQ	MAX - FREQ
957	DEGF	CANDLE FILTER OUTLET	63	1188.253	7.367	1172.400 01	1199.645 01

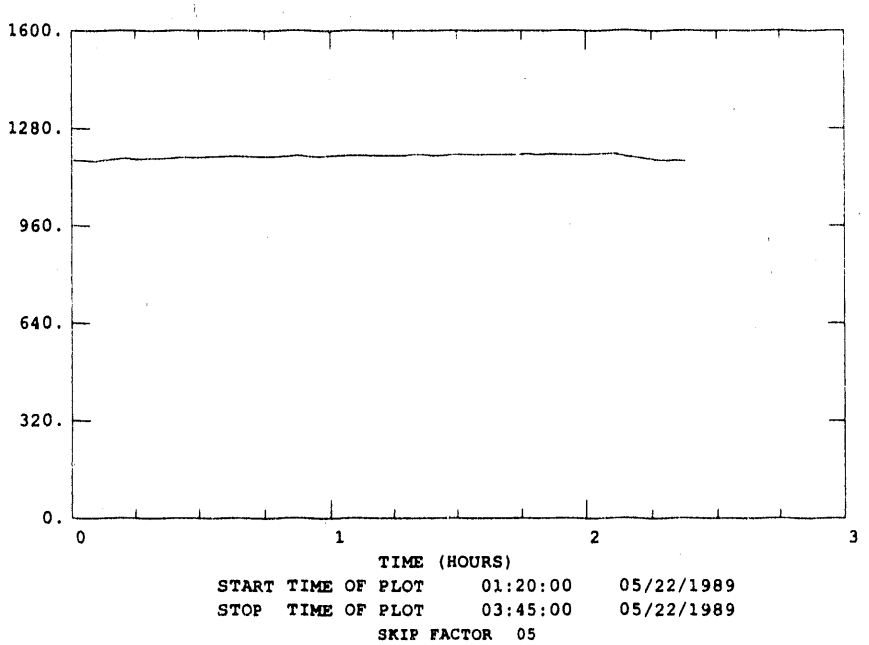

Figure 41. Disc Filter Outlet Temperature During Disc Filter Test DF4

SLOT	UNITS	DESCRIPTION	# SAMPLES	MEAN	ST DEV	MIN - FREQ	MAX - FREQ
1005	PSIG	ISO #2 PRESS.	19	23.495	4.149	15.671 01	31.542 01

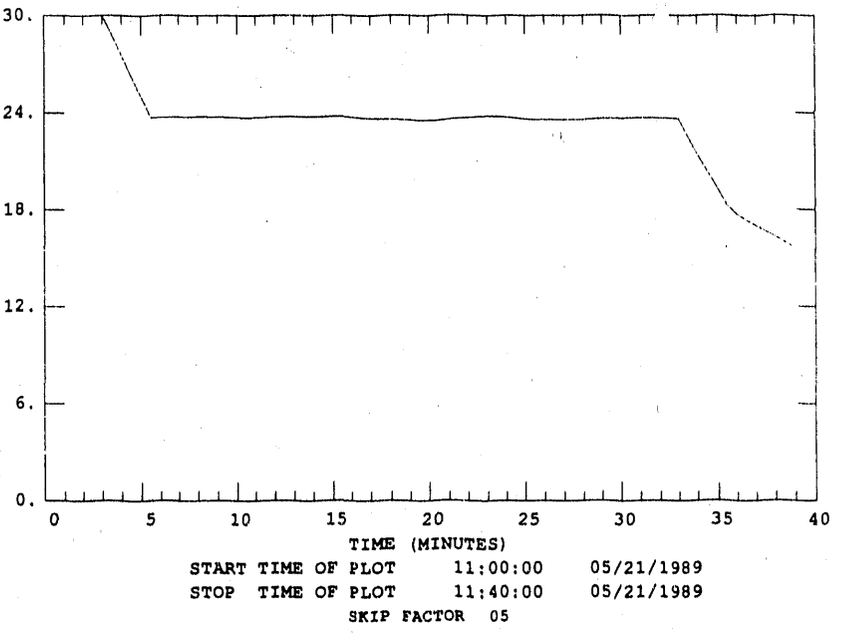

Figure 42. Disc Filter Vessel Pressure During Disc Filter Test DF4

SLOT	UNITS	DESCRIPTION	# SAMPLES	MEAN	ST DEV	MIN - FREQ	MAX - FREQ
994	"H2O	PATCH FILTER DP	23	12.617	5.017	2.789 01	17.878 01
3106	SCFH	PATCH FILTER HI FLOW	23	47.052	20.614	10.228 01	65.071 01
3114	FT/M	PATCH FILTER FACE VELOCITY	23	9.777	3.764	2.455 01	12.313 01

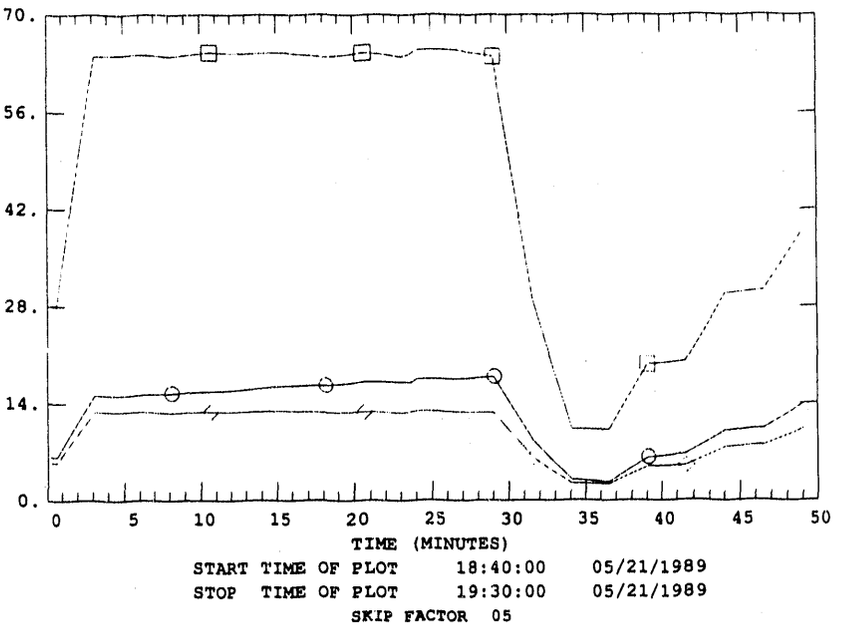

Figure 43. Pressure Drop, Flow Rate, and Face Velocity During Disc Filter Test DF5

SLOT	UNITS	DESCRIPTION	# SAMPLES	MEAN	ST DEV	MIN - FREQ	MAX - FREQ
957	DEGF	CANDLE FILTER OUTLET	23	1206.635	4.976	1197.441 02	1215.432 01

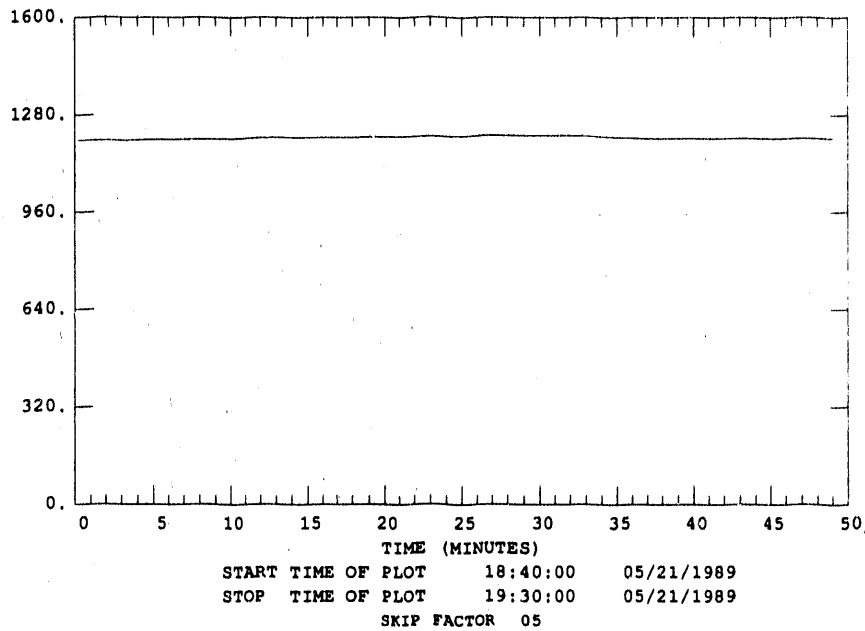

Figure 44. Disc Filter Outlet Temperature During Disc Filter Test DF5

SLOT	UNITS	DESCRIPTION	# SAMPLES	MEAN	ST DEV	MIN - FREQ	MAX - FREQ
1005	PSIG	ISO #2 PRESS.	23	20.998	3.918	13.890 01	23.982 01

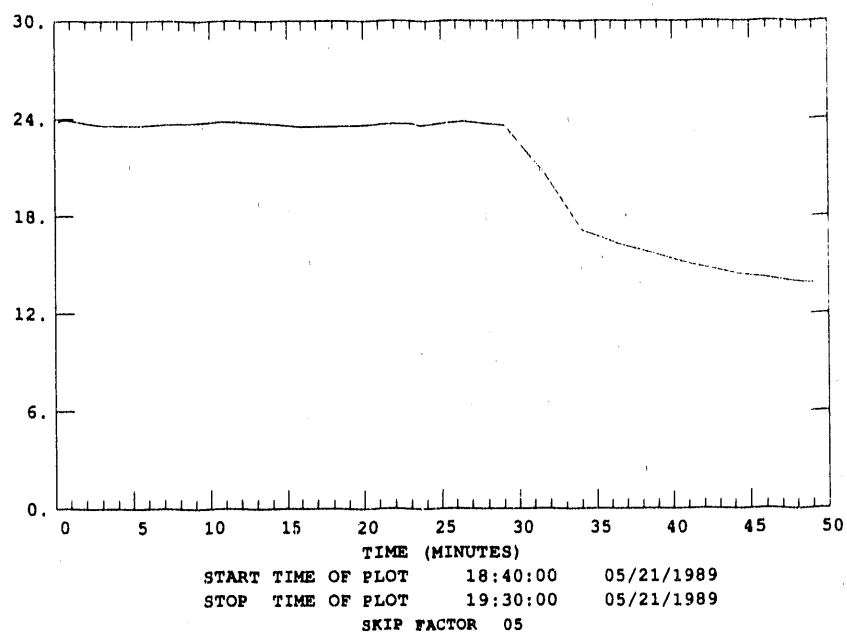

Figure 45. Disc Filter Vessel Pressure During Disc Filter Test DF5

	SLOT	UNITS	DESCRIPTION	# SAMPLES	MEAN	ST DEV	MIN - FREQ	MAX - FREQ
O	994	"H2O	PATCH FILTER DP	63	19.570	7.041	5.118 01	30.143 01
□	3106	SCFH	PATCH FILTER HI FLOW	63	55.941	15.064	8.851 01	66.328 01
◇	3114	FT/M	PATCH FILTER FACE VELOCITY	63	12.187	3.372	2.060 01	14.466 01

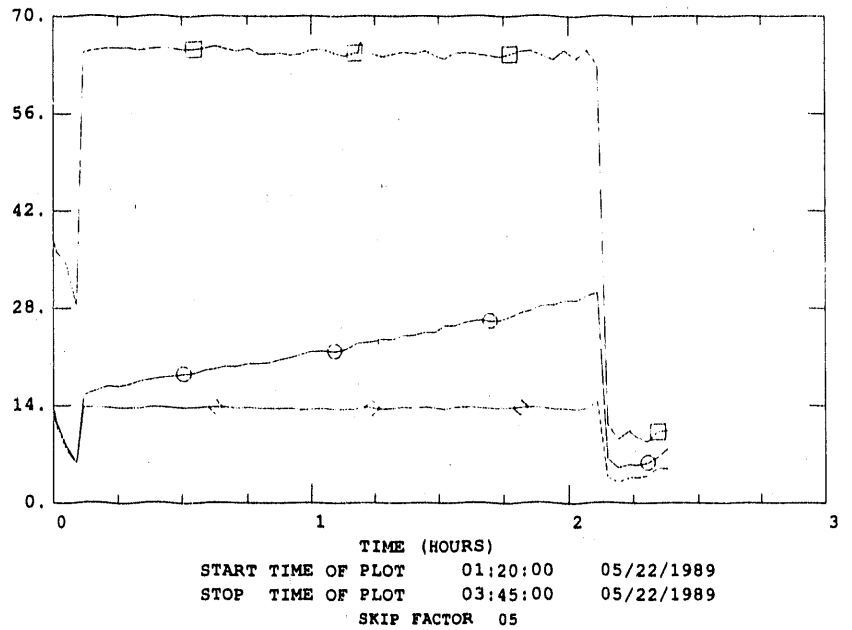

Figure 46. Pressure Drop, Flow Rate, and Face Velocity During Disc Filter Test DF6

SLOT	UNITS	DESCRIPTION	# SAMPLES	MEAN	ST DEV	MIN - FREQ	MAX - FREQ
957	DEGF	CANDLE FILTER OUTLET	63	1188.253	7.367	1172.400 01	1199.645 01

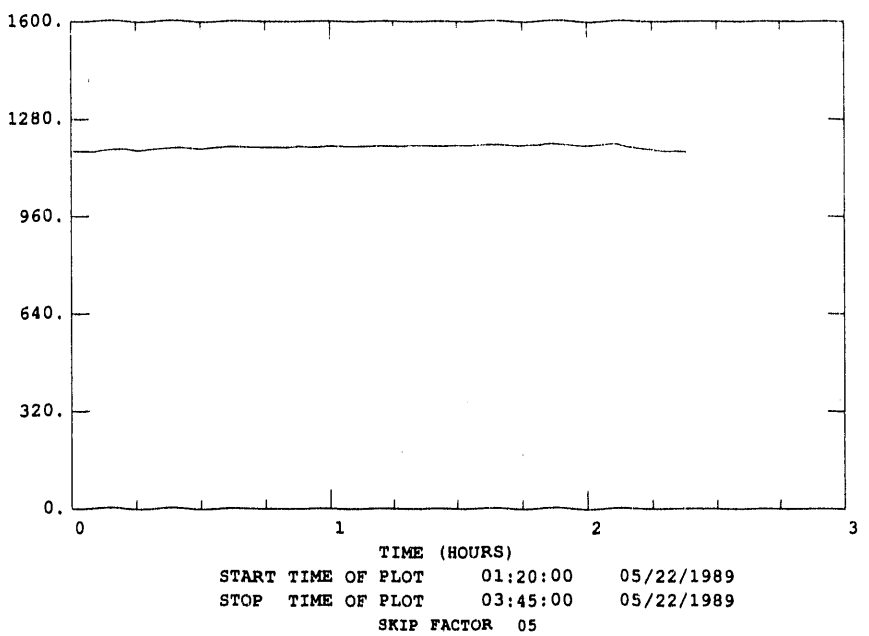

Figure 47. Disc Filter Outlet Temperature During Disc Filter Test DF6

SLOT	UNITS	DESCRIPTION	# SAMPLES	MEAN	ST DEV	MIN - FREQ	MAX - FREQ
1005	PSIG	ISO #2 PRESS.	63	11.001	6.325	1.487 01	24.669 01

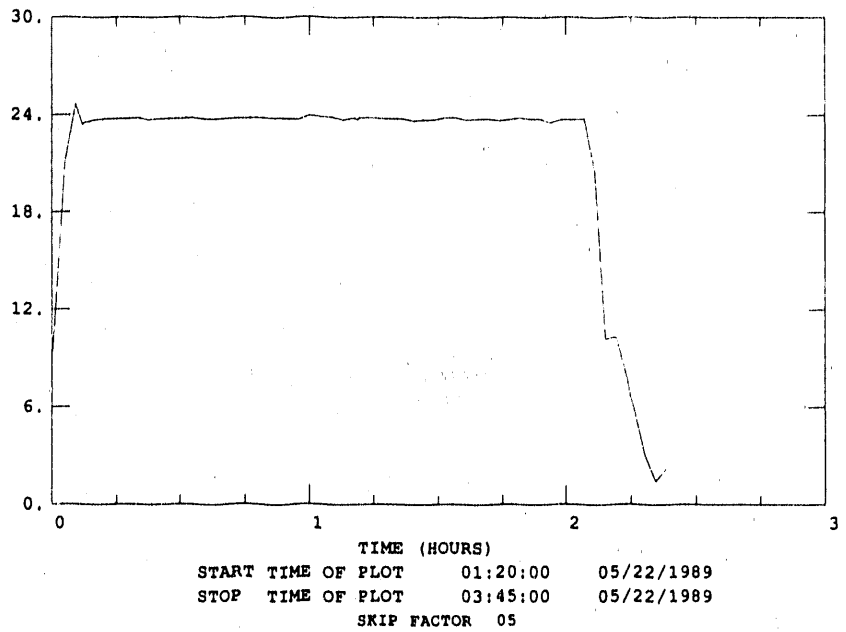

Figure 48. Disc Filter Vessel Pressure During Disc Filter Test DF6

SLOT	UNITS	DESCRIPTION	# SAMPLES	MEAN	ST DEV	MIN - FREQ	MAX - FREQ
994	"H2O	PATCH FILTER DP	108	25.863	7.640	4.097 01	36.800 01
3106	SCFH	PATCH FILTER HI FLOW	108	62.581	10.906	3.952 01	79.798 01
3114	FT/M	PATCH FILTER FACE VELOCITY	108	13.500	2.291	2.611 01	16.737 01

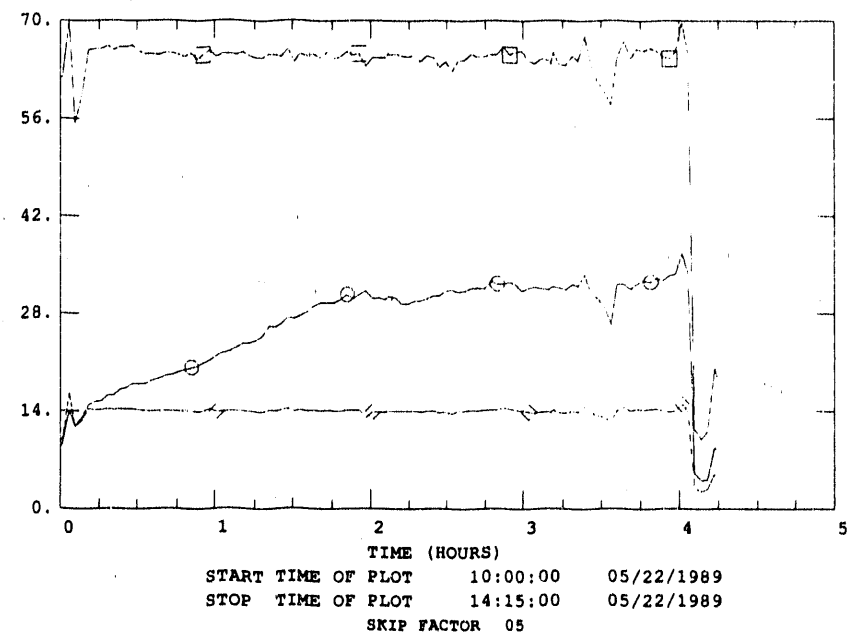

Figure 49. Pressure Drop, Flow Rate, and Face Velocity During Disc Filter Test DF7

SLOT	UNITS	DESCRIPTION	# SAMPLES	MEAN	ST DEV	MIN - FREQ	MAX - FREQ
957	DEGF	CANDLE FILTER OUTLET	108	1164.590	19.358	1068.983 01	1185.527 01

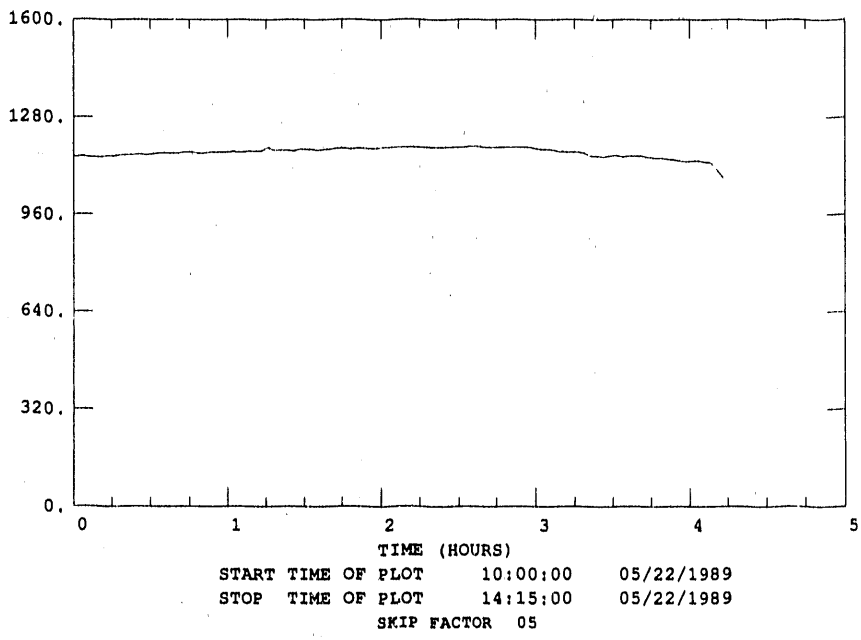

Figure 50. Disc Filter Outlet Temperature During Disc Filter Test DF7

SLOT	UNITS	DESCRIPTION	# SAMPLES	MEAN	ST DEV	MIN - FREQ	MAX - FREQ
1005	PSIG	ISO #2 PRESS.	108	23.833	2.332	16.897 01	37.602 01

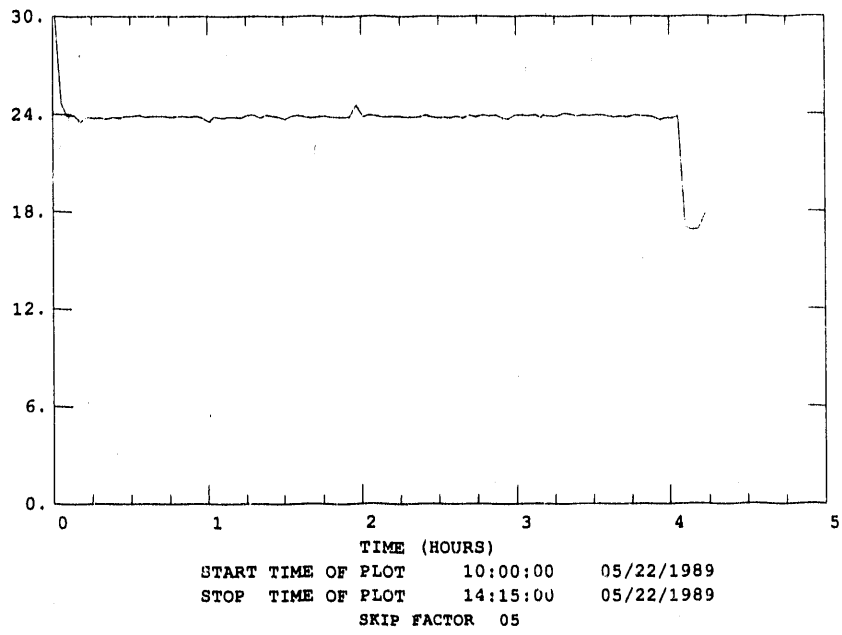

Figure 51. Disc Filter Vessel Pressure During Disc Filter Test DF7

SLOT	UNITS	DESCRIPTION	# SAMPLES	MEAN	ST DEV	MIN - FREQ	MAX - FREQ
994	"H2O	PATCH FILTER DP	213	32.898	9.426	-0.122 01	44.298 01
3106	SCFM	PATCH FILTER HI FLOW	213	62.741	11.686	0.753 01	103.496 01
3114	FT/M	PATCH FILTER FACE VELOCITY	212	17.311	2.356	1.340 01	28.633 01

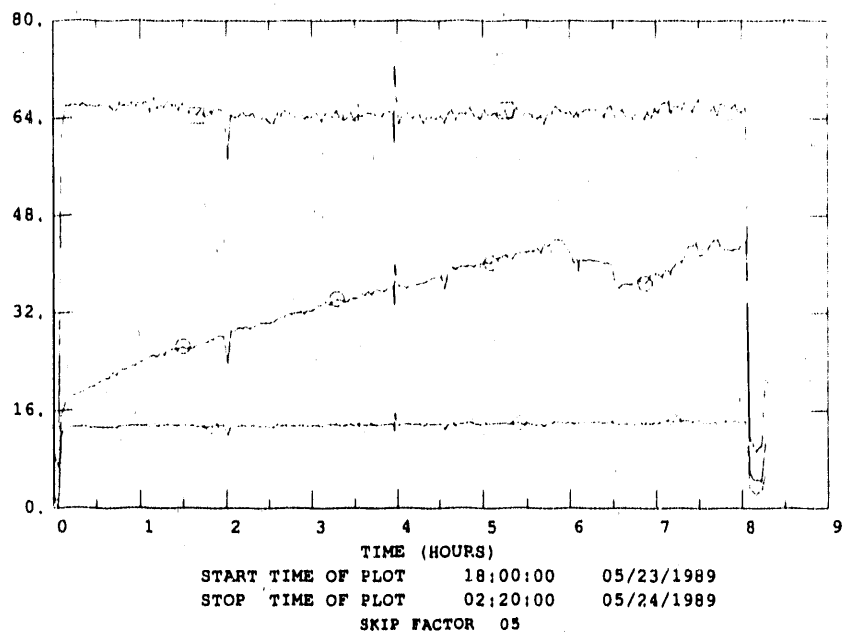

Figure 52. Pressure Drop, Flow Rate, and Face Velocity During Disc Filter Test DF8

SLOT	UNITS	DESCRIPTION	# SAMPLES	MEAN	ST DEV	MIN - FREQ	MAX - FREQ
957	DEGF	PATCH FILTER OUTLET	213	1185.329	16.086	1138.268 01	1203.213 01

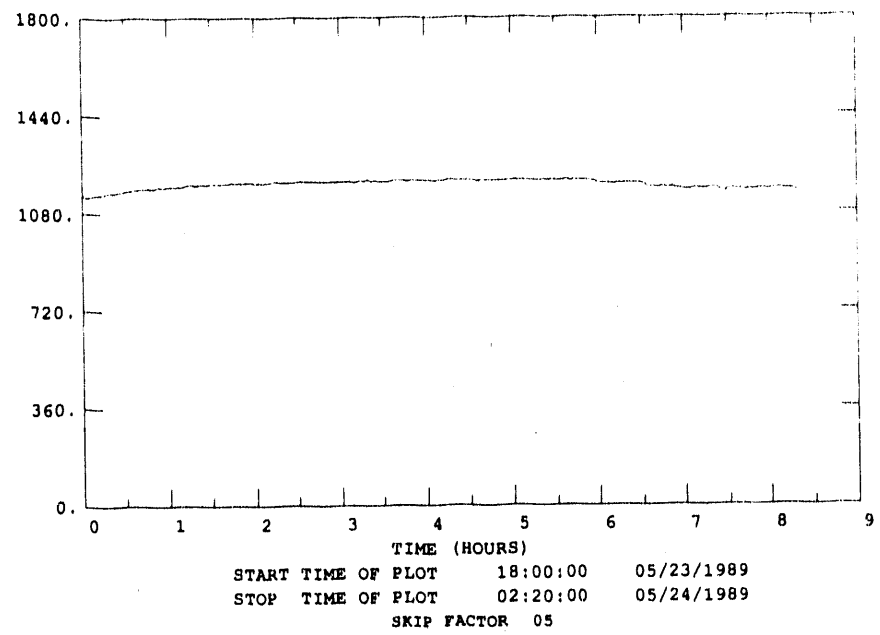

Figure 53. Disc Filter Outlet Temperature During Disc Filter Test DF8

SLOT	UNITS	DESCRIPTION	# SAMPLES	MEAN	ST DEV	MIN - FREQ	MAX - FREQ
1005	PSIG	ISO #2 PRESS.	213	23.083	1.453	15.296 01	24.326 01

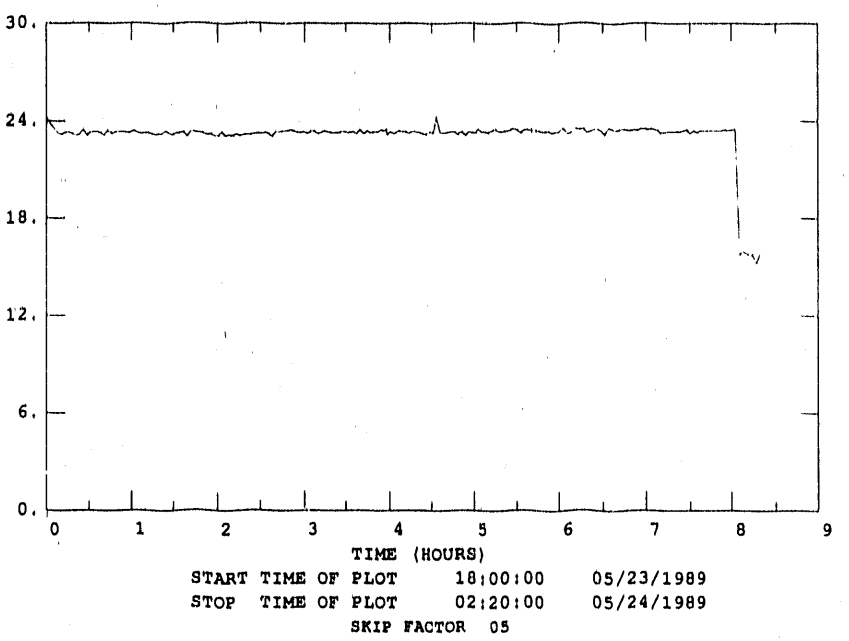

Figure 54. Disc Filter Vessel Pressure During Disc Filter Test DF8

	SLOT	UNITS	DESCRIPTION	# SAMPLES	MEAN	ST DEV	MIN - FREQ	MAX - FREQ
○	994	"H2O	PATCH FILTER DP	185	21.759	5.780	-0.501 02	30.989 01
□	3106	SCFH	PATCH FILTER HI FLOW	185	61.591	10.674	5.535 01	105.151 01
·	3114	FT/M	PATCH FILTER FACE VELOCITY	185	13.308	2.172	1.387 01	20.558 01

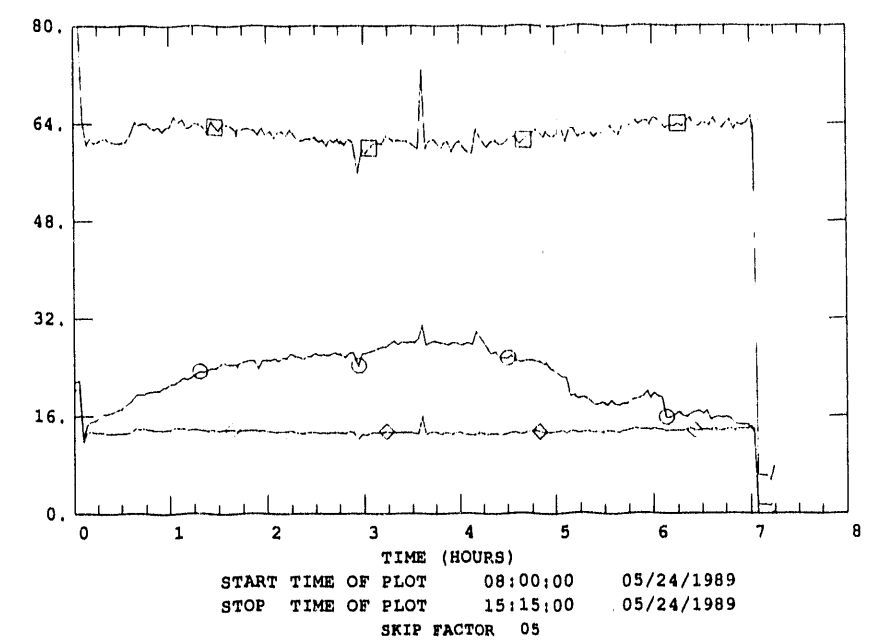

Figure 55. Pressure Drop, Flow Rate, and Face Velocity During Disc Filter Test DF9

SLOT	UNITS	DESCRIPTION	# SAMPLES	MEAN	ST DEV	MIN - FREQ	MAX - FREQ
957	DEGF	PATCH FILTER OUTLET	185	1181.236	37.895	1102.282 01	1232.137 01

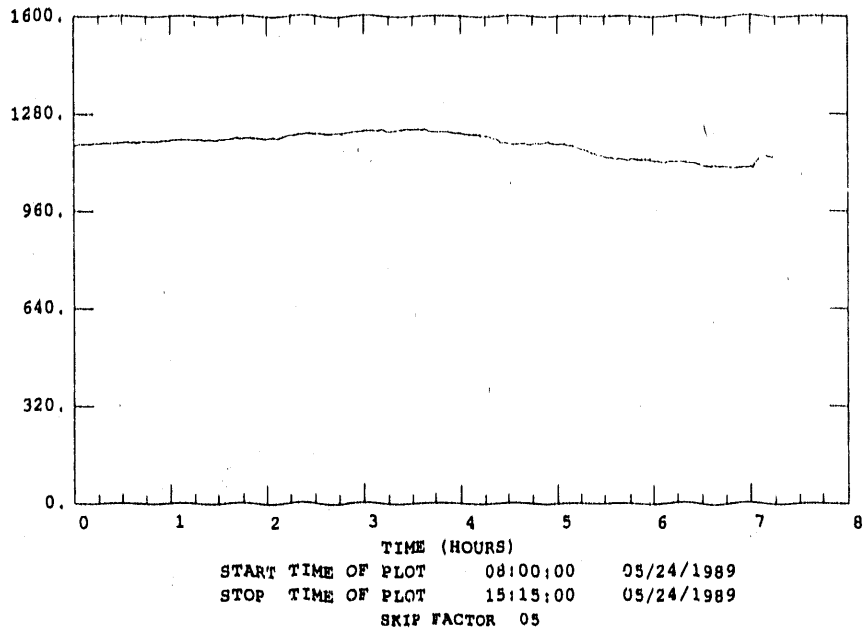

Figure 56. Disc Filter Outlet Temperature During Disc Filter Test DF9

SLOT	UNITS	DESCRIPTION	# SAMPLES	MEAN	ST DEV	MIN - FREQ	MAX - FREQ
A005	PSIG	ISO #2 PRESS.	185	23.549	1.061	17.109 01	31.042 01

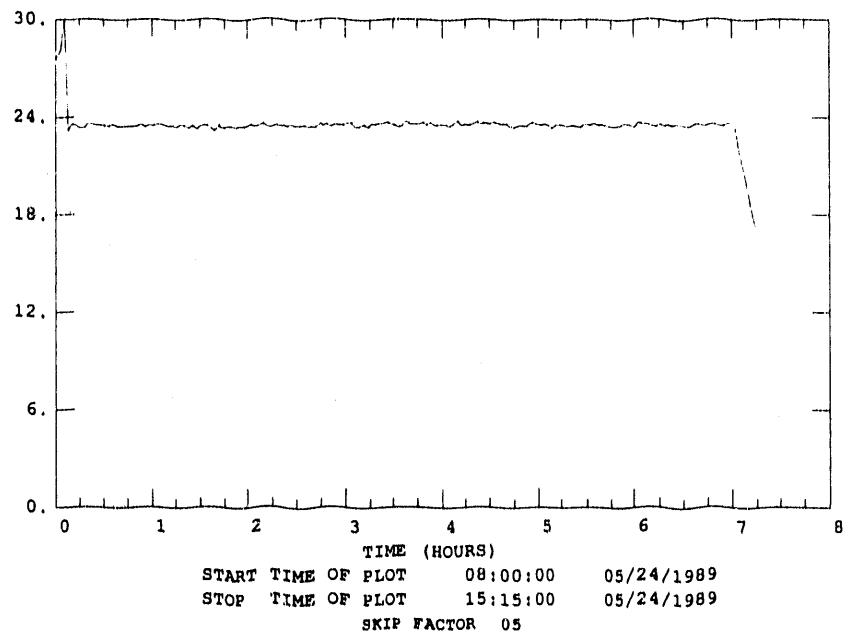

Figure 57. Disc Filter Vessel Pressure During Disc Filter Test DF9

SLOT	UNITS	DESCRIPTION	# SAMPLES	MEAN	ST DEV	MIN - FREQ	MAX - FREQ
994	"H2O	PATCH FILTER DP	367	35.923	10.484	0.184 01	51.985 01
3106	SCFM	PATCH FILTER HI FLOW	367	44.078	8.096	6.821 01	107.429 01
3114	FT/M	PATCH FILTER FACE VELOCITY	367	14.219	1.782	1.839 01	26.981 01

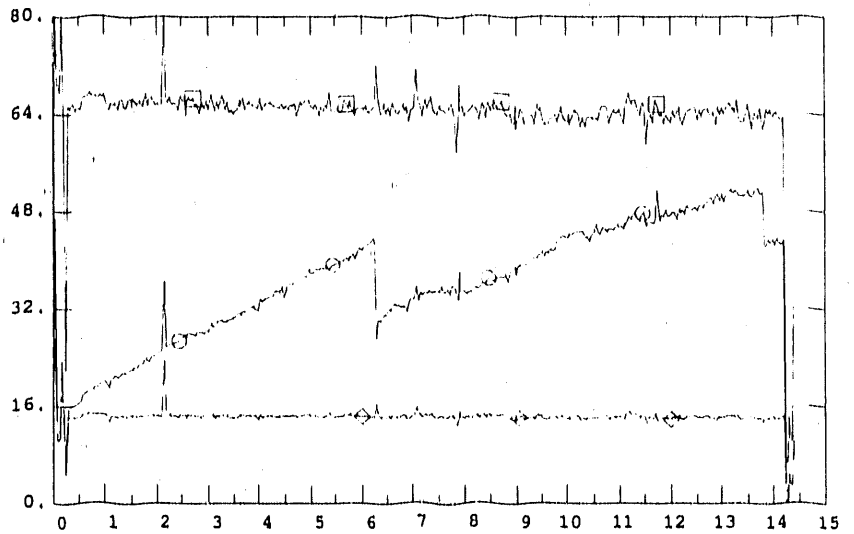

Figure 58. Pressure Drop, Flow Rate, and Face Velocity During Disc Filter Test DF10

SLOT	UNITS	DESCRIPTION	# SAMPLES	MEAN	ST DEV	MIN - FREQ	MAX - FREQ
957	DEGF	PATCH FILTER OUTLET	367	1168.358	14.721	1094.301 01	1193.905 01

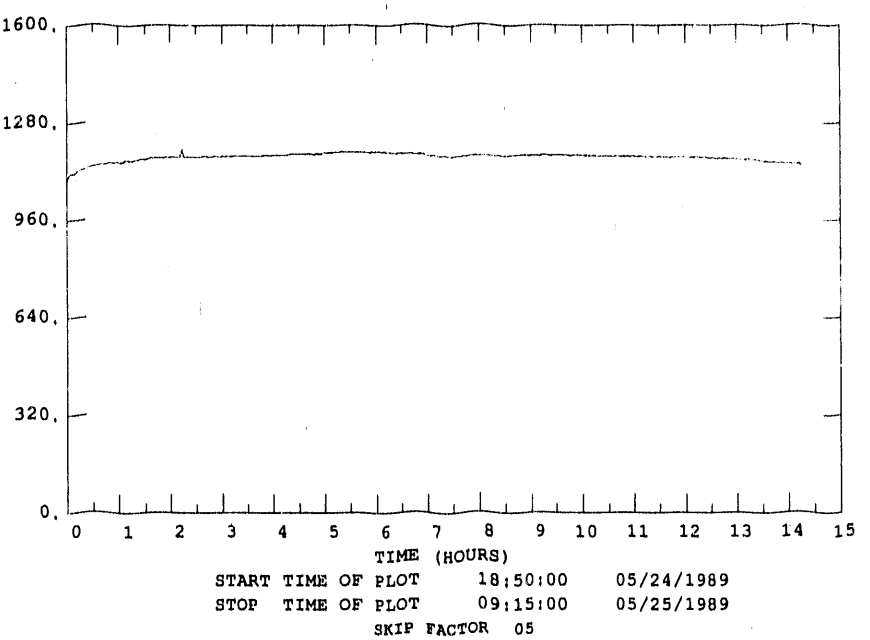

Figure 59. Disc Filter Outlet Temperature During Disc Filter Test DF10

SLOT	UNITS	DESCRIPTION	# SAMPLES	MEAN	ST DEV	MIN - FREQ	MAX - FREQ
1005	PSIG	ISO #2 PRESS.	367	23.540	2.029	1.053 01	36.727 01

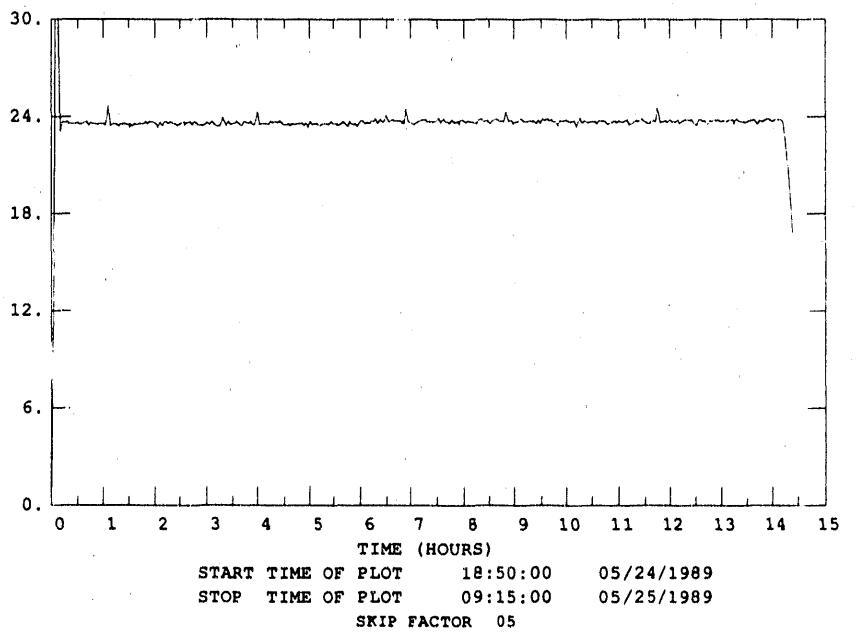

Figure 60. Disc Filter Vessel Pressure During Disc Filter Test DF10

	SLOT	UNITS	DESCRIPTION	# SAMPLES	MEAN	ST DEV	MIN - FREQ	MAX - FREQ
○	994	"H2O	PATCH FILTER DP	336	59.165	27.796	4.373 01	110.744 01
□	3106	SCFH	PATCH FILTER HI FLOW	336	65.382	4.689	11.157 01	85.277 01
△	3114	FT/M	PATCH FILTER FACE VELOCITY	336	14.605	2.310	2.429 01	21.230 01

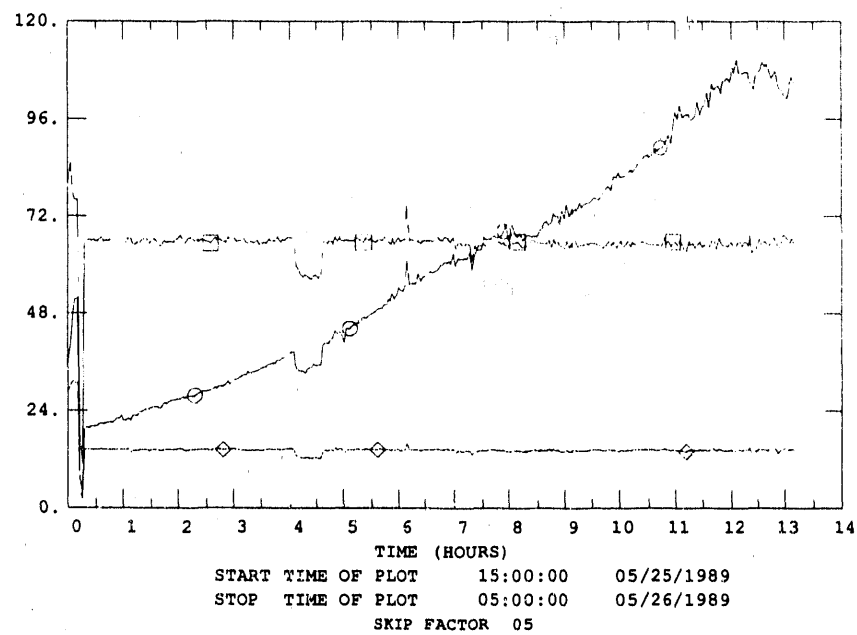

Figure 61. Pressure Drop, Flow Rate, and Face Velocity During Disc Filter Test DF11

SLOT	UNITS	DESCRIPTION	# SAMPLES	MEAN	ST DEV	MIN - FREQ	MAX - FREQ
957	DEGF	PATCH FILTER OUTLET	336	1151.899	7.052	1125.317 01	1165.977 01

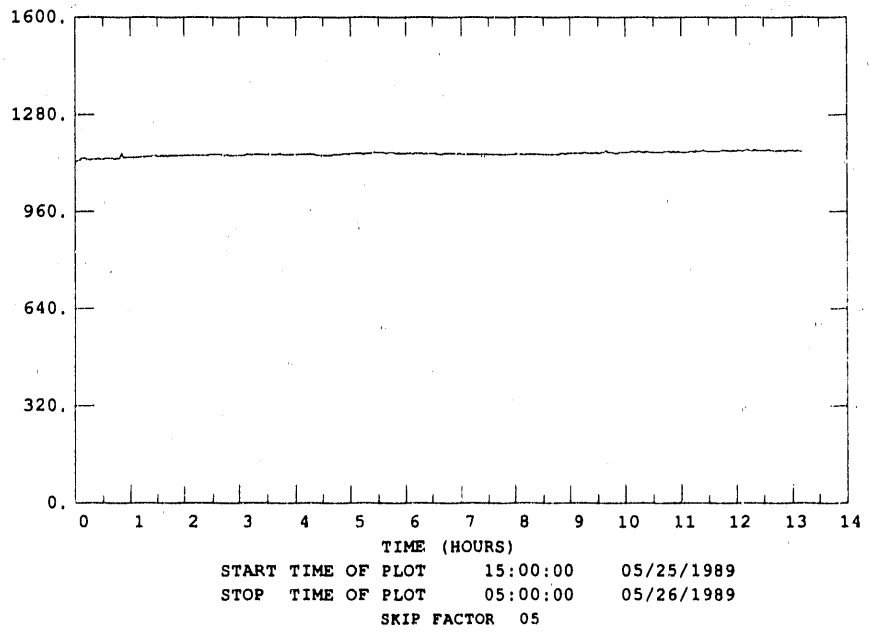

Figure 62. Disc Filter Outlet Temperature During Disc Filter Test DF11

SLOT	UNITS	DESCRIPTION	# SAMPLES	MEAN	ST DEV	MIN - FREQ	MAX - FREQ
1005	PSIG	ISO #2 PRESS.	336	23.264	2.189	5.921 01	24.481 01

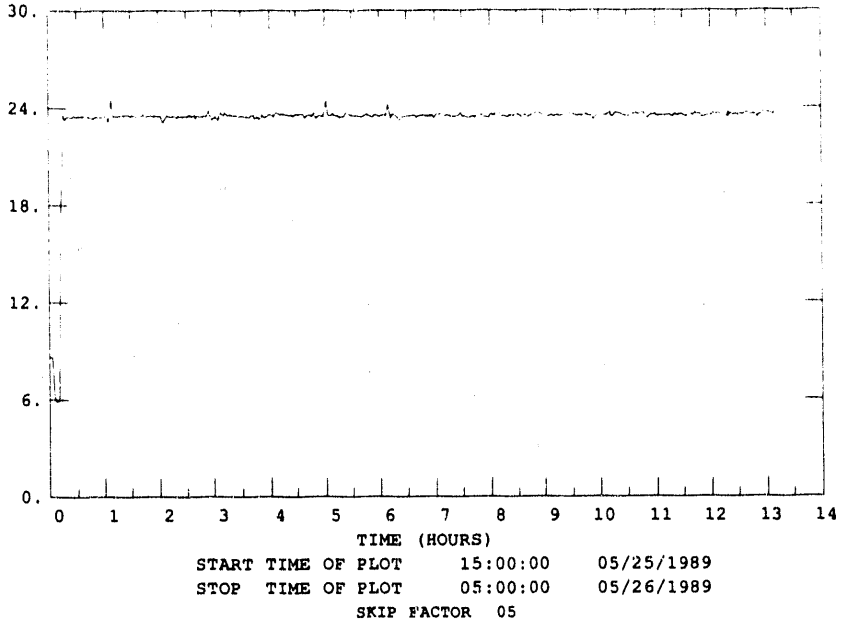

Figure 63. Disc Filter Pressure During Disc Filter Test DF11

Appendix D: Process Variables With Hot Nitrogen in the Disc-Filter Test Series

Presented in Table 11 is a list of process variables recorded when clean heated nitrogen was passed through the disc filter with a formed dust cake. The measured data were pressure drop, vessel pressure, temperature, and flow rate. The filter face velocity and K_2 values were calculated from these data. Both pressure drop and K_2 values are plotted against face velocity and are presented for each test. Data for Disc Filter Test DF10 was lost in a computer failure.

Table 11. Process Parameters When Hot Nitrogen Was Passed Through the Formed Dust Cake

Test ID	Flow (scf/h)	Pressure (psig)	Temperature (°F)	Face Velocity (ft/min)	ΔP (H_2O)	K2 (in H_2O ft min/lb)
DF1	10.37	25.09	1,178	2.00	9.88	7.97
	19.81	23.74	1,175	3.95	22.60	9.59
	29.75	22.50	1,174	6.13	34.39	9.36
	39.69	21.96	1,175	8.30	46.95	9.45
	49.40	22.76	1,176	10.12	55.87	9.17
	59.57	24.29	1,177	11.73	66.16	9.42
	69.28	25.34	1,179	13.30	76.05	9.58
	79.34	27.92	1,181	14.33	82.63	9.67
	88.84	30.53	1,186	15.16	89.94	10.01
	101.00	33.26	1,191	16.31	98.54	10.23
DF2	10.47	22.63	1,326	2.35	4.19	5.62
	20.25	23.10	1,324	4.48	8.62	6.84
	30.15	23.52	1,322	6.59	12.50	6.61
	40.21	23.89	1,320	8.70	16.89	7.00
	50.46	24.86	1,317	10.63	20.38	6.81
	59.70	26.29	1,316	12.13	23.81	7.20
	69.17	27.90	1,314	13.51	26.82	7.40
	79.24	30.59	1,313	14.55	29.66	7.86
	89.03	31.77	1,314	15.94	31.47	7.31
	81.45	13.94	1,306	23.55	92.66	24.19
DF3	10.12	19.36	1,181	2.29	13.11	5.14
	20.00	16.95	1,174	4.84	33.04	6.36
	30.31	20.05	1,170	6.67	45.58	6.37
	39.95	20.30	1,168	8.72	62.06	6.68
	49.46	20.89	1,168	9.39	77.29	7.92
	59.77	21.78	1,169	12.52	92.49	6.98
	70.36	23.23	1,171	14.19	110.50	7.42
	79.24	24.86	1,174	15.35	121.20	7.54
	89.04	26.33	1,176	16.65	127.50	7.28
	106.70	26.55	1,179	19.88	153.00	7.32
DF4	10.41	17.35	1,204	2.53	3.08	1.32
	19.79	14.04	1,201	5.36	7.89	3.81
	30.59	14.22	1,201	8.24	12.41	4.14
	39.37	14.48	1,203	10.52	15.89	4.18
	49.08	13.81	1,206	13.45	19.80	3.79
	59.23	15.20	1,207	15.49	23.66	4.32
	69.11	13.34	1,212	19.33	30.07	4.58
	78.47	12.53	1,217	22.67	36.10	4.92
	89.15	13.96	1,223	24.55	39.55	5.08
	95.60	13.77	1,227	26.57	48.76	7.24

Table 11. Process Parameters When Hot Nitrogen Was Passed Through the Formed Dust Cake
(Continued)

Test ID	Flow (scf/h)	Pressure (psig)	Temperature (°F)	Face Velocity (ft/min)	ΔP (H_2O)	K2 (in H_2O ft min/lb)
DF5	10.31	16.52	1,207	2.58	2.97	0.58
	20.14	15.03	1,205	5.29	6.68	1.39
	29.77	14.12	1,205	8.07	10.42	1.59
	39.70	13.70	1,205	10.92	14.12	1.61
	49.74	13.98	1,207	13.56	17.67	1.67
	59.58	14.72	1,210	15.86	20.88	1.76
	69.50	14.45	1,213	18.71	25.10	1.93
	78.87	16.57	1,216	19.83	26.73	1.97
	88.87	18.11	1,220	21.34	29.52	2.22
	101.50	19.92	1,223	23.14	32.51	2.36
DF6	10.66	3.02	1,172	4.60	7.48	2.29
	20.13	4.33	1,172	7.89	13.42	2.57
	30.16	7.04	1,170	10.61	19.96	3.24
	39.56	9.22	1,171	12.65	25.51	3.75
	49.84	10.74	1,174	15.01	31.12	3.95
	59.04	12.10	1,176	16.90	36.09	4.18
	69.31	13.41	1,178	18.94	41.29	4.34
	79.11	14.23	1,179	21.02	46.64	4.49
	89.21	15.48	1,182	22.76	51.29	4.61
	102.60	17.03	1,184	24.93	56.92	4.72
DF7	10.38	16.93	1,122	2.43	4.29	1.15
	19.50	17.89	1,065	4.28	8.84	1.67
	30.33	19.38	1,005	6.11	13.46	1.94
	39.37	21.40	945	7.19	17.29	2.30
	49.33	23.08	898	8.32	21.70	2.66
	59.22	23.92	863	9.51	26.29	2.94
	69.52	25.17	838	10.61	30.52	3.14
	79.02	26.33	817	11.53	34.42	3.33
	89.31	27.68	800	12.45	38.14	3.47
	99.50	29.72	787	13.10	41.43	3.64
DF9	10.29	14.35	1,129	2.64	0.73	-3.77
	19.32	18.09	1,118	4.36	2.1	-2,63
	29.60	20.50	1,105	6.17	3.4	-2.22
	44.18	20.88	1,093	9.04	6.45	-1.31
	49.58	21.20	1,092	10.05	8.26	-0.72
	59.05	22.67	1,090	11.49	10.37	-0.27
	69.17	23.73	1,093	13.11	12.71	0.08
	79.24	24.59	1,075	14.52	16.72	1.11
	88.93	26.54	1,032	15.09	18.66	1.67
	108.60	24.44	990	18.87	24.88	2.21

Table 11. Process Parameters When Hot Nitrogen Was Passed Through the Formed Dust Cake
(Continued)

Test ID	Flow (scf/h)	Pressure (psig)	Temperature (°F)	Face Velocity (ft/min)	ΔP (H_2O)	K2 (in H_2O ft min/lb)
DF8	10.03	15.77	1,164	2.51	4.55	2.17
	19.93	15.69	1,160	4.98	11.07	3.72
	29.40	17.27	1,151	6.95	17.23	4.70
	39.41	18.91	1,150	8.85	24.46	5.77
	49.64	19.74	1,149	10.88	32.21	6.51
	59.20	20.68	1,152	12.63	40.21	7.33
	68.65	21.73	1,154	14.26	47.11	7.79
	79.36	23.17	1,149	15.81	52.00	7.75
	89.04	25.19	1,149	16.84	57.51	8.22
	101.50	26.84	1,161	18.58	64.05	8.32
DF11	15.99	3.00	1,127	6.73	13.36	1.39
	20.04	10.05	1,121	6.00	33.13	6.53
	29.92	11.02	1,120	8.62	59.92	8.64
	39.37	11.16	1,123	11.30	83.92	9.34
	48.86	10.44	1,126	14.46	115.70	10.19
	58.12	9.25	1,132	18.12	142.70	10.00
	67.36	9.22	1,137	21.09	168.10	10.14
	77.01	9.84	1,142	23.58	192.00	10.39
	76.43	10.71	1,148	22.68	214.00	12.30
	77.12	11.83	1,151	21.96	230.00	13.84

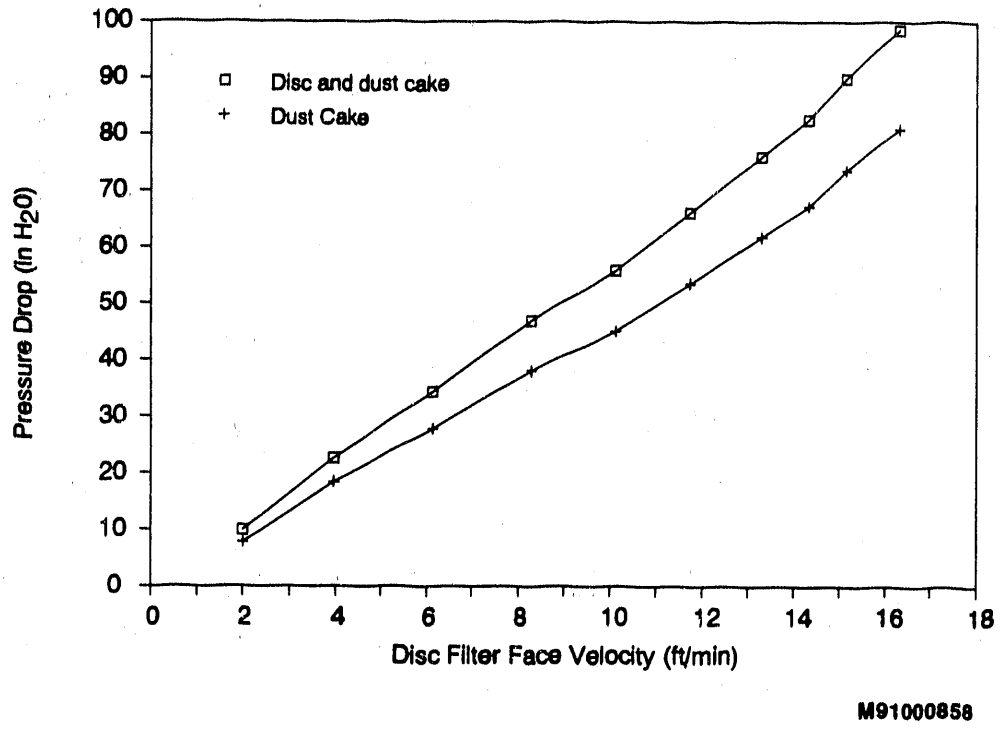

Figure 64. Effect of Face Velocity on Pressure Drop Through Disc Filter and Dust Cake for Disc Filter Test DF1

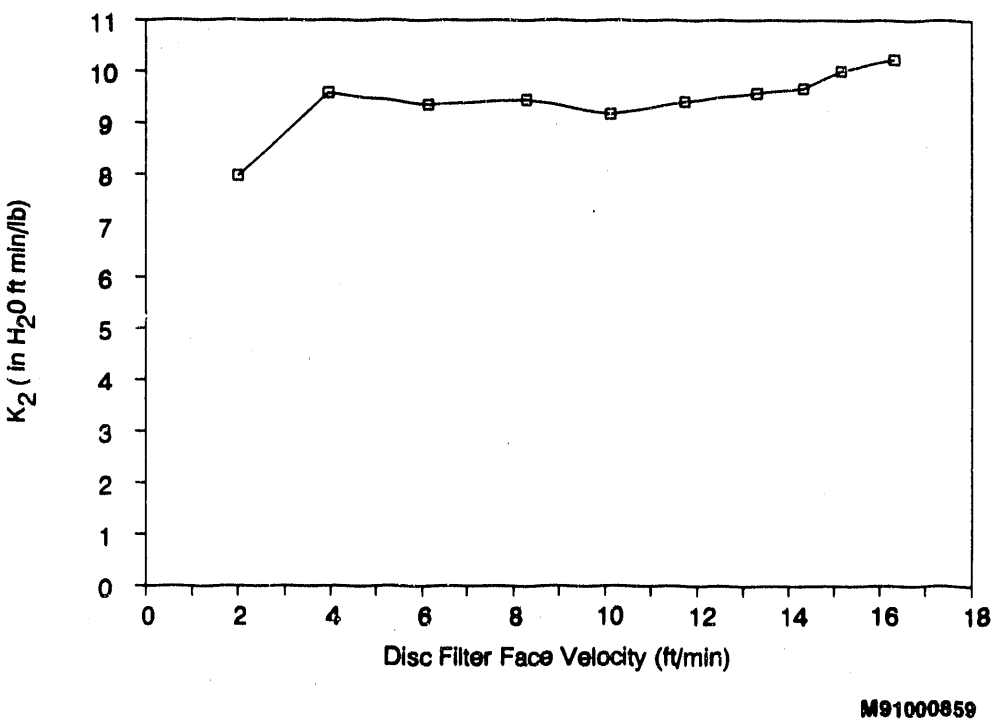

Figure 65. Effect of Face Velocity on K_2 for Disc Filter Test DF1

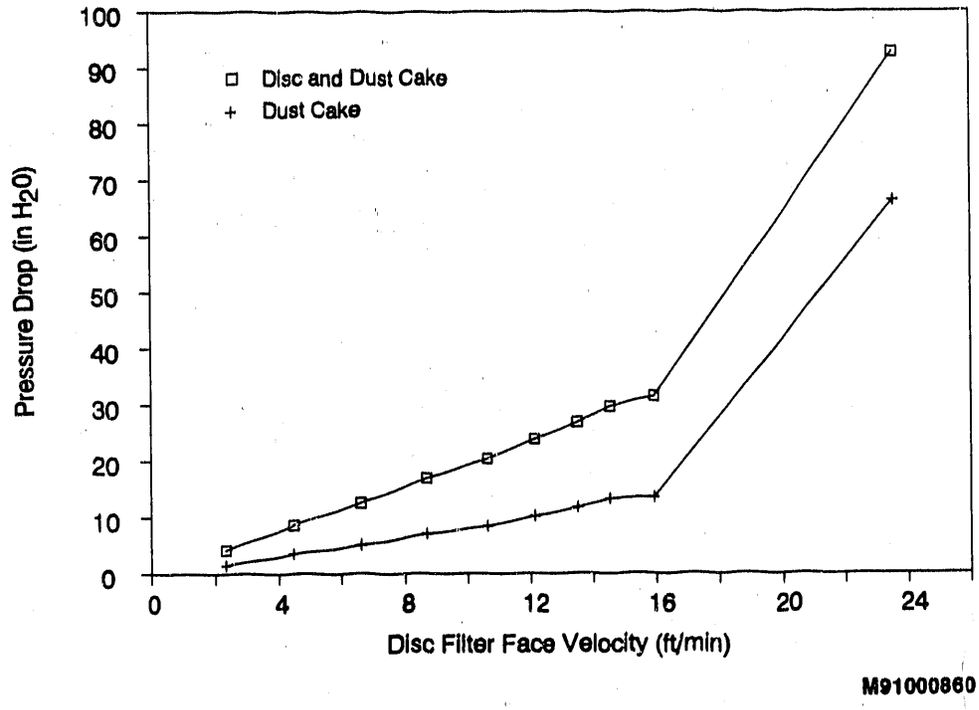

Figure 66. Effect of Face Velocity on Pressure Drop Through Disc Filter and Dust Cake for Disc Filter Test DF2

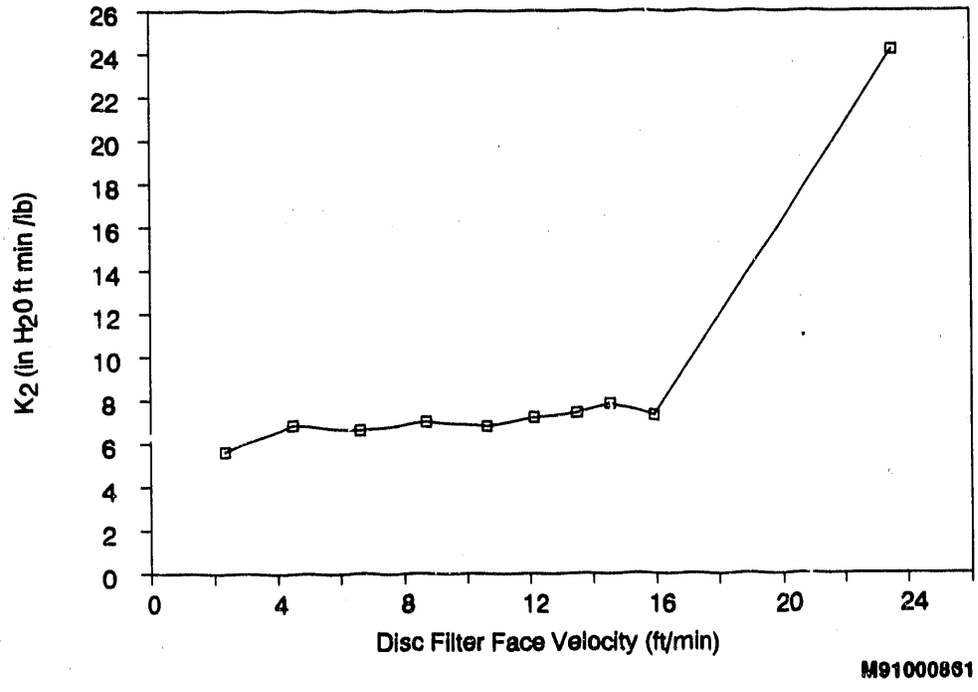

Figure 67. Effect of Face Velocity on K_2 for Disc Filter Test DF2

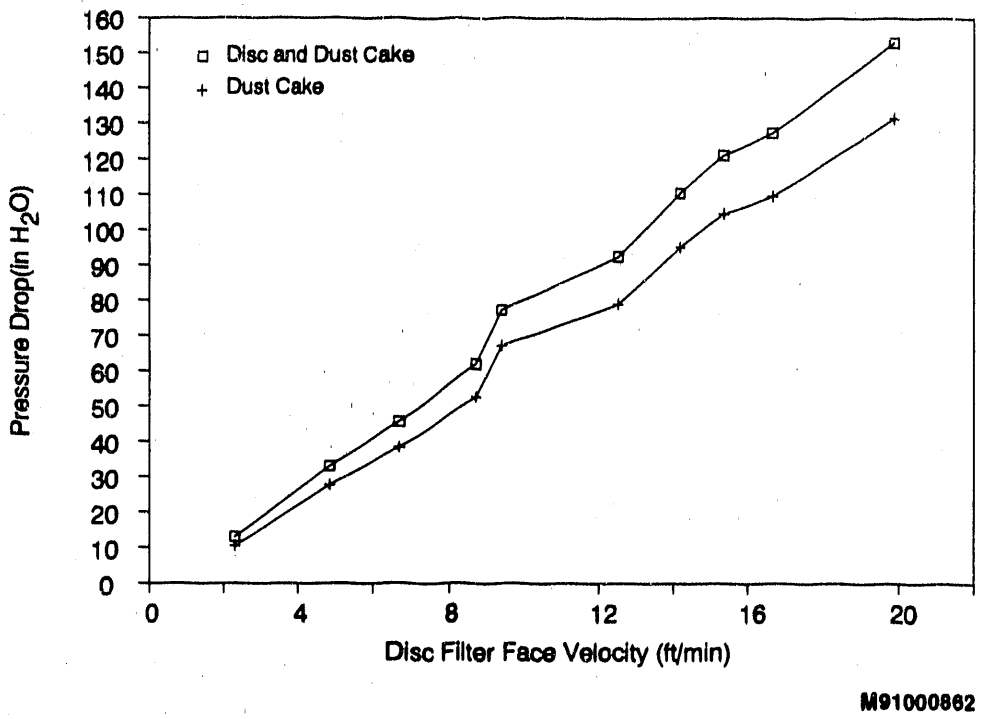

Figure 68. Effect of Face Velocity on Pressure Drop Through Disc Filter and Dust Cake for Disc Filter Test DF3

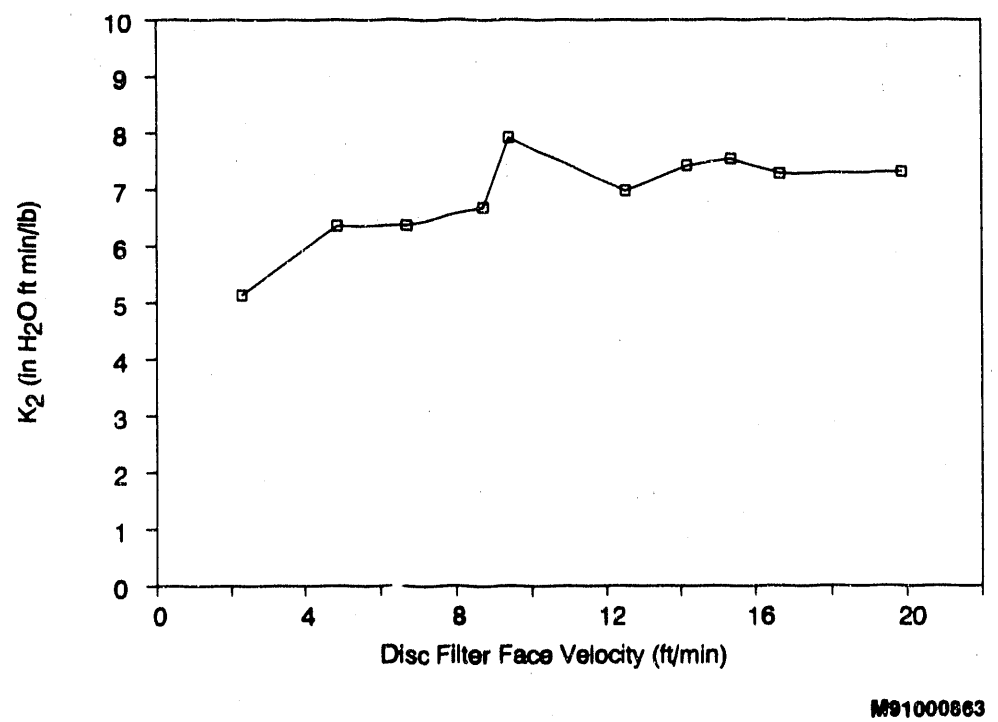

Figure 69. Effect of Face Velocity on K_2 for Disc Filter Test DF3

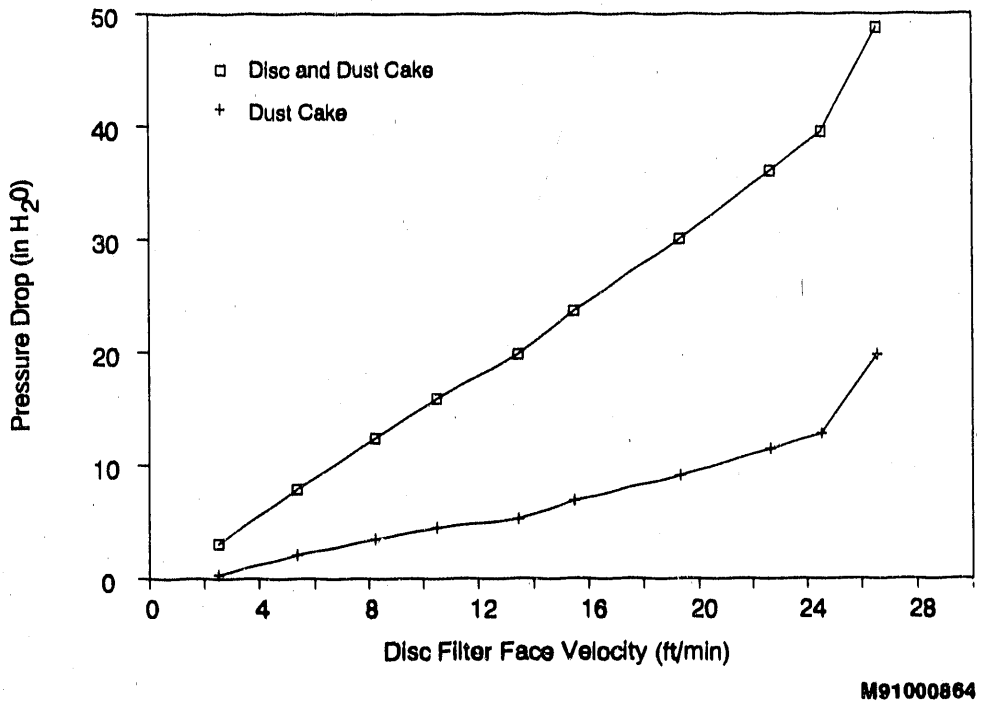

Figure 70. Effect of Face Velocity on Pressure Drop Through Disk Filter and Dust Cake for Disc Filter Test DF4

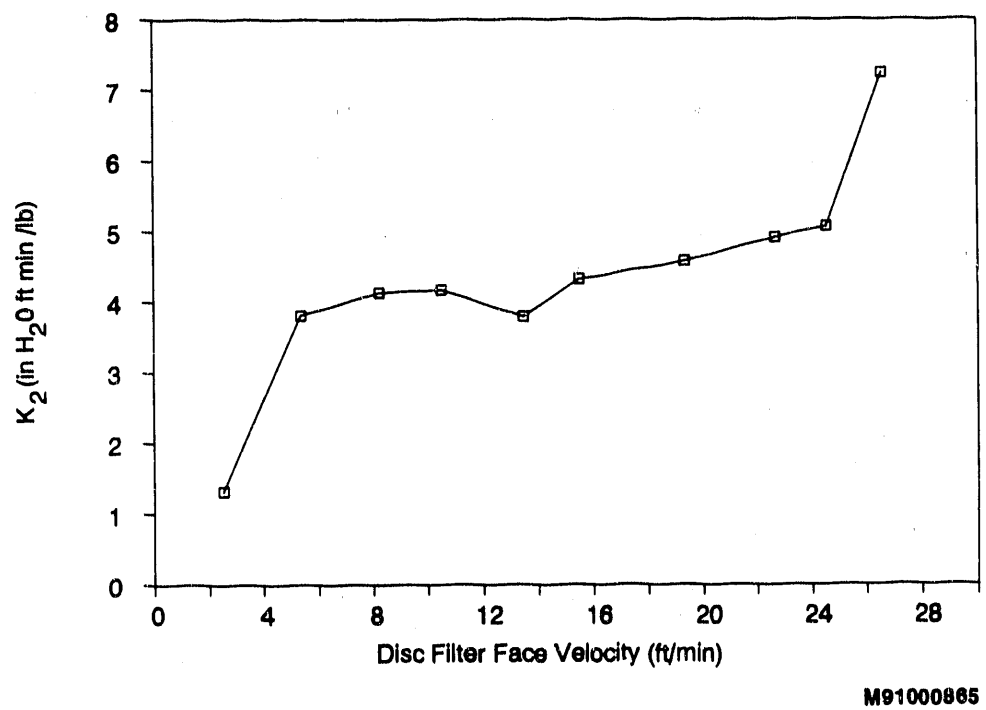

Figure 71. Effect of Face Velocity on K_2 for Disc Filter Test DF4

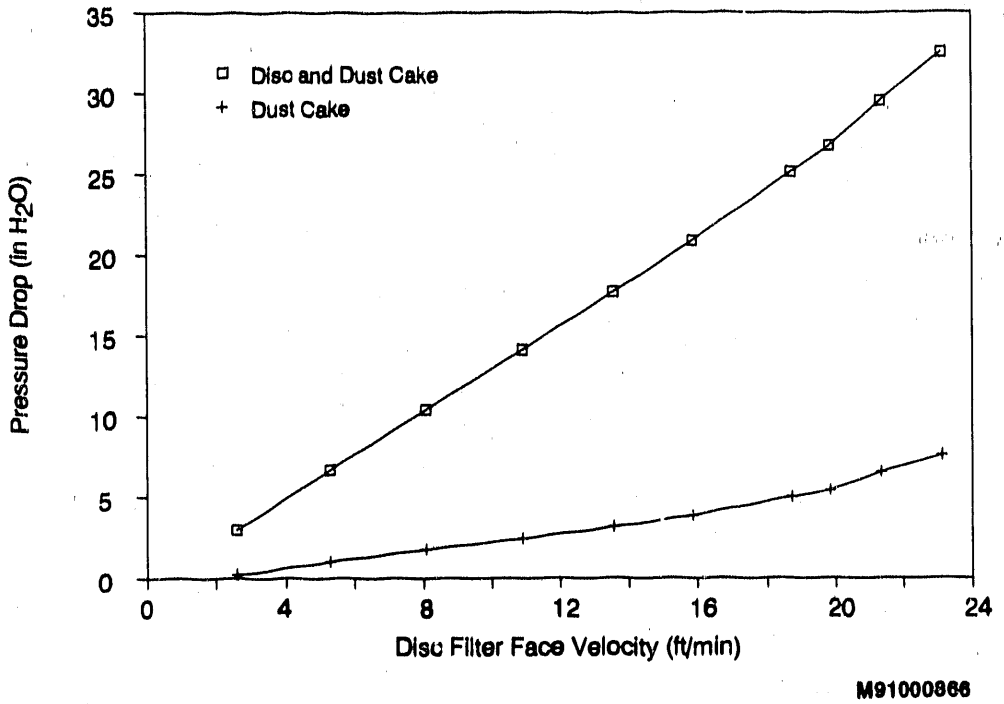

Figure 72. Effect of Face Velocity on Pressure Drop Through Disc Filter and Dust Cake for Disc Filter Test DF5

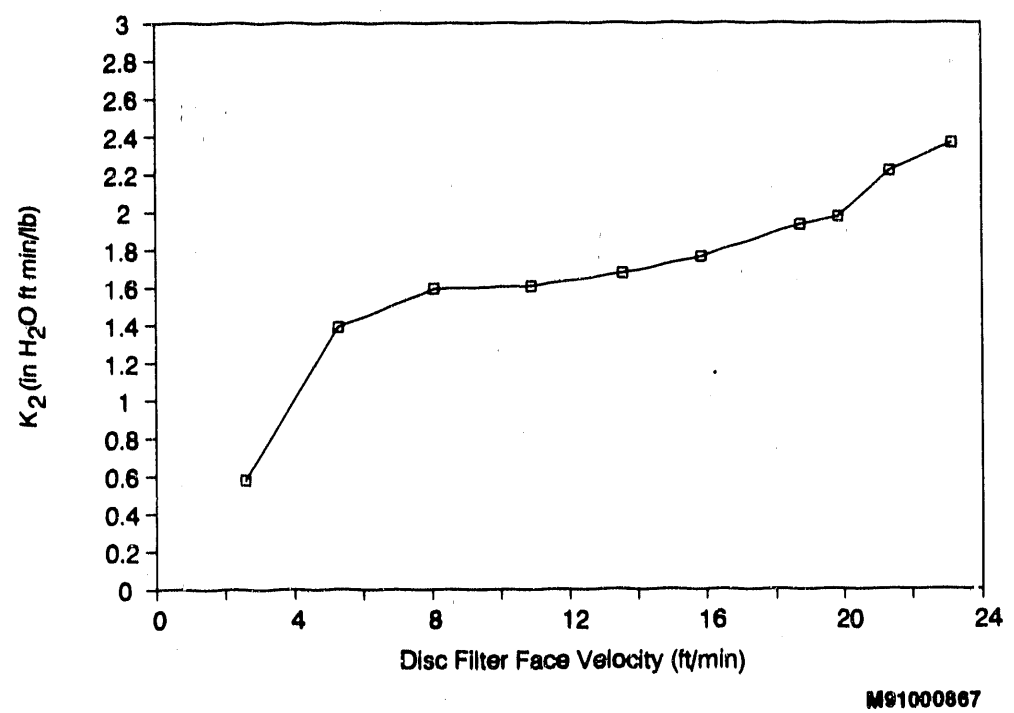

Figure 73. Effect of Face Velocity on K_2 for Disc Filter Test DF5

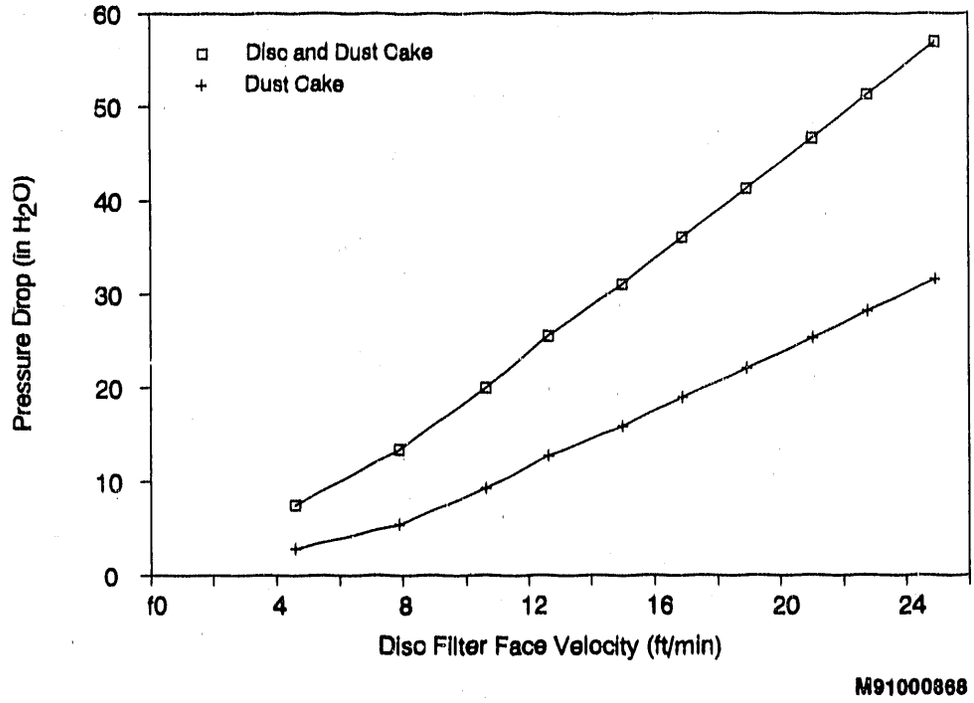

Figure 74. Effect of Face Velocity on Pressure Drop Through Disc Filter and Dust Cake for Disc Filter Test DF6

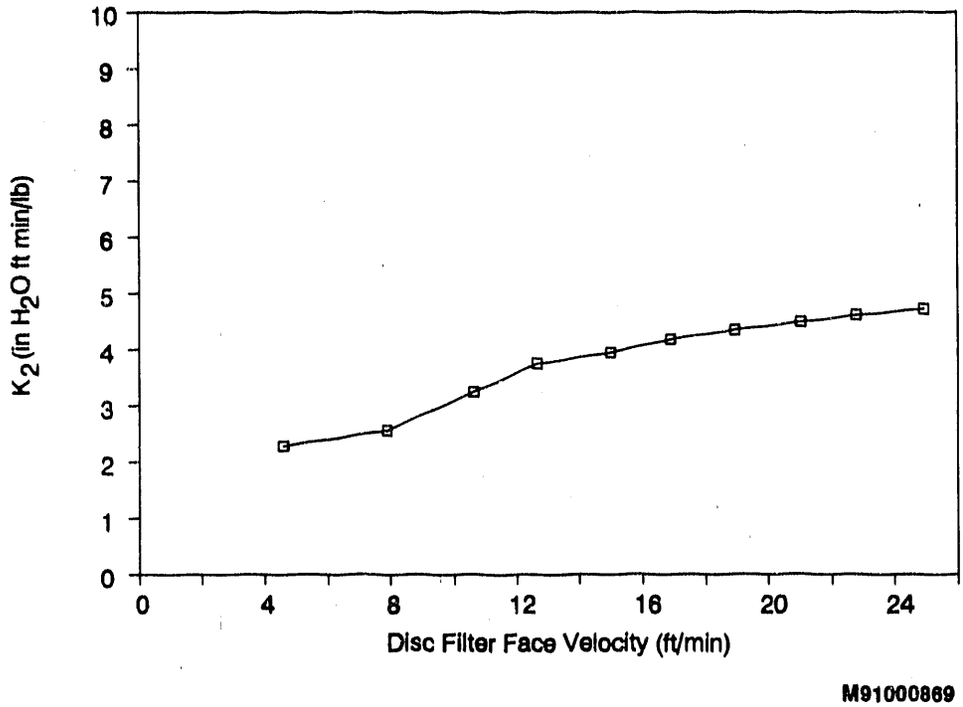

Figure 75. Effect of Face Velocity on K_2 for Disc Filter Test DF6

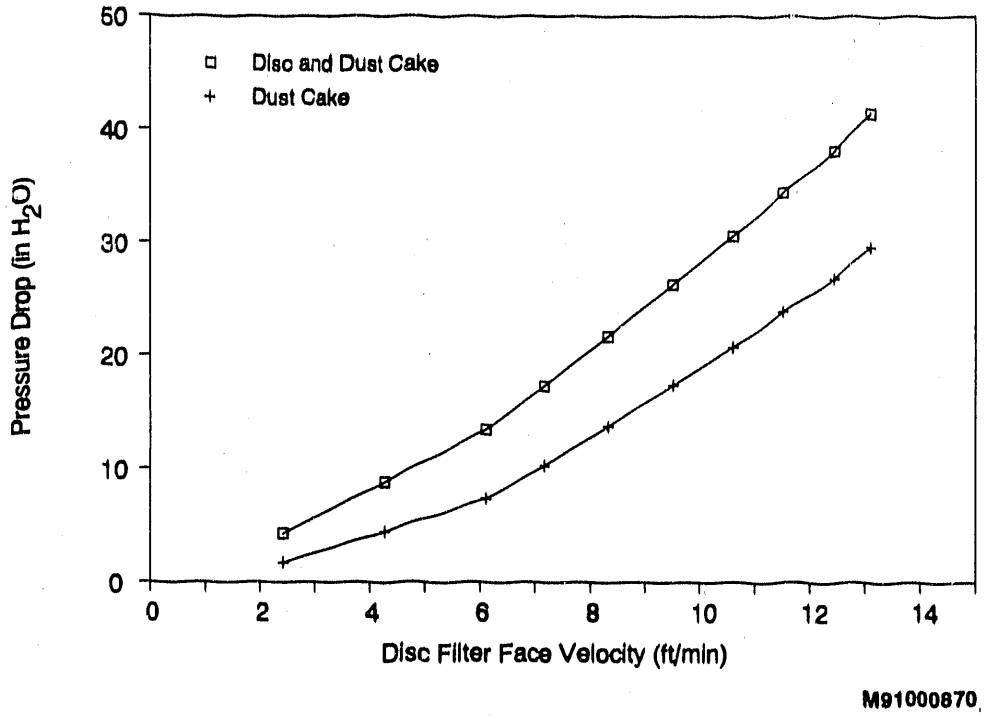

Figure 76. Effect of Face Velocity on Pressure Drop Through Disc Filter and Dust Cake for Disc Filter Test DF7

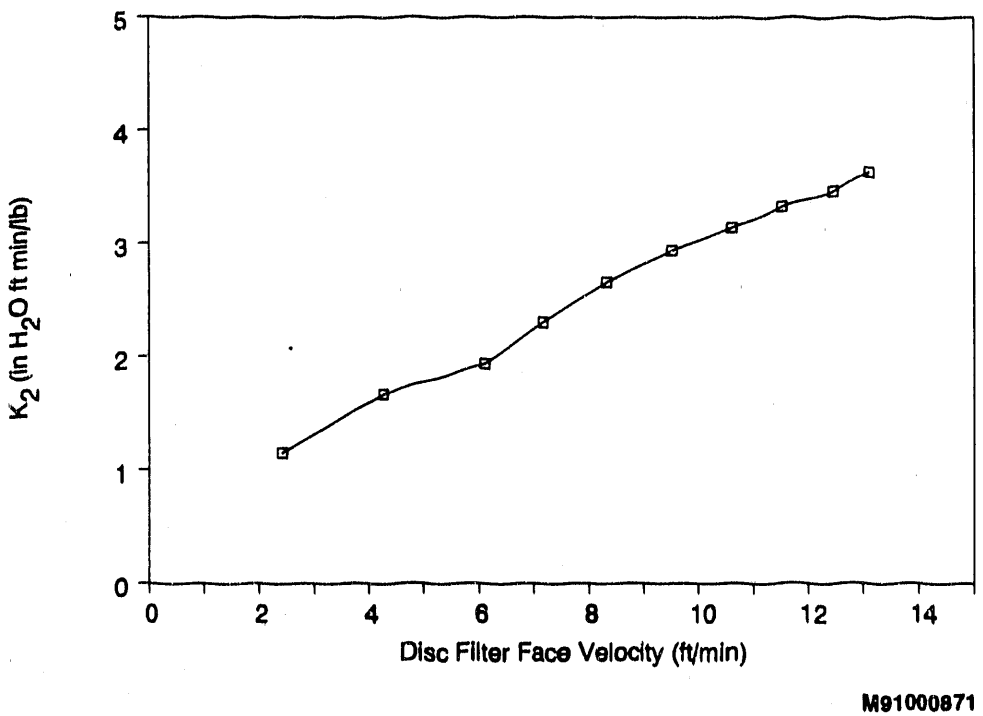

Figure 77. Effect of Face Velocity on K_2 for Disc Filter Test DF7

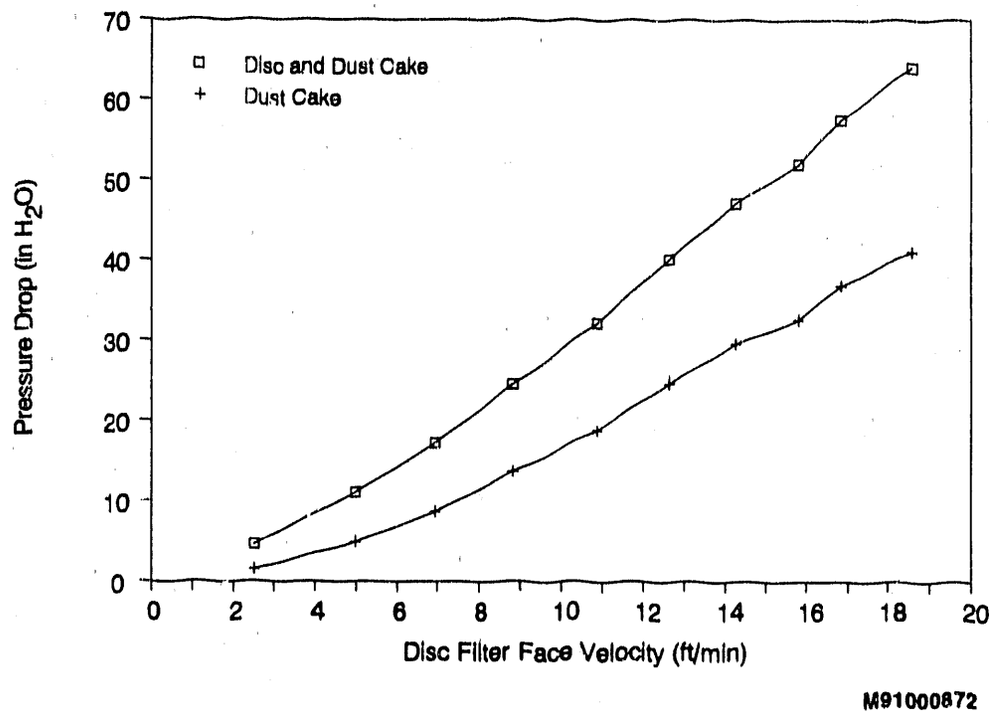

Figure 78. Effect of Face Velocity on Pressure Drop Through Disc Filter and Dust Cake for Disc Filter Test DF8

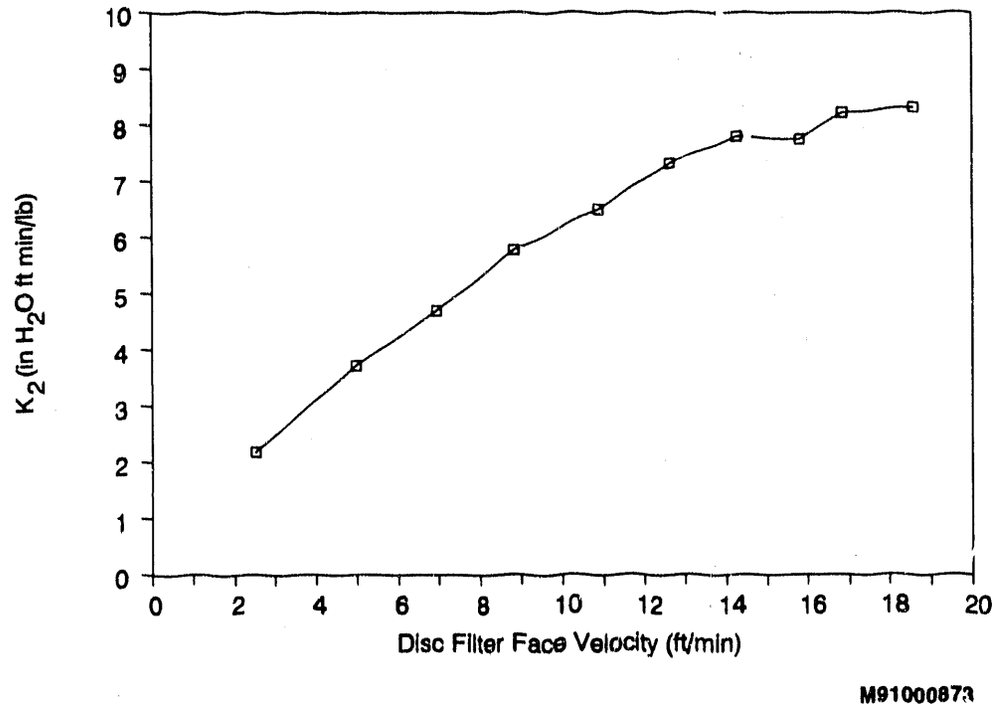

Figure 79. Effect of Face Velocity on K_2 for Disc Filter Test DF8

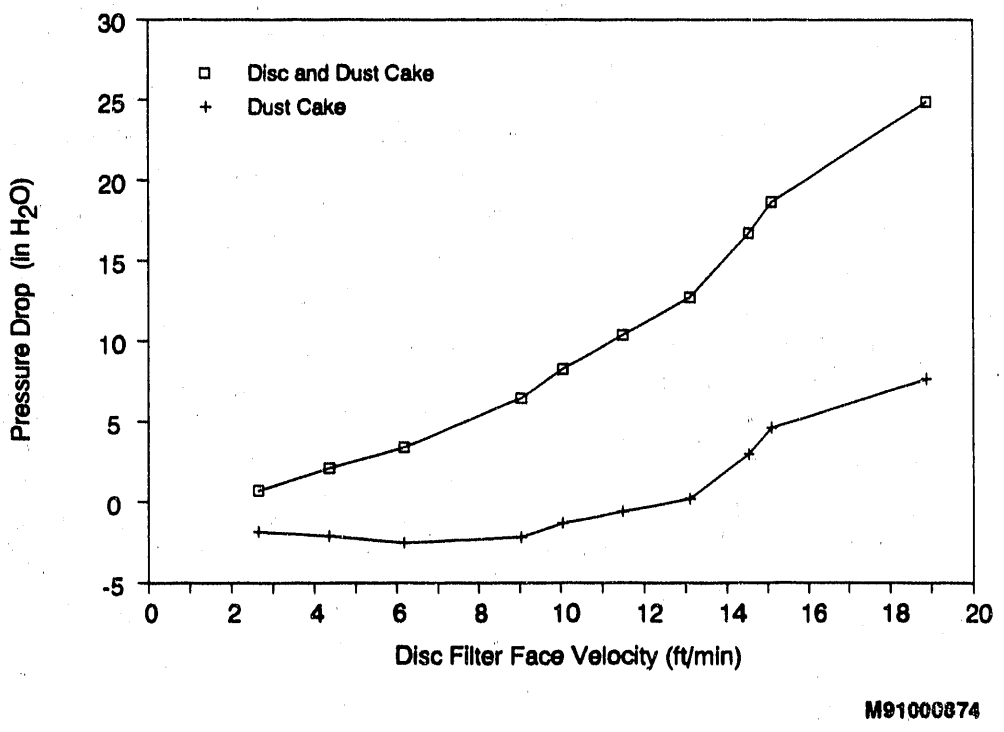

Figure 80. Effect of Face Velocity on Pressure Drop Through Disc Filter and Dust Cake for Disc Filter Test DF9

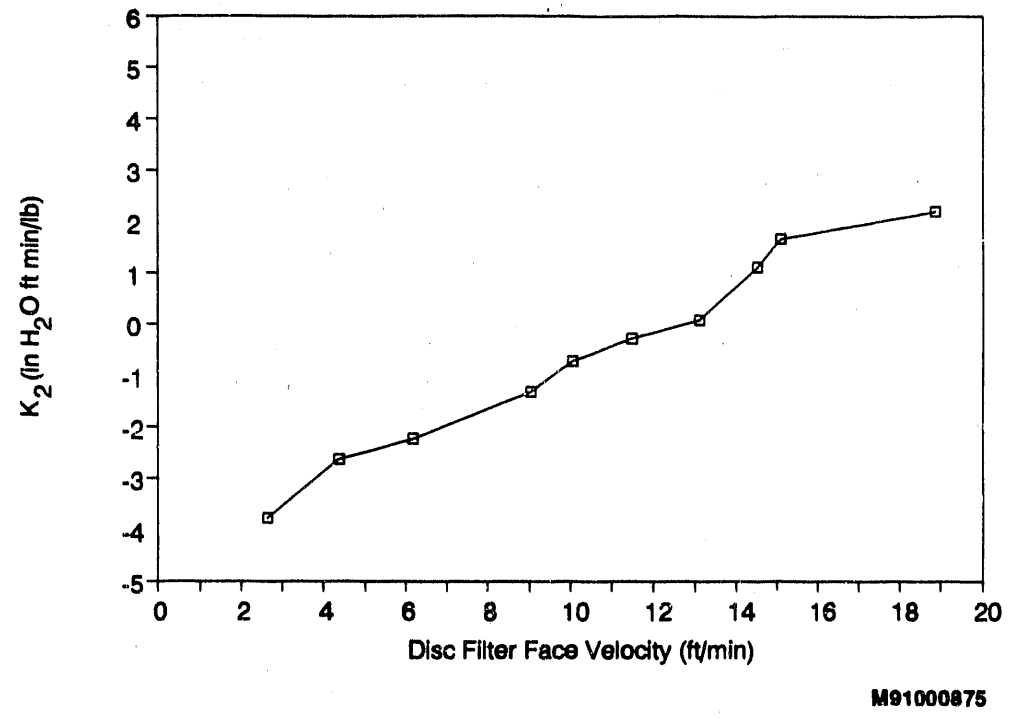

Figure 81. Effect of Face Velocity on K_2 for Disc Filter Test DF9

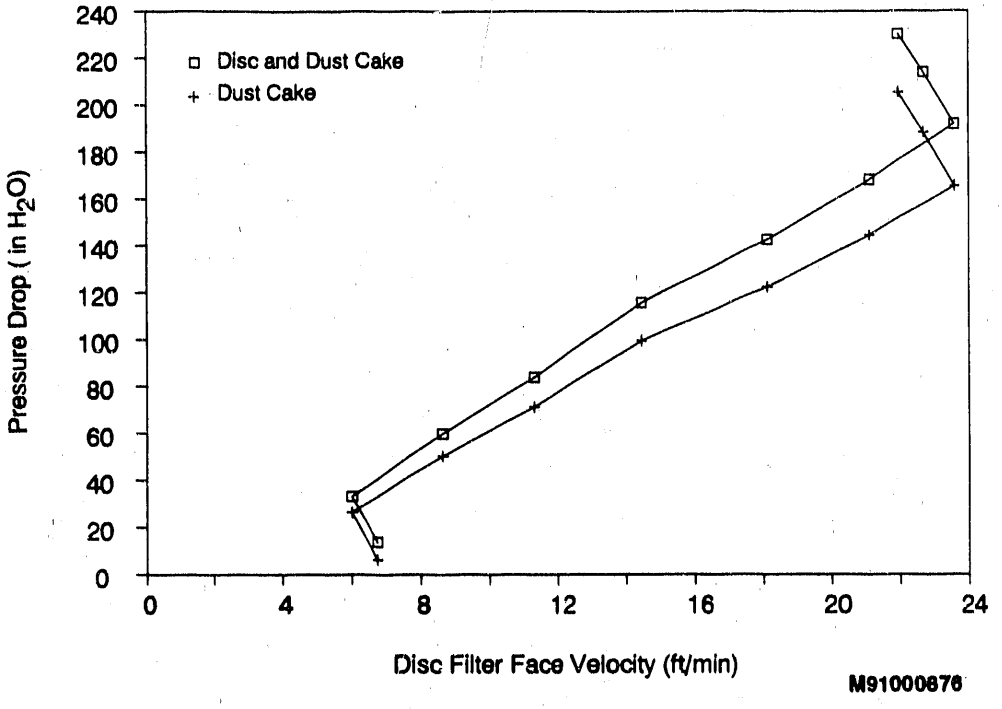

Figure 82. Effect of Face Velocity on Pressure Drop Through Disc Filter and Dust Cake for Disc Filter Test DF11

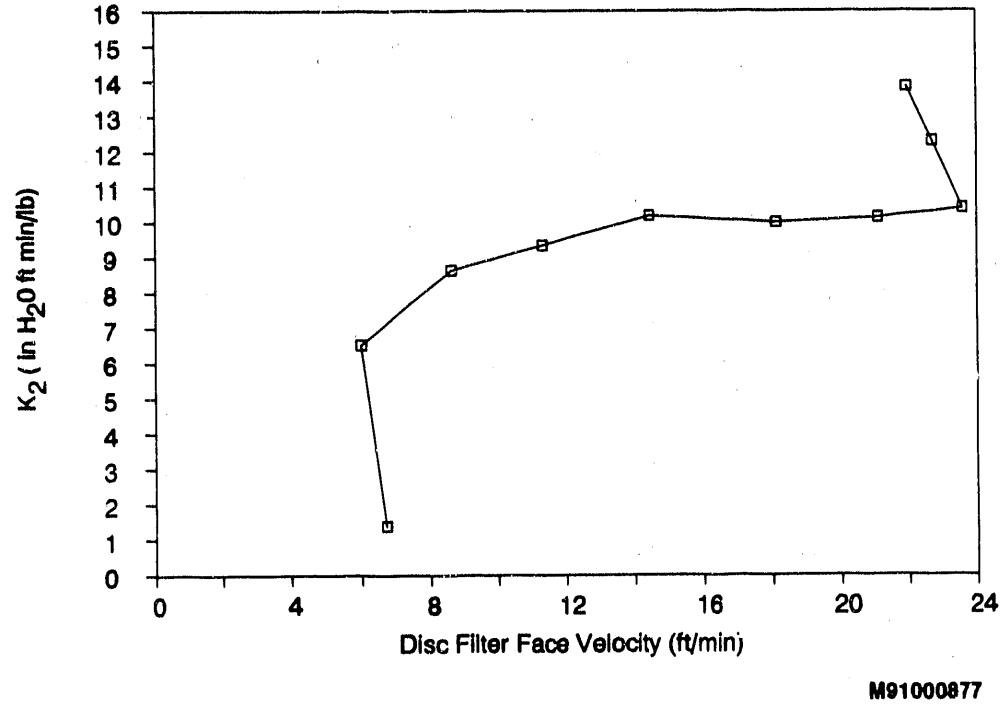

Figure 83. Effect of Face Velocity on K_2 for Disc Filter Test DF11

Appendix E: SEM, Chemical, and Physical Analyses of Dust Cakes in the Candle-Filter Test Series

The scanning electron microscope (SEM) photographs show bedding planes on the "cracker-like" dust cakes as rings concentric with the outside surface of the candle filter. SEM photographs taken perpendicular to the bedding planes would also be perpendicular to the candle filter surface. Photos taken parallel to the bedding plane were tangent and longitudinal to the candle filter surface, but were elevated from the filter surface to examine the inner regions of the cracker-like cake. The material used for the SEM photographs was taken from the cracker-like samples formed during each test. The separate specimens (three for each test) analyzed in Table 12 were grab samples used to determine the mean particle size for each test. These samples were selected based on their apparent carbon content.

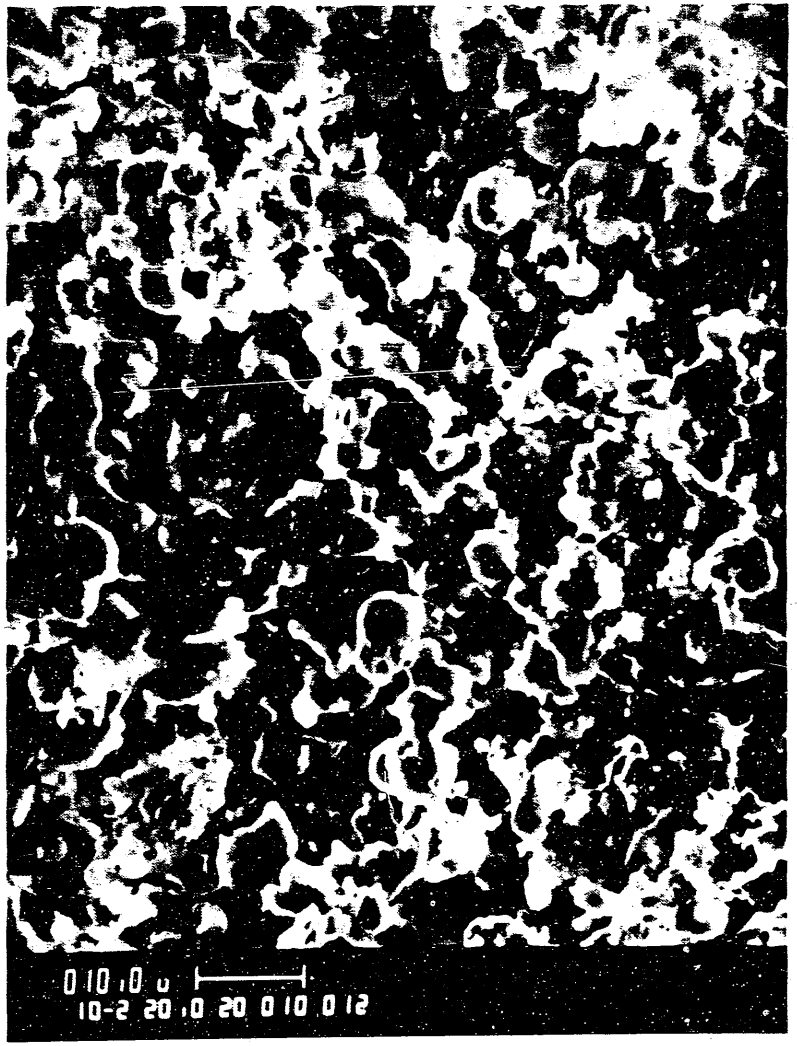

Figure 84. SEM of CF1 Dust Cake Perpendicular to the Bedding Plane

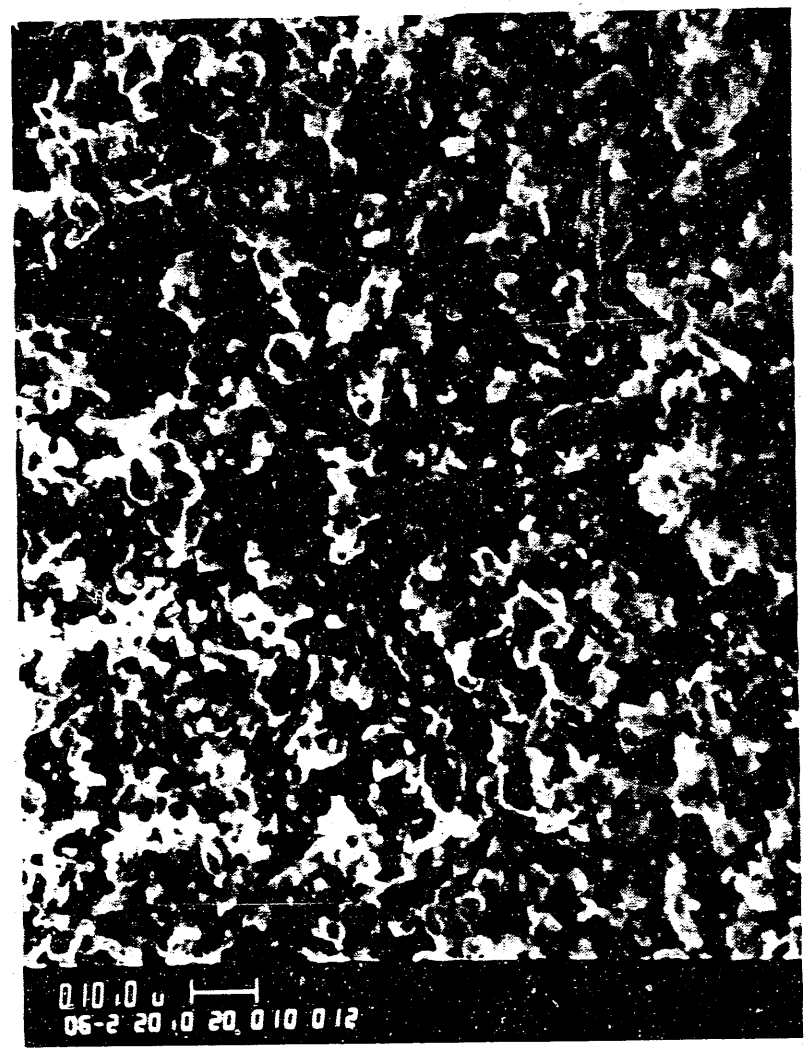

Figure 85. SEM of CF1 Dust Cake Parallel to the Bedding Plane

Figure 86. SEM of CF1 Dust Cake Perpendicular to Bedding Plane at Higher Magnification

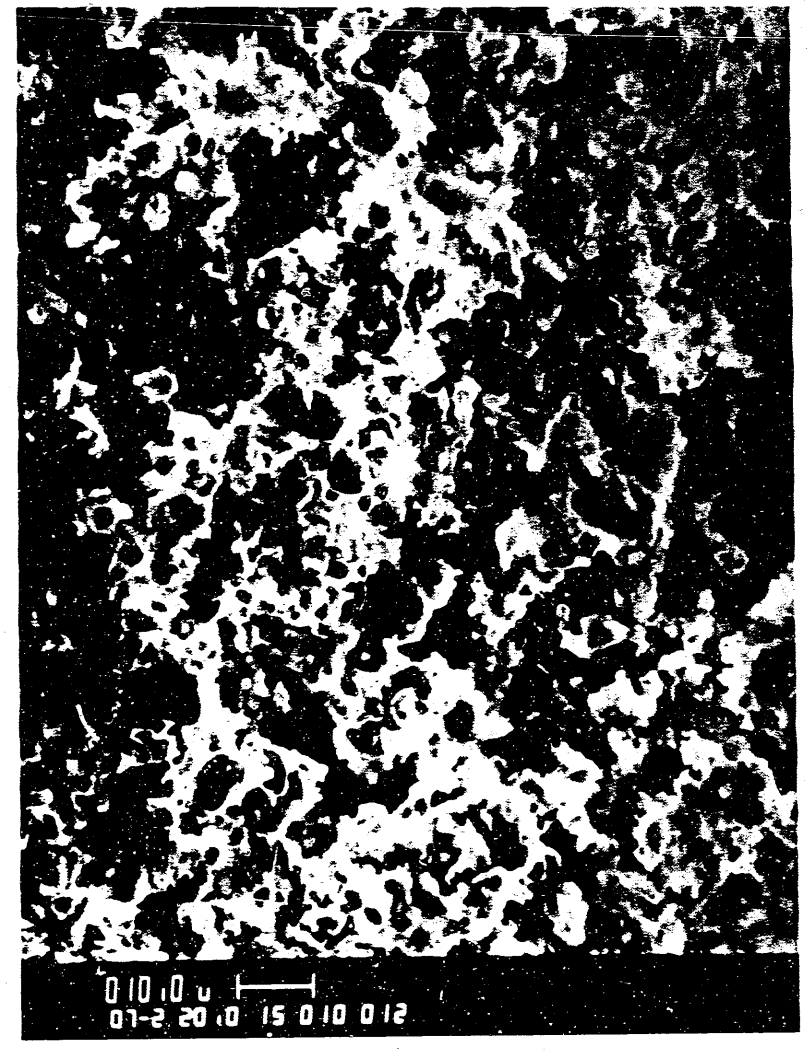

Figure 87. SEM of CF2 Dust Cake Perpendicular to the Bedding Plane

Figure 88. SEM of CF3 Dust Cake Perpendicular to the Bedding Plane

Figure 89. SEM of CF3 Dust Cake Perpendicular to Bedding Plane at Higher Modification

Table 12. Laboratory Analysis of Candle-Filter Dust Cakes

Parameter	CF1			CF2			CF3		
	R11-1	R11-2	R11-3	R12-1	R12-2	R12-3	R13-1	R13-2	R13-3
Mean Particle Size (by volume) (μm)	6.66	8.51	5.32	15.06	10.16	8.64	9.80	8.21	6.80
Mean Particle Size (by population (μm)	2.57	3.02	2.66	4.42	3.98	3.65	3.45	3.23	2.17
Density (by helium) (g/cc)	2.78	2.80	2.80	2.84	2.75	2.80	2.86	2.68	2.87
BET Surface Area (via nitrogen) (m^2/g)	6.43	8.15	1.57	27.66	3.79	1.55	17.91	3.22	1.55
Pore Volume, Adsorption (via N_2) (cc/g)	0.0063	0.0058	0.0047	0.0105	0.0049	0.0024	0.0080	0.0058	0.0024
Ash (%)	94.25	91.80	97.96	77.32	95.58	98.16	86.55	98.85	99.73
Carbon (%)	3.30	4.94	0.86	17.74	2.12	3.33	10.22	0.57	0.20
Nitrogen (%)	< 0.02	0.05	0.06	0.27	0.02	0.08	0.17	< 0.01	< 0.01
Total Sulfur (%)	6.866	6.808	4.899	6.698	5.734	8.122	5.868	7.64	--
Sulfur (%)	4.43	4.15	3.66	3.21	4.02	5.22	3.82	4.97	4.80
Hydrogen (%)	< 0.01	< 0.01	< 0.01	0.38	0.09	< 0.01	0.19	0.08	0.16
Moisture (%)	0.49	0.44	0.22	0.74	0.18	0.15	0.99	0.22	0.14
K_2O (%)	2.285	1.960	1.926	0.840	1.783	1.684	1.806	2.16	--
SiO_2 (%)	38.4	38.5	39.0	33.9	39.2	36.3	39.2	37.5	--
Fe_2O_3 (%)	5.39	5.76	5.32	5.66	6.34	5.51	5.86	4.96	--
MgO (%)	2.109	2.271	2.421	2.890	2.070	1.902	1.996	--	--
ZnO (%)	0.0078	0.0067	0.0087	0.0049	0.0067	0.0073	0.0065	0.009	--
SrO (%)	0.114	0.093	0.137	0.056	0.095	0.107	0.096	--	--
CaO (%)	16.560	18.758	16.775	30.492	16.961	14.645	16.706	13.46	--
P_2O_5 (%)	0.290	0.309	0.292	0.425	0.297	0.271	0.288	0.26	--
Al_2O_3 (%)	18.88	17.97	18.70	13.29	19.09	17.74	18.97	19.47	--
TiO_2 (%)	0.84	0.72	0.88	0.36	0.75	0.75	0.73	--	--
MnO (%)	0.006	0.006	0.006	0.005	0.003	0.002	0.004	0.00	--
Ash Fusion ID (°F)	2,120	--	--	--	--	2,180	--	--	2,260
Ash Fusion ST (°F)	2,220	--	--	--	--	2,305	--	--	2,345
Ash Fusion HT (°F)	2,235	--	--	--	--	2,345	--	--	2,365
Ash Fusion FT (°F)	2,290	--	--	--	--	2,450	--	--	2,470

Note: We could not perform elemental analysis by XRF on Sample R13-3 because the pellet fell apart.

Appendix F: Laboratory Characterization of Filter Dust by Southern Research Institute

Appendix F is a table listing Southern Research Institute's standard laboratory analysis of dust samples from the candle filter test series.

Table 13. Laboratory Analysis of Dust Samples

Parameter	Sample Identification CF1	CF2	CF3
Specific Surface Area (m^2/g)	5.2	20.3	13.3
Uncompacted Bulk Porosity (%)	86.0	72.4	81.8
Estimated Dust Cake Porosity (%)	83	--[1]	80
Drag-Equivalent Diameter (μm)	1.23	4.05	1.81
Relative Gas Flow Resistance (in H_2O ft min/lb)	3.0	1.3	2.4

[1] The estimated dust cake porosity was not determined since the sample contained a significant amount of unburned char particles with a high surface area. Consequently, the relative gas flow resistance was calculated with the uncompacted bulk porosity.

5:900531tk.1m

END

DATE FILMED

06 / 24 / 91